7

- NASA CR-147440

E7.6-10204

PACIFIC SOUTHWEST and ROCKY MOUNTAIN Forest and Range Experiment Stations

FOREST SERVICE U.S. DEPARTMENT OF AGRICULTURE

EVALUATION OF SKYLAB (EREP) DATA FOR FOREST AND RANGELAND SURVEYS

(E76-10204) EVALUATION OF SKYLAB (EREP) DATA FOR FOREST AND RANGELAND SURVEYS Final Report (Pacific Southwest Forest and Range Experiment) 282 p HC $9.25 CSCL 08F

N76-19512

Unclas
G3/43 00204

Cover page: an enlarged portion (4X) of a Skylab S190B color photograph taken on November 30, 1973. Clark Hill Reservoir and the Savannah River are shown in the center. Interstate 20 and the outer fringe of Augusta, Georgia, can be seen in the lower right corner. This black-and-white reproduction was made from a color internegative. The scale is approximately 1:250,000.

EVALUATION OF SKYLAB (EREP)

DATA FOR FOREST AND RANGELAND SURVEYS

by

Robert C. Aldrich, Principal Investigator
and
Robert W. Dana
Edwin H. Roberts
Wallace J. Greentree
Nancy X. Norick
Thomas H. Waite

Pacific Southwest Forest and Range Experiment Station
Berkeley, California 94701

Richard E. Francis
Richard S. Driscoll

Rocky Mountain Forest and Range Experiment Station
Fort Collins, Colorado 80521

Frederick P. Weber

Forest Economics and Marketing Research Staff
Washington, D.C. 20250

Final Report

December 1, 1975

Registration Number 418

Contract Number T-4106B

NASA Technical Monitor: Clayton D. Forbes, NASA, Johnson Space Center, Experimental Development and Integration Branch, Mail Code TF6, Houston, Texas 77058

Forest Service

U.S. Department of Agriculture

ABSTRACT

Four widely separated sites--near Augusta, Georgia; Lead, South Dakota; Manitou, Colorado; and Redding, California--were selected as typical sites for forest inventory, forest stress, rangeland inventory, and atmospheric and solar measurements, respectively. Skylab photographic data were examined monocularly or stereoscopically by photo interpreters using a variety of magnifying interpretation devices. Land use, forest types, physiographic sites, plant communities, and other natural resource cover types, as well as forest stress, were interpreted and mapped. Microdensitometric techniques and computer-assisted data analysis and sampling procedures were developed and tested against ground truth.

Results indicated that Skylab S190B color photography is good for classification of Level I forest and nonforest land (90 to 95 percent correct) and could be used as a data base for sampling by small- and medium-scale photography using regression techniques. The accuracy of Level II forest and nonforest classes, however, varied from fair to poor. Pine and hardwood could be separated as classes 70 to 95 percent of the time. Agricultural classes--cropland, idle land, and abandoned land--as well as grassland, could not be separated on November Skylab imagery. Water was classified in most instances as bare soil (sedimentation) and grassland. Similar classification problems were encountered using both photo interpretation and computer-assisted procedures with S190B color film and the results were also much alike. The use of color infrared photographs would improve classification considerably.

Random and systematic sampling designs were tested for measuring forest area proportions using a digitized ground truth map for one county.

The variance in forest area proportion was always less using systematic sampling. Systematic sampling, using digitized Skylab S190B optical densities and linear discriminant functions for postsampling stratification, reduced variance in forest area proportions at the lower sampling rates--at sampling fractions above 0.0004, the advantage decreased rapidly.

Results of plant community classification tests indicate that both visual and microdensitometric techniques can separate Deciduous, Coniferous, and Grassland classes to the Region level in the ECOCLASS[1] hierarchical classification system. The classification accuracy was over 90 percent by visual techniques on both Skylab and supporting aircraft photography. Deciduous, however, was date, film-type, and scale dependent. Using microdensitometry on Skylab photographs, an accuracy of over 80 percent was achieved--Deciduous was film-type dependent.

There was no consistency in classifying tree categories at the Series level by visual photo interpretation. Conifers were classified more often (80 percent) on Skylab photos, whereas Aspen was most accurate on aircraft photos. Under certain conditions, Grassland plant communities were classified at accuracies greater than 80 percent on Skylab photos, but on aircraft photos they were consistently better than 80 percent regardless of conditions. Results of microdensitometric techniques were variable and highly dependent on date, film type, and scale.

---

[1]Pfister, Robert D., and John C. Corliss, task force cochairmen. 1973. ECOCLASS-a method for classifying ecosystems. Report on file at Forestry Sciences Laboratory, Intermountain Forest and Range Experiment Station, Missoula, Montana.

Only the Conifer and Grassland Region classes were successfully mapped on both Skylab and underflight photographs--over 80 percent accuracy. Plant communities mapped at the Series level agreed with ground truth 80 percent of the time, but only if class-complexes were formed. Cultural features could be mapped by visual techniques more successfully on underflight photographs than on Skylab photographs. Computer-assisted mapping of cultural features was unsuccessful.

The relationship between ground measurements and large-scale photo measurements of foliar cover had a correlation coefficient of > 0.75. Some of the relationships, however, were site dependent.

A comprehensive evaluation of Skylab data showed that mountain pine beetle infestations could not be detected on color-combined multiband black-and-white, normal-color, and color infrared photographs from the S190A multiband camera system. All positive identifications were made on S190B terrain mapping camera color photographs. Infestations detected were always over 26 meters (85 feet) in the longest dimension. On one site, only infestations over 50 meters (164 feet) could be detected. Poor detection was blamed on timing of the imagery (June) and low sun angle. Optimum viewing was achieved with a microscopic viewer on a good-quality light table at a scale of 1:75,000. Stereoscopic viewing was preferred over monocular viewing and resulted in fewer commission errors. Infestations could not be detected by computer processing of the five usable channels from the 13-channel multispectral scanner (S192).

Wide-band terrain reflectance measured from a low-flying aircraft was found linearly correlated with radiance measured by Skylab S190A and S190B and LANDSAT-1 (ERTS-1) sensors. The results support the

proposition that the regression coefficients are a measure of the path radiance and a quantity representing the product of total irradiance and beam transmittance at the time of the satellite overflight. These coefficients should be useful to correct for solar and atmospheric effects in extending spectral signatures in computer-aided classification of satellite imagery.

PREFACE

This is the final report of an investigation to evaluate the usefulness of the Skylab Earth Resources Experiment Package (EREP) data in identifying forest, rangeland, nonforest, water, and forest stress as a first level of resource information. The experiments reported here were performed under a Memorandum of Understanding (Contract No. T-4106B) between the National Aeronautics and Space Administration/Johnson Space Center (NASA/JSC) and the United States Department of Agriculture (USDA). The research was conducted by the combined professional staff members of the Remote Sensing Work Unit, Pacific Southwest Forest and Range Experiment Station (PSW), Berkeley, California, and the Remote Sensing Work Unit, Rocky Mountain Forest and Range Experiment Station (RM), Fort Collins, Colorado. Robert C. Heller was originally identified as Principal Investigator and Robert C. Aldrich, Richard S. Driscoll, and Frederick P. Weber were identified as coinvestigators. Robert C. Aldrich was made Principal Investigator upon the retirement of Mr. Heller in August 1974. Technical Monitors for NASA were Ryborn R. Kirby and Clayton D. Forbes.

The original research proposal was submitted to NASA on April 26, 1971, and entitled "Inventory of Forest and Rangeland Resources, Including Forest Stress." Portions of the proposal and the Statement of Work (SOW) were amended effective August 28, 1974. Amendments were necessary because some Skylab data were lacking and, in some instances, the data were either too poor in quality to analyze or did not meet the requirements set out in the proposal.

The contract began on March 7, 1973, and was to be completed in a period of 14 months. An extension to 30 months was obtained due to

operational problems that delayed receipt of Skylab data for all test sites until September 1974. The last data were received on March 24, 1975.

All Skylab data required to complete the amended contract were furnished by NASA/JSC. The Earth Resources Aircraft Program (ERAP) Office at NASA/JSC furnished high-altitude color infrared (CIR) transparencies and/or aircraft multispectral scanner data for all test sites.

During the period covered by this report, research was under the administrative direction of Benjamin Spada, Assistant Director, PSW, and Harold A. Paulsen, Jr., and William A. Laycock, Assistant Directors, RM. The authors gratefully acknowledge Professor Robert C. Heller, College of Forestry, Wildlife, and Range Sciences, University of Idaho, who, prior to his Forest Service retirement in August 1974, coordinated the original proposal and gave valuable technical direction to this research. As might be expected in a program of long duration, many professional and nonprofessional staff members, not included among the authors, have contributed to the effort involved in these experiments. Richard J. Myhre, Scientific Photographer, PSW, was responsible for all photographic work required by the investigators and for all reproductions used in the Forest Inventory and Solar and Atmospheric Measurement sections of this report. Marilyn Wilkes and Bruce McArthur, PSW, did a large part of the computer programming required for data analysis and computer-assisted classification. Emanuel E. Moellman, Machinist, PSW, made special equipment mountings and fabricated special devices required by the investigators. Anne L. Weber, Work Unit Clerk, PSW, assisted in editorial review, typing, and administrative tasks. Tomiko Hiromoto, Clerk-Typist, PSW, Diane M. Christensen, Work Unit Clerk, RM, Jacie Sneed, Work Unit Clerk, RM, and Dixie L. Kinderknecht, Work Unit Clerk, RM, performed typing and general administrative functions.

A large number of temporary, summer, part-time, and Work Study employees assigned to the PSW and RM Work Units during the contract period also made contributions to the studies:

Joseph Afong, PSW

Greg R. Johnson, RM

Mike Keyes, PSW

Roy A. Mead, RM

Dorothea Pigman, PSW

David L. Shanks, RM

Phillip Shaw, RM

Emanuel Suhl, PSW

Julian Suso, PSW

Peter E. Wikoff, RM

The S192 data analysis reported in the Forest Stress section was completed by subcontract with the University of Kansas Space Technology Center. The analysis was performed by Dr. Robert Haralick of the Remote Sensing Laboratory, assisted by Mr. Gary Minden, a graduate student in the Department of Electrical Engineering.

Intentionally left blank.

TABLE OF CONTENTS

GLOSSARY

Alpha (α): (Also see Beta) The conditional probability of the X_1 and X_2 values, given a fixed classification category (C).

Band: One of the wavelength bands of the electromagnetic spectrum sensed by a multispectral scanner (MSS) or passed by a band-pass filter and recorded on photographic film.

Band Pair: Any two defined wavelength bands of the electromagnetic spectrum used in signature analysis.

Band-pass: Used to describe optical filters that allow only defined portions of the electromagnetic spectrum to pass to the sensor surface.

Beta (β): (Also see Alpha) The conditional probability such that with X_1 and X_2 values fixed, the value for the classification category (C) is allowed to vary.

Bias: The difference between the expected value of a statistic over all possible samples and the true population value of that statistic.

Color composite: A false-color reconstruction of multiband photographs created from two or more filtered photographic bands. The four filtered bands on Skylab (S190A) were 0.5-0.6 μm (station 6), 0.6-0.7 μm (station 5), 0.7-0.8 μm (station 1), and 0.8-0.9 μm (station 2).

Computer-compatible tape (CCT): A reconstruction of Skylab MSS data or digitized photographic optical densities in magnetic tape form suitable for computer analysis.

Confusion matrix: A tabular presentation of classification data showing the proportion of actual types that were classified as each of the predicted types.

Contingency table: A table in which contingency is the difference in the table cells between actual frequency and expected frequency, assuming that the two characteristics are independent from a probability standpoint.

Convolution window: A two-dimensional (X, Y) mathematical smoothing process applied to a digital data array to improve classification. In the simplest form, data for adjoining pixels are added together to improve classification. This process usually results in poorer resolution.

Data element: A single picture element of digital image density recorded on computer-compatible tape by a microdensitometer. The size of the element varies with the microdensitometer aperture.

EAI: Electronics Associates Incorporated. Data plotter Model 430 used to plot land-use maps in color from CCT's of microdensitometer data analysis.

IDECS: Acronym for image descrimination enhancement combination system (University of Kansas).

Irradiance: The amount of light measured on a surface. In physics, the radiant flux density on a given surface. Usually expressed in watts per square meter.

Multispectral scanner (MSS): For Skylab, an electronic optical line scanning device (S192) that collects reflected and emitted radiation in 13 spectral intervals (bands) of the visible, near-IR, and thermal-IR regions of the electromagnetic spectrum. The S192 has a conical line scan which meant line scan data had to be straightened for computer analysis.

Pixel (also called digital element): A single picture element of digital image data recorded on Skylab MSS and microdensitometer computer-compatible tapes. A single pixel of MSS data covers approximately 79

meters square (260 feet square). A pixel of microdensitometer data used in this experiment covers approximately 0.08 hectare (one-fifth of an acre).

Postsampling stratification (PSS): Stratified sampling in which the strata assignments are unknown or are not used at the time of sample selection.

Prior: In statistics, a probability determined before further observation trials are made or a probability based on a prior trial and related to further trial experiments. In digital data analysis, a probability based on ground observations and used as a weighting factor to improve classification.

Radiance: The brightness of an object as seen from a remote observation point. In physics, it is a measure of the power radiating from a unit area of a source through a unit solid angle. Typical units of radiance are watts/meter^2-steradian.

Reserved decision: An assignment made by the decision rule when no category has high enough likelihood of being correct. The cell is left blank or unclassified.

Resolution cell: (See pixel).

Sampling fraction: Proportion of units sampled to the total number of units in the population.

Set intersection rule: The intersection of two sets of categories with elements common to both.

Spatial region growing process: Unassigned resolution cells are assigned to a category label of a resolution cell closest to it.

Threshold: A beginning value selected from a data array to define a signature for classification. The threshold value can be changed by trial and observation to improve classification.

UTM: Universal Transverse Mercator map projection.

ZTS (Zoom Transfer Scope): An optical instrument for transferring data from a small-scale photograph to a larger scale photograph or map. The scale change range is from 1X to 13X. Manufactured by Bausch and Lomb Optical Company.

SUMMARY

A 30-month-long investigation of Skylab photographic and multispectral scanner data products was made to test potential applications for forest and range surveys. Four separate studies were conducted to test classification of land use and forest and range vegetation, detection of stress on forest vegetation, and measurement of solar and atmospheric effects in satellite imagery. Sites selected for these studies were near Augusta, Georgia; Manitou, Colorado; the Black Hills of South Dakota; and Redding, California. The Manitou and Black Hills sites were used in previous remote sensing studies of aircraft photography and LANDSAT-1 (ERTS-1) multispectral scanner data.

Skylab data were supplied by NASA as photographic transparencies or computer-compatible tapes for analysis by photo interpretative and computer-assisted techniques. Photographic products included duplicates of S190B terrain mapping camera exposures on color or color infrared (CIR) films. Also included were color and CIR duplicate transparencies and four black-and-white (B&W) duplicate transparencies from the S190A multispectral camera. The four B&W bands representing four spectral regions of the visible spectrum were combined into false-color composites. Computer-compatible tapes included unstraightened conical scan data recorded from the 13-channel multispectral scanner (S192). Different instruments and methods were used at each site to satisfy separate experimental requirements and peculiar problems encountered. The approaches to the experimental objectives also varied considerably at each site.

Generally speaking, the Skylab photographic data were found useful at two resource-oriented sites for broad classification. Land-use classes,

such as forest and nonforest, and range vegetation classes at the Region level (Deciduous, Coniferous, and Grassland) were distinguished with acceptable accuracy when checked against ground truth. Maps produced from digitized optical film densities, measured on color film, were acceptable for forest classes but unacceptable for nonforest. Regardless of interpretation technique, Level II nonforest classes could not be accurately identified on color film, and plant communities at the Series level could not be classified with consistency on any film/season combination.

Forest stress, in the form of mountain pine beetle-killed ponderosa pine, was detected only on Skylab's terrain mapping camera photography. However, no individual trees and only infestations over 26 meters (85 feet) in the longest dimension could be detected. Mountain pine beetle infestations could not be detected by analysis of S192 multispectral scanner data. Both photographic data and multispectral data were acquired in June--a period of low insect activity and a period when little discolored foliage remains on the trees killed by the previous year's bark beetle population. Had data been available for September, a period of high insect activity and increasing dead-tree discoloration, results might have been more encouraging.

Additional Conclusions:

1. Systematic or random-sampling designs can be overlaid upon digitized photographic data by computer and classified into broad forest-nonforest classes for estimating area proportions. Acceptable results will depend on improving both the classification system and the classification procedure.

2. Enlargements of Skylab terrain camera photographs (1:125,000) can be used with conventional photo interpretation techniques to estimate proportions of broad land cover classes within large political or administrative boundaries in two-stage sampling designs.

3. Skylab and high-altitude aerial photographs can be used to map areal extent of Conifer and Grassland classes with greater than 90 percent accuracy.

4. Paved and gravel roads, utility corridors constructed within the past 10 years, large mining excavations, and clusters of buildings can be mapped on enlarged Skylab photographs.

5. Radiance from Skylab S190B and LANDSAT sensors were linearly correlated with wide-band terrain reflectance. Coefficients of the regression will be useful as linear conversion coefficients for extending spectral signatures in computer-aided classification using satellite imagery.

Summaries of the individual studies composing this report follow. If Skylab-quality data should become available on a recurring basis, further investigation is needed to support, clarify, and extend these results.

Forest Inventory - Three independent studies were made of the potential application of Skylab photographic data in (1) forest resource evaluation, (2) sampling designs for computer application, and (3) automated land classification and mapping. Multispectral scanner data were not analyzed due to time constraints caused by a required late change in the test site location.

Sixteen land-use and forest classes, at three levels, were originally defined for both human and computer-assisted classification. Two types of photographic data were used in the tests--multiband false-color

composites of S190A data for September 12, 1973, and S190B color for November 30, 1973. These photographs were enlarged to a scale of 1:125,000, 1:250,000, and 1:500,000 for interpretation. Ground truth for forest resource evaluation was provided by a 1971 forest survey. High-altitude CIR photographs (1:120,000) and ground checks were used to map one county into two forest and two nonforest classes for a sampling design study. To evaluate computer-assisted classification, two study blocks were mapped into 31 Level III and Level IV land-use classes on high-altitude CIR photographs and corrected using ground observations.

In one forest resource evaluation, land-use proportions were estimated for a four-county area. The estimate of forest area was within 2 percent of the 1971 Forest Survey figure for the four counties. By individual counties, the estimates were within 2 percent for three of the four counties. With the exception of pasture and idle land, the four-county estimates were all close to ±1 percent of the 1971 Forest Survey estimates. A quasi-operational application test using regression techniques in one county estimated forest area 3 percent above the Forest Survey estimate. The sampling error was ±3.53 percent.

Using computer-simulation techniques, sampling designs were tested with a digitized ground truth map and digitized Skylab photographic data for one county. The variance in forest area using systematic sampling was always smaller than when using simple random sampling. When a digitized type-map classified from Skylab S190B microdensitometer data was used in a postsampling stratification strategy, the variance of the forest area estimate was smaller than that for systematic sampling alone--but only when the sample intensity was low.

Computer-assisted analysis of microdensitometer scans made on Skylab S190B color photographs separated forest land from nonforest land with an accuracy of approximately 95 percent. Pine and hardwoods could be separated with an accuracy of approximately 70 percent.

Forest inventory studies in the Augusta, Georgia, site showed that Skylab S190B photographs provide a good base for Level I forest classification. Conventional photo interpretation will provide acceptable area estimates for some nonforest classes; however, idle land, pasture, and water were difficult to separate on normal-color film.

Range Inventory - Classification of range plant communities was based on the ECOCLASS system. Identification at two levels--three Region and eight Series classes--was attempted. Skylab photographs from the S190A multiband camera and the S190B terrain mapping camera (June and August 1973), high-altitude aircraft photographs (June and August 1973), and Forest Service-acquired large-scale photography were used in the tests. Both visual and microdensitometer techniques were tested.

Training and test sample cells were selected for interpretation tests on a restricted random basis. To be selected, a specific plant community had to occupy an area at least 500 meters square (1,635 feet square). A 10-percent sample was picked at random from each plant community class for field validation. Overlays of sample cell locations and plant community keys were used to aid interpretation. Procedures were also developed to map cultural features from Skylab photographs. In a separate study, foliar cover estimates made on large-scale color photographs were compared with measurements made on ground transects.

Photo interpreters classified Grassland and Conifer Region classes with a mean accuracy of 98 percent or greater on both Skylab and support aircraft photography regardless of date or film type. The Deciduous (Aspen) class was identified with 80 percent or greater accuracy on the August CIR aircraft photographs, but the accuracy on Skylab photographs was not acceptable. Tree Series classification was inconsistent. Aspen was classified with 80 percent accuracy on August CIR aircraft photographs, but the accuracy on Skylab photographs was unacceptable. The coniferous Series class accuracies were date, film-type, and scale dependent. For instance, the Douglas-fir class was accurately classified on June CIR Skylab photographs but not on aircraft photographs. Lodgepole Pine and Ponderosa Pine classes were interpreted accurately on Skylab color photographs for June but not on aircraft photographs. June color and CIR medium-scale aircraft photographs were best for interpreting the Spruce/Fir class. The greater accuracies at smaller scales were probably due to the mixing of tree species into homogeneous units with a dominant species signature and a lower resolution. Within the grassland Series, Shortgrass had a classification accuracy of 95 percent or greater on both Skylab and aircraft photographs regardless of date or film type. Wet Meadow had a classification accuracy greater than 90 percent on both June and August aircraft photographs regardless of film type or scale. Classification of Wet Meadow was also acceptable on both color and CIR Skylab photographs taken in August. Mountain Bunchgrass was not accurately classified on Skylab photographs, but on the August aircraft photographs the classification was acceptable regardless of film type or scale. Topographic slope and aspect, mountain shadows, ecotones, season, and class-mixing affected classification of plant communities.

Microdensitometer point-sampling of Region level Conifer, Deciduous (Aspen), and Grassland classes showed significant differences in mean optical densities at the 95 percent probability level. However, the Deciduous class could be separated from the other classes with significant differences only on color film. Ponderosa Pine was the only coniferous Series class that showed a significant difference in mean optical density with the other three conifers, regardless of date or film type. Spruce/Fir and Lodgepole Pine were not separable at any date or on any scale or film type. The mean optical density for Aspen was significantly different from the Conifer classes, but the differences were dependent upon date, scale, and film type. Douglas-fir was separable from the other three conifers on both the June CIR and August color S190A Skylab photographs. Grassland classifications at the Series level varied in acceptability. However, Shortgrass, Mountain Bunchgrass, and Wet Meadow did have mean optical density differences which were significant on August S190A color photographs. Optical density was more dependent on community mixing than the growth stage of the plants at the time (season).

Both Skylab and aircraft photographs were useful to map the areal extent of Conifer and Grassland. These two classes were usually mapped with greater than 90 percent accuracy. The Deciduous class could not be mapped with acceptable accuracy at either the Region or the Series level. Series level conifer and grassland could be mapped with acceptable accuracy only if class-complexes were formed. Class-complexes were Ponderosa Pine/Douglas-fir, Lodgepole Pine/Spruce/Fir, Shortgrass/Mountain Bunchgrass, and Wet Meadow.

Paved and gravel roads, utility corridors constructed within the last 10 years, larger mining excavations, and clusters of buildings could

be mapped on Skylab photograph enlargements. On the other hand, 1:100,000 scale aircraft photographs were needed to map dirt roads, minor earth excavations, utility corridors older than 10 years, and individual buildings. Foliar cover and plant litter measured on large-scale CIR photographs of non-diverse grasslands were related to ground measurements with a correlation coefficient of 0.75. This is considered acceptable for range surveys. The relationship for foliar cover of shrubs was acceptable only on diverse grasslands.

Forest Stress Detection - An evaluation of Skylab data in the Black Hills showed that mountain pine beetle infestations in ponderosa pine could not be identified on any S190A multiband camera system photographic product. All positive identification of bark beetle infestations were made on color photographs taken by the S190B terrain mapping camera. To be detected, infestations had to exceed 26 meters (85 feet) in the longest dimension. On one site, only infestations over 50 meters (164 feet) in size could be detected. Infestations over 100 meters (328 feet) in the longest dimension were located with 100 percent accuracy. The optimum viewing scale with a stereomicroscope was about 1:75,000. Best results were obtained when viewing on a high-quality, variable high-intensity light table; however, stereoscopic viewing was preferred and usually resulted in fewer commission errors than monocular viewing. Interpretation on a rear-projection viewer with high magnification was judged to be inferior to microscopic viewing on a light table.

The June Skylab imagery used in this analysis was considered poorly timed for stress detection. All dead ponderosa pine in the site were killed during the previous year and had lost most of their discolored

foliage before the Skylab pass. Since the distinct red-orange color of dead tree foliage is used for recognition, many infestations were missed. Also, the early morning low-sun angle, at the time of the Skylab missions, made interpretation difficult in the steep terrain of the Black Hills because west- and north-facing slopes were in shadow.

Ponderosa pine trees killed by the mountain pine beetle were not detected by computer processing of 13-channel multispectral scanner (MSS) data (S192). Only five bands of the MSS were usable and misregistration of the data seriously detracted from the analysis results. Attempts to correct the registration improved classification somewhat in several instances, but beetle-killed trees were not identified. The MSS data were collected on a June 9, 1973, pass and not during early September--the period of peak spectral response of beetle-killed trees.

The analysis for stress detection in this report was a compromise due to the lack of Skylab data during the time of year of maximum insect activity and maximum spectral response of stressed trees. Late August through mid-September is considered the best period for detecting mountain pine beetle-caused stress. A Skylab earth resources pass was requested and scheduled during that period (September 18, 1973) and correlative data needed in the analysis were collected by ground-based instruments on that date. However, the Skylab earth resources sensors were turned off unexpectedly during the pass without explanation. Thus, the results of the analysis in this report cannot be considered conclusive and further investigation is required to determine if forest stress can be detected on Skylab-quality remote sensing data.

Measurement of Forest Terrain Reflectance - Terrain radiance and solar irradiance data gathered on or near the Earth's surface could contribute to the interpretation and full utilization of calibrated satellite data. One contribution is the estimation of temporal and locational variations in solar and atmospheric effects on satellite imagery for earth resource investigations.

This report describes efforts to make airborne radiance and irradiance measurements and use them to compute terrain reflectance values. These values (when correlated with satellite radiance of the same terrain elements) yield a first-order measure of solar and atmospheric properties at the time of a satellite overpass. Treating satellite radiance as the dependent variable, the correlation procedure produces an additive coefficient which is the path radiance and a multiplicative coefficient representing the product of total irradiance and beam transmittance.

The airborne system for reflectance measurements consisted of an upward-pointing irradiance meter, a downward-pointing radiometer, a silicon vidicon camera (for support imagery) and associated data-recording instruments. Spectral matching to the bandwidths of Skylab S190A and LANDSAT-1 MSS sensors was achieved for all three airborne sensors.

The S190A photographs were scanned by a digital microdensitometer. Programs were written to convert microdensity values to diffuse density and subsequently to effective film exposure. Finally, a camera radiance equation was used to compute the satellite radiance from film exposure values. The utilization of film samples, and the sensitometric package (provided by NASA) necessary for these conversions, is fully outlined.

The analysis of one set of Skylab photographs and one set of LANDSAT-1

images resulted in a high linear correlation between satellite radiance and reflectance. The derived path radiance values are in agreement with other published values.

The reflectance measurement technique presents two possible advantages over other empirical methods. One is that the results are derived in terms of the satellite scale of units without concern for the calibration accuracy of ground-based or airborne radiometers. The other is that, during stable periods in terrain reflectance properties, the reflectance measurements need not be made on the same day as the satellite overpass.

Intentionally left blank

INTRODUCTION

High-resolution sensors operating on board manned space laboratories may play an important part in forest and rangeland surveys in the future. Although conventional aerial photographs have been an aid in resource surveys for several decades, the role of the more sophisticated remote sensors is growing in importance every year. This can be attributed to several factors: (1) costs of acquiring resource data by conventional methods are rapidly increasing, (2) more resource data is required at shorter intervals to measure rapid changes in land use that affect the environment, (3) urban and recreational uses of land are encroaching upon available resources and alternate sources must be planned and provided for, and (4) there is a continuing need for up-to-date resource information for day-to-day land management decisions and program planning. The earth resources sensors on board the NASA Skylab (SL) Spacecraft from May 1973 until February 1974 were capable of providing high-resolution resource data. Unlike LANDSAT satellites, however, Skylab provided only one opportunity to evaluate the sensors and the concept of manned space laboratories for resource surveys.

The Skylab Earth Resources Experiment Package (EREP) was supported by three low earth-orbit missions. These were designated SL-2, SL-3, and SL-4. For each mission a three-man crew was launched in a space vehicle to dock with the Skylab Workshop (SWS) already in orbit: SL-2, launched on May 15, 1973, continued for 28 days; SL-3, launched on July 13, 1973, continued 74 days; and the SL-4 mission, launched on November 14, 1973, continued 84 days. The Skylab experiment was completed on February 8, 1974. During each mission, the Skylab Workshop

was in a circular orbit approximately 235 nautical miles (435 km) above the earth. Earth resources coverage was confined by this orbit to the Earth's surface lying between the Equator and 50 degrees north latitude and between the Equator and 50 degrees south latitude.

Objectives

The original objectives of this investigation as outlined in the NASA contract proposal were these:

1. To test the hypothesis that Skylab data will permit identification of forest, rangeland, nonforest, water resources, and forest stress.

2. To determine the gains to be made in using satellite imagery as a first level of information when coupled with aircraft underflights and ground examinations in a multistage and multiseasonal sampling system for quantification of the forest-related resources.

3. To compare the utility and cost effectiveness of various data and interpretation modes--such as single-channel versus multispectral-channel data and human versus automated interpretation--to separate and identify forest and rangeland resources.

A number of modifications in specific objectives were necessary at each of the four study sites used in the investigation. These changes were necessary due to a number of operational and technical problems that developed during the course of the Skylab experiment. For instance, a lack of Skylab coverage for the Atlanta study site made it necessary to move the forest inventory study to an area north of Augusta, Georgia. This move was made in March 1974 after the Skylab experiment had been completed. This precluded obtaining any supporting aircraft flights or

ground truth at the time of the Skylab passes. Thus, the multiseasonal photographic and the multispectral scanner data evaluations were eliminated from the study. Proper filters for the multispectral camera were omitted during the November 30, 1973, Skylab pass over the Augusta site and prevented our combining these data for analysis. In the Black Hills, a Skylab pass scheduled for September 18, 1973, was cancelled at the last moment. Biophysical data collected on the ground during the pass could not be analyzed. As a result there was no Skylab data or corollary biophysical data in the proper time frame to analyze for stress detection.

Originally the analysis at all sites was to include all data types and all interpretation techniques. Because of insufficient data and time constraints, however, these were modified. Human photo interpretation techniques were used at all sites. Microdensitometric analysis of photographic data was used on the Augusta and Manitou sites, and an analysis of the multispectral scanner data was performed by a subcontractor for the Black Hills site. These modifications made it impossible to make cost comparisons between all methods.

Study Areas

Experiments were conducted in four widely separated locations across the country (fig. 1). We had originally planned to use the same sites as those used in evaluations of aircraft imagery and LANDSAT-1 (ERTS-1) data--Atlanta, Georgia, for forest inventory; the Black Hills in South Dakota for forest stress; and Manitou, Colorado, for range inventory. By retaining these sites, firsthand knowledge of conditions accumulated over a period of years could be used in the analysis, and comparisons

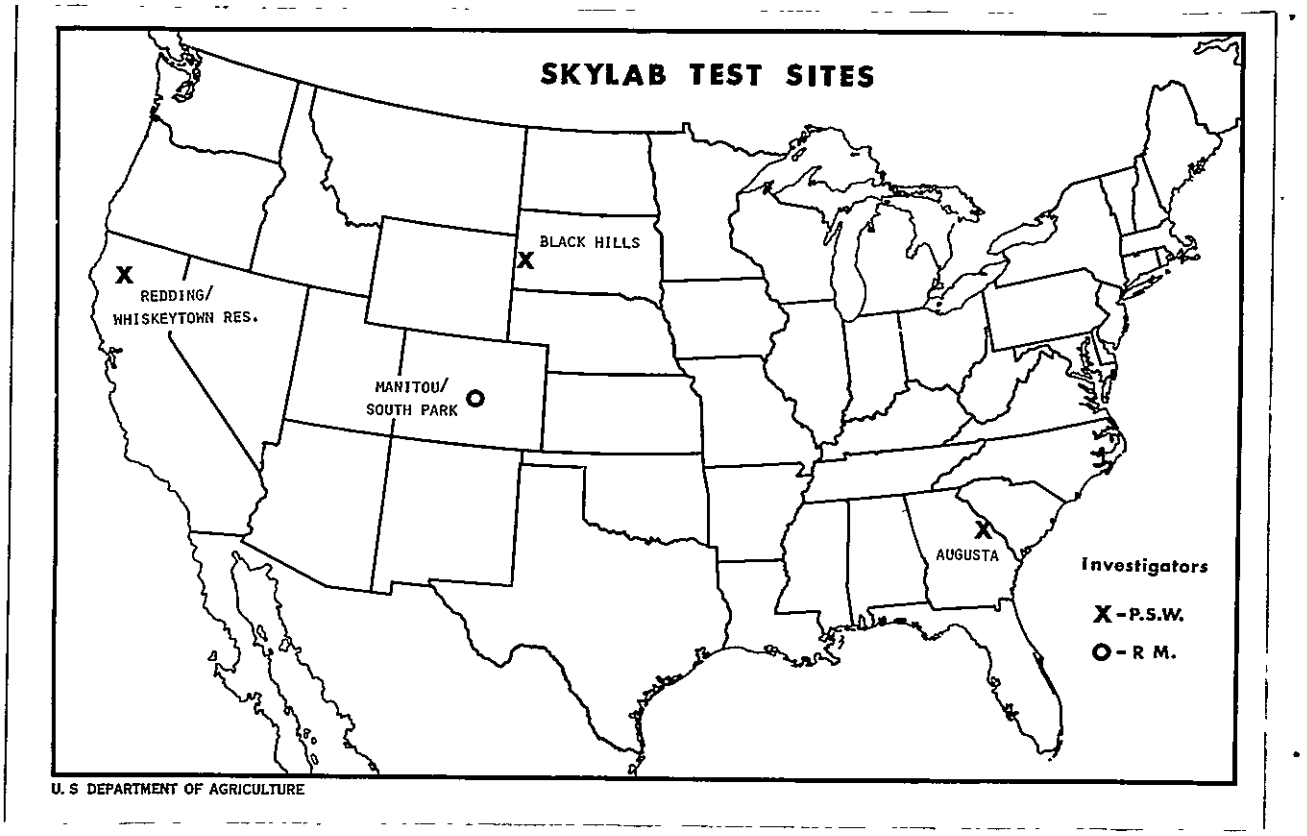

Figure 1.--The study areas indicated on this map were used for different phases of the Skylab data evaluation: Augusta, Georgia - forest inventory; Manitou, Colorado - rangeland inventory; Black Hills, South Dakota - forest stress from mountain pine beetle; Redding, California - solar and atmospheric effects on data evaluation.

could be made between systems. However, due to problems in acquiring data for the Atlanta site, two new sites were selected to carry out studies originally proposed for this area.

Of the original sites, only Atlanta was not covered during the entire Skylab experiment. The study to develop techniques for measuring and correcting for atmospheric interference, originally located at Atlanta, was moved to a new site near Redding, California. The site selection was made early in the SL-4 mission so that both Skylab and aircraft underflights could be scheduled for the same day. The forest inventory study was moved to an area near Augusta, Georgia. As a result, the study was redesigned, new ground truth was collected 1 year following the best SL-4 pass (November 30, 1973), and comparisons between Skylab, aircraft, and ground data were made from this new beginning.

The forest inventory site just north of Augusta, Georgia, is representative of a large portion of the Southeastern United States where a high level of forest management is taking place and rapid changes are occurring. Forests here occupy 75 percent of the land area and are found in large contiguous bodies as well as in small woodlots intermingled with nonforest land. Pulpwood, wildlife, and recreation are three major uses of the forest land in this area. With a major lake, varied forest practices, and many forest and field borderlines, this area is a challenge to the photo interpreter.

Rangelands such as the Manitou, Colorado, site are important national resources and need to be inventoried, protected, and managed. They are becoming more valuable as our food and fiber supplies become more critical. An orderly system of classifying vegetation according

Intentionally left blank.

to its relation to other plants and animals and its potential for vegetative development (ECOCLASS) has been devised by Forest Service ecologists. This hierarchical system was used to determine the level at which Skylab data can accurately assess range vegetation types.

On the third site, in the Black Hills of South Dakota, a severe outbreak of mountain pine beetle (Dendroctonus ponderosae Hopk.) has killed several hundred thousand ponderosa pine trees (Pinus ponderosa Laws.) over the past 10 years. Early detection of the dying pines, which discolor to a yellow and yellow-red hue, would assist forest managers in assessing the severity of the outbreak and in planning control and salvage operations--particularly if the assessment can be done accurately and quickly from either manned or unmanned satellites.

The Whiskeytown Reservoir-Redding, California site was selected as an alternate site for the experiment to measure low-altitude reflectance as an aid for quantitative analysis of Skylab photographs. This site consisted of one east-to-west flight line from the reservoir to the Redding Airport. Land-use and vegetative conditions along this strip were rather limited because of a partial cloud cover. Only mixed oak and digger pine (Pinus sabiniana Dougl.), ponderosa pine, brush species, and water were available for reflectance measurements. The topography ranged from rolling hills to moderately steep foothill slopes and deep

gullies. A light, variable cirrus overcast was present during both the aircraft and Skylab passes.

Data and Techniques

Six EREP sensors were on board the Skylab Workshop. These consisted of a multispectral photographic camera (S190A) with six high-precision matched lenses, an earth terrain camera (S190B), an infrared spectrometer (S191), a 13-channel multispectral scanner (S192), a microwave radiometer/scatterometer and altimeter (S193), and an L-Band radiometer (S194). Only S190A, S190B, and S192 data were evaluated in the studies reported here. We originally intended to use S191 infrared spectrometer data to evaluate the effects of the atmosphere; however, due to a lack of coverage that could be related to ground truth measurements, this part of the experiment was eliminated.

S190A data were provided by NASA/JSC in the form of 2¼" x 2¼" film transparencies. For each EREP pass over a test site, a set of six pictures was received. A set consisted of one color infrared (CIR), one high-resolution color, and four black-and-white transparencies. Of the black-and-white transparencies, two were duplicates of panchromatic film and two were duplicates of infrared sensitive film. Special filters used on the camera lenses separated the visible and reflected infrared spectrum into bands for multispectral analysis. The films and filtered portions of the spectrum are as follows:

Film Type	Filtered Spectral Region
	Wavelength/micrometers
Panatomic-X B&W	0.5 to 0.6
Panatomic-X B&W	0.6 to 0.7
IR Aerographic B&W	0.7 to 0.8
IR Aerographic B&W	0.8 to 0.9
Aerochrome IR Color	0.5 to 0.88
Aerial Color	0.4 to 0.7

For each site covered by an EREP pass, a set of contact duplicate transparencies (5" x 5") was received for all S190B coverage. These transparencies were either normal color or color infrared, depending on the requirements of the greater number of investigators on each pass. This often resulted in obtaining normal color when CIR was preferred.

Computer-compatible tapes (CCT's) with S192 multispectral scanner data were received for only the Black Hills test site. These tapes were used by a subcontractor to classify stressed ponderosa pine under attack by the mountain pine beetle. The tapes, with 13 channels of MSS data, covered six discrete bands in the visible spectrum, six discrete bands in the reflected infrared, and one single thermal infrared band from 10.2 to 12.5 micrometers. The spectral band covered by each MSS channel is shown below:

Band Number	Spectral Coverage (micrometers)
1	0.41 to 0.46
2	0.46 to 0.51
3	0.52 to 0.56
4	0.56 to 0.61
5	0.62 to 0.67
6	0.68 to 0.76
7	0.78 to 0.88
8	0.98 to 1.08
9	1.09 to 1.19
10	1.20 to 1.30
11	1.55 to 1.75
12	2.10 to 2.35
13	10.20 to 12.50

Techniques and instruments used by the investigators to analyze Skylab photographic data varied from one site to the next. In both the forest and the range inventory investigations, a Bausch and Lomb Zoom Transfer Scope (ZTS)[2] was used for mapping and dual image correlations. In the Black Hills investigation, a Bausch and Lomb 240 Zoom Stereo Microscope was used to test a wide range of image magnifications for stress

[2]Trade names and commercial enterprises or products are mentioned solely for necessary information. No endorsement by the U. S. Department of Agriculture is implied.

detection--both stereoscopically and monocularly. The investigator here also used a Variscan rear-projection viewer to interpret images at magnifications up to 29.5 times. On the forest inventory site, conventional photo interpretation was carried out with both an Old Delft Scanning Stereoscope and a lamp magnifier. A Photo Data Systems (PDS) automatic scanning microdensitometer and process computer were also used to scan and record optical density on one S190B color photograph for computer-assisted classification. At the range inventory site a General Aniline and Film Corp. (GAF) microdensitometer was used to relate film density to plant communities. Similarly, a point-sampling technique was used at the Manitou site to classify plant communities by conventional interpretation. Interpretations were verified on ground-truth maps prepared from high-altitude color infrared photography and ground checks. At the Augusta site, existing forest inventory photo samples and ground subsamples provided a basis for land-use and forest-type evaluations. The investigator at the Black Hills site systematically scanned each sub block study site to detect bark beetle-killed trees--the trees were counted, infested spots were mapped, and the Skylab interpretation verified on aerial photography or by aerial observations.

During the studies described here, large quantities of data were gathered over a long period of time. Many of the techniques used were developed and modified in light of required changes in the analysis plan and from experience. In this report, only enough detail has been included to help the reader understand what was done and evaluate the results. The report is intended primarily to aid those who may be using manned earth resources satellite data in forestry applications in the future.

Intentionally left blank.

FOREST INVENTORY

Forest Area Estimates, Sampling Design, and Automated Land Classification

Robert C. Aldrich, Edwin H. Roberts, Wallace J. Greentree, Nancy X. Norick, and Thomas H. Waite

The Skylab studies conducted near Augusta, Georgia, are part of a continuing research program to improve extensive forest inventory techniques. Intensive inventory techniques relate to individual forest stands as small as 2 hectares (5 acres) whereas the research reported here deals with the measurement of resource conditions within broad natural, administrative, and political boundaries using sampling procedures. Additional information about specific locations within the survey boundaries is useful but is not usually required.

Three independent studies were carried out by the investigators to evaluate Skylab photographic data for national forest resource surveys:

1. An evaluation of Skylab S190A and S190B photographic data for classifying forest and related land use. This study includes a quasi-operational one-county forest evaluation.

2. A study to determine an effective method for sampling digitized remote sensing data. This study includes a one-county evaluation of sampling designs and sampling intensity using optical densities from an S190B color photograph.

3. A study of microdensitometer techniques for classifying forest and related land use on Skylab S190B photography. Two 10,000-meter-square (6.22-mile-square) blocks are used as experimental areas to map Level II and Level III land-use classes.

Background

Synoptic vertical photographs taken from space platforms are of considerable interest to forest inventory specialists. In March 1969, foresters found that color infrared photographs taken by Apollo 9 astronauts could be used to stratify forest land into broad classes (Langley and others 1969; Aldrich 1970). This first-level stratification was used in a multistage forest inventory in the Mississippi Valley and it increased sampling efficiency by over 58 percent. Interest in multistage sampling strategies using satellite imagery coupled with aircraft photography and ground observations has increased as a result (Draeger and others 1971; Kuusela and Poso 1972; Hildebrandt 1973; Nichols 1974).

Land-use classification has been the first stage in extensive nationwide forest resource inventories since the early 1940's. This classification is usually done by photo interpreters on available medium-scale panchromatic aerial photographs. Many times these photographs are 5 to 10 years old at the time they are used. Since the primary purpose of land-use classification is to determine an accurate forest area base for expanding forest resource statistics, changes in land use since the photographs were taken can be a serious problem. If the forest area base is not accurate, data from ground subsamples expanded by a forest area expansion factor can be inaccurate. Unless up-to-date photography or other remote sensing imagery is available on a wide area basis, it will be very difficult to adequately measure the changes in the forest area base.

In 1969, a research program was begun by the PSW Remote Sensing Work Unit to study high-altitude aircraft photography and satellite imagery for land use and forest classifications as a first level of information in

resource surveys. These studies were conducted under the Earth Resources Survey Programs sponsored by NASA. A study near Atlanta, Georgia, using 1:400,000 and 1:120,000 CIR aerial photography, showed that forest land could be identified correctly over 96 percent of the time regardless of scale (Heller and others 1973). During this study, techniques for classifying land use by optical film density were investigated with only limited success. Multispectral scanner data from aircraft flights over two 4,049-hectare (10,000-acre) study blocks were also analyzed. Although land-use classifications were reasonably accurate, distortions in the processed data were a limiting factor (Weber and others 1973). In 1973, LANDSAT-1 (ERTS-1) MSS data for the Atlanta test site were studied by both conventional photo interpretation techniques and by computer-assisted classification procedures (Heller and others 1974). Interpreters could correctly classify Level I information (forest, nonforest, water) over 96 percent of the time on false-color photo composites. Computer-assisted classification using four bands of scanner data was 94 to 96 percent correct for the Level I classes. Neither human nor machine classification could separate Level II information with a high degree of accuracy.

From the LANDSAT-1 (ERTS-1) studies it was concluded that, with improved spectral and spatial resolution, satellite imagery could provide the required first-level information required in extensive forest inventory sampling strategies. Skylab data provided an opportunity to investigate and substantiate this conclusion using both human and machine-assisted classification procedures.

Intentionally left blank.

Study Area

The study site near Augusta, Georgia, (fig. 2) lies in the Piedmont physical division and is part of Georgia Forest Survey Unit 4.[3] The area is typical of a large part of the Southern United States with both broad contiguous bodies of forest land and small farm woodlots mingled with nonforest land use. Forest land is 75 percent of the total land area. Major forest types are loblolly pine (Pinus taeda L.) oak-pine, oak-hickory, and oak-gum-cypress. Topography is gently rolling to hilly with many narrow stream valleys. Principal land uses are forest, grassland (pasture), urban, and water. Agriculture is not a major land use though scattered grain and row crops are found throughout the area. The Clarks-Hill Reservoir forms the eastern boundary and is the site of homes, hunting and fishing, and other recreational uses. Major forest disturbances are caused by forest management practices and development of recreation home sites.

Classification Systems

Because of the diversity of techniques used in these studies it was necessary to use a variety of classification systems. Although somewhat

---

[3]The Forest Survey is a branch of the Division of Forest Economics and Marketing Research, U.S. Forest Service, USDA.

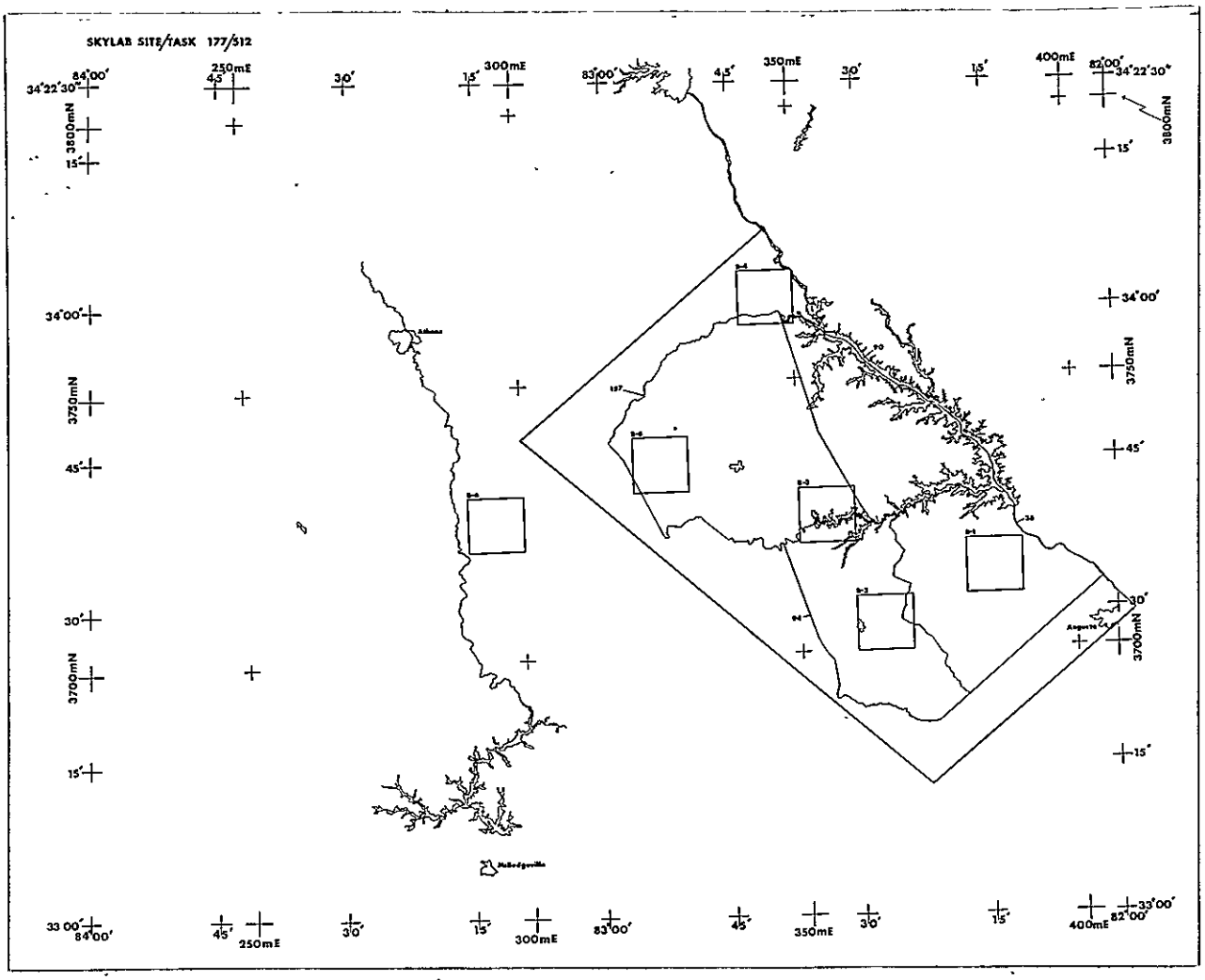

Figure 2.--The Augusta site, used for evaluating Skylab data in forest inventory, includes four counties. Two intensive study sites (2 and 4) were used for computer-assisted mapping with digitized photographic film densities.

different in nomenclature, these systems have the same objective, e.g., to measure the forest area within an error of ±3 percent per million acres (404,858 hectares).

The classification system used in the forest resource evaluation study included 10 individual land-use classes (table 1). Not all of these classes, however, were found within the four-county site. In some portions of the study the five agricultural classes were combined to conform with the system used by the Forest Survey in their first-level stratification on aerial photographs.

The forest sampling design study in McDuffie County used a classification heirarchy of three Level I and two Level II classes. Forest land, nonforest land, and water were mapped at Level I for the purpose of building a base for testing computer sampling designs. Two Level II classes--pine and deciduous forest--were also delineated to see if they could be separated and stratified on Skylab data digitized by microdensitometer.

To test the use of computer classification algorithms developed for LANDSAT-1 (ERTS-1), a classification system of four levels was developed for Skylab (table 2). The land area in two 10,000-meter-square (6.22-mile-square) blocks was mapped to a 0.4-hectare (1-acre) minimum using this system. On five randomly selected 1,000-meter (.62-mile) sub blocks within the test blocks, forest land was classified by three stand-size classes to help explain variations in the Skylab film densities.

Table 1. A land-use hierarchy adapted from the Forest Service Resource Data Standards Handbook[1] and Forest Survey Manual for the Southeast.[2]

Classification	Definition
Forest Land	Areas .4 hectare (1 acre) or larger in size and capable of supporting more than 10 percent cover by forest trees and not developed for nonforest use.
Cropland	Land currently being utilized to produce agricultural crops that are harvested directly and not indirectly as pasture forage consumed by livestock.
Idle Farmland	Former cropland, orchards, improved pasture, and farm sites not tended within the past 2 years and presently less than 10 percent stocked with trees.
Improved Pasture	Land currently improved for grazing by cultivation, seeding, irrigation, or clearing of brush and trees.
Grassland	Land other than improved pasture on which the primary natural cover is grass and forbs.
Other Agriculture	All other farm land not used for crops, idle, or pasture. Includes farmstead, buildings, and service areas.
Marsh and Swampland	Land temporarily or partially covered by water and poorly drained land capable of supporting more than 10 percent cover of swamp vegetation (marsh grasses, cattails, etc.). Does not include spruce bogs, cypress land, or other hydric forest sites.
Urban and Other Areas	Areas within the legal boundaries of cities and towns; suburban areas developed for residential, industrial, or recreational purposes; schoolyards; cemeteries; roads; railroads; airports; beaches; powerlines and other rights-of-way; or other nonforest land not included in any other specific land class.

Census Water	Streams, sloughs, estuaries, and canals more than .2 kilometers (1/8 of a statute mile) in width; and lakes, reservoirs, and ponds more than 16.2 hectares (40 acres) in area.
Noncensus Water	Streams, sloughs, estuaries, and canals less than .2 kilometer (1/8 of a statute mile) in width; and lakes, reservoirs, and ponds less than 16.2 hectares (40 acres) in area. Minimum width of streams, etc., is 9.1 meters (30 feet) and minimum size of lakes, etc., is 9.1 meters (30 feet) in diameter.

[1]Forest Service Handbook, Chapter 1309.13, U.S. Department of Agriculture, Forest Service.

[2]Forest Survey Manual for the Southeast, Parts 1 through 5, 1968, U.S. Department of Agriculture, Forest Service, Southeastern Forest Experiment Station, Asheville, North Carolina. Definition of Terms, Pages D-1 through D-9.

Table 2. A land-use classification hierarchy for remote sensing and ground information sources compatible with current nationwide forest resource evaluation objectives. Color definitions are based on high-altitude color infrared photography and simulated color infrared composites of LANDSAT data.

Classification	Color definitions (based on Munsell 1920-60, ISCC-NBS 1975)
I FOREST LAND	
II Conifer III Pine Pine-Hardwood IV Seedling and Sapling Poles Sawtimber	Density of conifer stands, number of hardwoods mixed in stand, and stand size influence color value and chroma. Dense stands are darker with less chroma. In the fall, before advanced hardwood coloration and leaf fall, conifer stands appear dark purplish red. Separation between Conifer and Hardwood classes is less distinct in fall than in winter or early spring. Where hardwoods and conifers are mixed in stands, hardwood color predominates, and stand is usually classified as Hardwood. In spring before hardwoods are foliated, conifers appear moderate to dark purplish red. Seedlings and saplings on prepared sites appear lighter than poles and mature sawtimber with closed canopies.
II Deciduous Hardwood III Upland Hardwood Bottomland Hardwood IV Seedling and Sapling Poles Sawtimber	Stands appear moderate grayish purplish red in fall and pale purple to moderate purplish red in spring. In fall, upland hardwoods cannot be distinguished from bottomland hardwoods. In spring, before foliation, upland hardwoods appear pale purple to light grayish purplish red. Bottomland hardwoods are generally a moderate purplish red. Stand size class (texture), density of crown canopy, and ground cover influence color value, density, and chroma but to a lesser extent than in conifer stands.
I NONFOREST LAND	
II Grassland III Undisturbed Grass Disturbed Grass Dead Grass (Annual) New Improved Grass	Grassland appears deep pink in both fall and spring; sometimes mistaken for immature cropland in spring.

II Cropland	Mature crops in fall appear bluish gray to grayish blue. In spring, immature crops appear deep pink and may be mistaken for grassland.
III Immature Grain Immature Row Crop Mature Crop Harvested Crop Orchard Farmsteads	
II Bare Soil	In fall and spring bare soil appears cream colored on LANDSAT imagery. There is no distinction between plowed agricultural fields and sites prepared for new commercial developments. Generally in spring most areas of bare soil are newly plowed fields either recently or soon-to-be planted.
III Plowed Fields Erosion Urban (site preparations) Rock Outcrop	
II Wild Vegetation	In fall, areas range from grayish purple of idle land to grayish purplish red of abandoned land to deep pink of Kudzu vine. Marsh and alder swamps are a moderate purple because of wet background. In spring, idle land becomes light grayish red to dark pink because of influx of new infrared-reflectant vegetation. Abandoned-transitional land (reverting to forest), on the other hand, is grayish purplish red and marsh and alder swamps are grayish violet. Deciduous Kudzu vine, purplish gray in the spring, easily separates itself from all other vegetation when fall and spring images are viewed together.
III Idle Land Abandoned Land Transitional Kudzu Marshland Alder Swamp	
II Urban	Areas are light blue in the fall and very pale blue in the spring. Unfortunately, because of low resolution of LANDSAT data, secondary roads, minor roads, and most utility lines are not resolved.
III Transportation Utilities Home Developments Commercial Developments Recreation	
I WATER	
II Water	Water is dark greenish blue in fall and light greenish blue in spring. Farm ponds of less than .4 hectare (1 acre) can be seen on LANDSAT images if there is sufficient contrast with background.
III Clear Lakes & Ponds Turbid Lakes & Ponds Rivers & Streams	

Skylab Data

Restrictions imposed by short missions, seasonal data requirements, and the scientists' lack of control over scheduling reduced the probability of obtaining a clear photographic day for Skylab data collection. For this reason, remotely sensed data were not obtained for the original inventory test site near Atlanta, Georgia. To complete the proposed research, an alternate site was selected after the Skylab experiment had been completed and all data tabulated. This meant that SL-3 and SL-4 data for the new site were already 4 to 6 months old and precluded gathering any time-dependent ground truth.

The Skylab data used in these studies include only S190A and S190B photography (fig. 3). The photography was taken on September 12 (SL-3) and November 30, 1973 (SL-4)(table 3).

The SL-3 S190A multiband photography was combined and enhanced on an I^2S additive color viewer. A color internegative was made of the combined image following the technique described by Myhre for combining LANDSAT-1 (ERTS-1) film chips (Heller and others 1974). From the internegative 1:500,000 and 1:250,000 enlargements were made on color transparency film. These films were used in combination with S190B color transparencies for forest and land-use classification. When used together with an S190B transparency the lower resolution and graininess of the S190A composite caused eye fatigue. The effect was to increase interpretation time. Although the spectral information was helpful in making land-use and forest-type decisions, it is felt that high-resolution CIR film from the S190B terrain camera would have been much more useful. We did not use the S190A CIR or color films in our analysis because, after a careful review of the

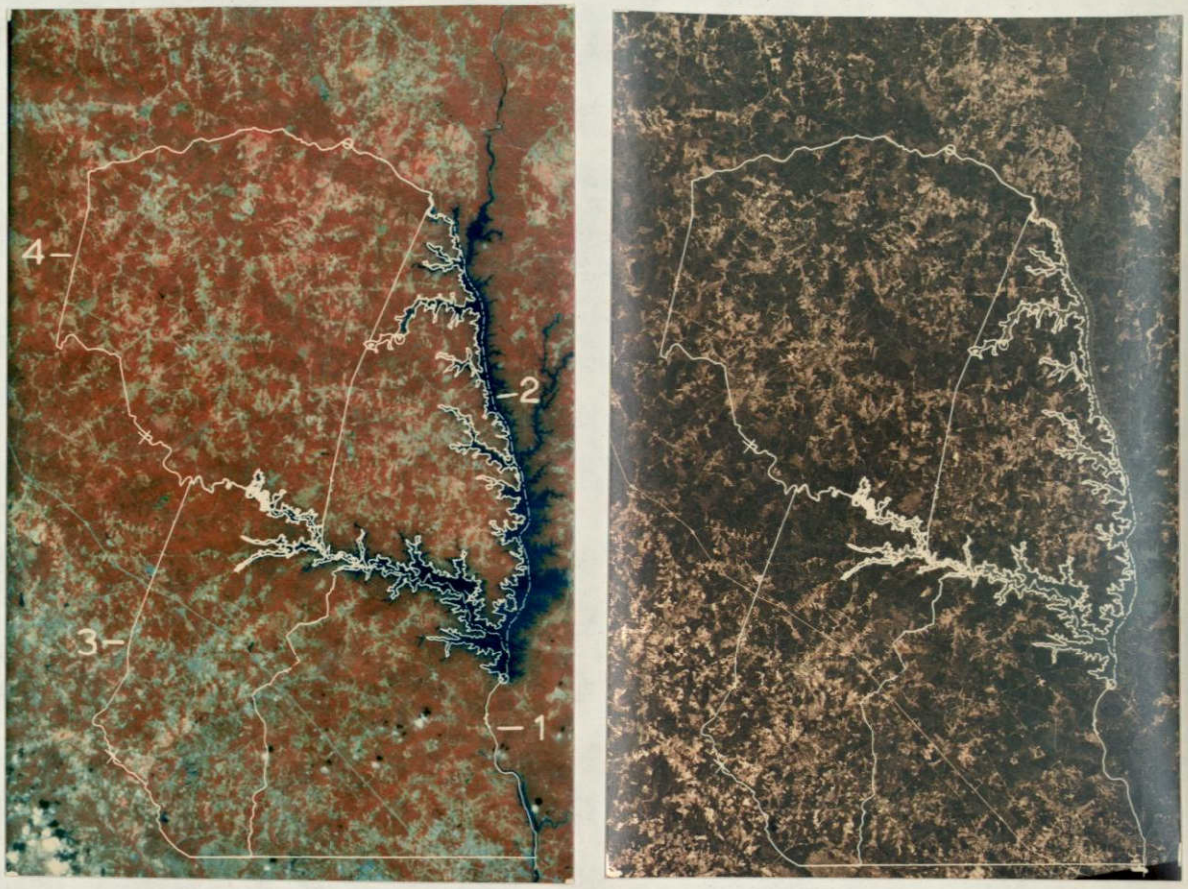

Figure 3. A Skylab S190A multiband composite for September 12, 1973, (left) and a Skylab S190B color photograph for November 30, 1973, (right) were used in the data analysis. The area outlined includes four counties identified in the left-hand photograph: (1) Columbia, (2) Lincoln, (3) McDuffie, and (4) Wilkes. Photographic scale is approximately 1:850,000.

Table 3. Skylab data used in the forest inventory studies; Augusta, Georgia.

Sensor System	Skylab Mission	Pass No.	Track No.	Mag. No.	Frame No.	Film Type[1]	Band Width
S190A	SL-3	36	43	40	111, 112	Pan, SO-022	0.5-0.6 μm
	SL-4	54	19	52	69, 70, 71	Pan, SO-022	0.6-0.7 μm
						IR, 2424	0.7-0.8 μm
						IR, 2424	0.8-0.9 μm
						Color, SO-356	0.4-0.7 μm
						CIR, SO-127	0.5-0.88 μm
S190B	SL-3	36	43	86	284, 285	Color, SO-242	0.4-0.7 μm
	SL-4	54	19	90	46, 47		

[1]Each Skylab mission used the same film types.

materials, we felt that they contained only redundant information and at a lower resolution than the S190B imagery.

The S190A multiband photography for SL-4 (November 30, 1973) could not be used in the analysis because the films had been exposed without filters.[4]

Of the two sets of photographs produced by the S190B terrain camera, only the SL-4 (November 30, 1973) could be effectively used. The SL-3 photographs (September 12, 1973) were low in contrast, there was a general haze condition present, and there was no overlap for stereoscopic viewing. The SL-4 photographs, on the other hand, were taken on a clear day, contained reasonably good contrast between land uses and forest conditions, and had 60 percent overlap for stereoscopic viewing. We found this photography most useful for forest inventory purposes because (1) a single photograph includes 8 to 10 counties, (2) a photograph can be enlarged to 1:125,000 without loss of information, and (3) a scaled map overlay of county boundaries can be used on the photograph without serious photographic distortion problems.

Generally speaking, forest land can be easily separated from nonforest land on S190B color photographs. There are some conflicts, however, with shadows, small bodies of water, streams, and idle land. Where forest land borders on nonforest land, shadows cast by timber stands on west- and northwest-facing edges blend with the forest and can cause misclassification bias in favor of forest land. Small bodies of water within forested areas are

---

[4]SKYLAB PROGRAM, Sensor Performance Report, Volume I (S190A), MSC-05528, National Aeronautics and Space Administration, L. B. Johnson Space Center. September 6, 1974. p. 3-6d.

not easily separated from the surrounding forest--particularly pine forest--because, to the eye, both features have the same density and hue. Although small bodies of water within hardwood stands show more contrast with surrounding features, they too can be misinterpreted as pine. Idle land in many instances appears very similar to abandoned land stocked with hardwood and pine saplings. The difference is very subtle and can cause a bias in favor of forest land.

Pine land is easily separated from the deciduous hardwoods in November. The separation is made by density (tone) and hue to a limited extent. Pine is much darker than the leafless deciduous forest, and the ground cover under the deciduous forest is a gray-green. Because of a limited range in color hues, pasture, cropland, idle land, and wild range are difficult to separate. Graininess of the film gives the impression of texture that interpreters look for in idle, abandoned, or transitional land-use types. Unfortunately, pasture land with this artificial texture appears very much like idle land. This can be a problem in breaking down land use beyond broad classes.

All major roads and secondary roads are clearly visible as are utility corridors. However, woods roads are difficult to see and secondary roads are not resolved where they pass through areas of little contrast--agriculture land, primarily.

Ground Truth

Ground truth for the forest inventory studies came from a number of sources. High-altitude color infrared (CIR) photography, Forest Survey ground sample data, and field checks were used independently, or together, as a basis for evaluating Skylab data interpretation. Because we lacked

ground and aerial photographic support for these studies at the time of the Skylab pass (November 30, 1973), we had to rely very heavily on high-altitude CIR photography taken on April 25, 1974. The quality of these photographs was excellent.

In the forest resource evaluation study we used both Forest Survey ground plot and 16-point cluster classifications made in 1971. These classifications included first- and second-level information for land use and forest stratification. Since the data were 2 years old at the time of this study, subsamples of locations were checked on high-altitude CIR photographs taken within 5 months following the Skylab pass. With only minor differences in agricultural use, the photographs reflected land-use conditions at the time of the Skylab pass and showed where changes had occurred since the ground data were collected.

The ground truth for the forest sampling design study was derived from the April 1974 CIR photography and a ground check in December 1974 that included nearly 20 percent of the county.

Initial ground truth for the automated land classification study was obtained using the April 1974 CIR photography. Photographs were selected from the coverage for two 10,000-meter-square (6.2-mile-square) sample blocks to be used in developing and testing digitized Skylab film densities for land classification. These two blocks were located by random selection from the total number of 10,000-meter UTM intersections within the four-county test site.

Ground truth maps were made for the two sample blocks in the following way:

1. The photo for each sample block was mounted on a Zoom Transfer

Scope and enlarged five times to match a USGS 1:24,000 quadrangle sheet used as control (fig. 4). A 1,000-meter (0.62-mile) grid template (10 x 10 grid) was placed over the outlined block on the control map to facilitate mapping.

2. Four forest and 27 nonforest classes (Level III) were delineated within each 1,000-meter (0.62-mile) grid cell.

3. In five randomly selected 1,000-meter (0.62-mile) cells, forest land was further subdivided into three stand-size classes: (1) seedlings and saplings, (2) poles, and (3) sawtimber. Recognition of the classes was based on a combination of crown closure, crown size, amount of bare soil, and the arrangement of vegetation. These refined delineations were needed to explain discrepancies in automated classification.

In early December 1974, a trip was made to the test site to check map classifications and to observe conditions that could have an effect on land-use interpretation. To aid in this effort, enlargements of the aerial photographs were made on which land use, forest conditions, and other observations were recorded directly in the field. Several photographic examples of local forest management practices that were found to affect image interpretation are shown in Figure 5. Examples of land use on Skylab and high-altitude CIR were used in photo interpretation aids (fig. 6).

Finally, after the ground checks had been completed, the ground truth maps were adjusted and corrected where necessary. The maps were photographed and both prints and film overlays made to the scale of digital maps produced by the computer-assisted classification procedures. The map for block 4 was used to develop training sets for the computer classification algorithm and the map for block 2 was used to test the system once it was developed.

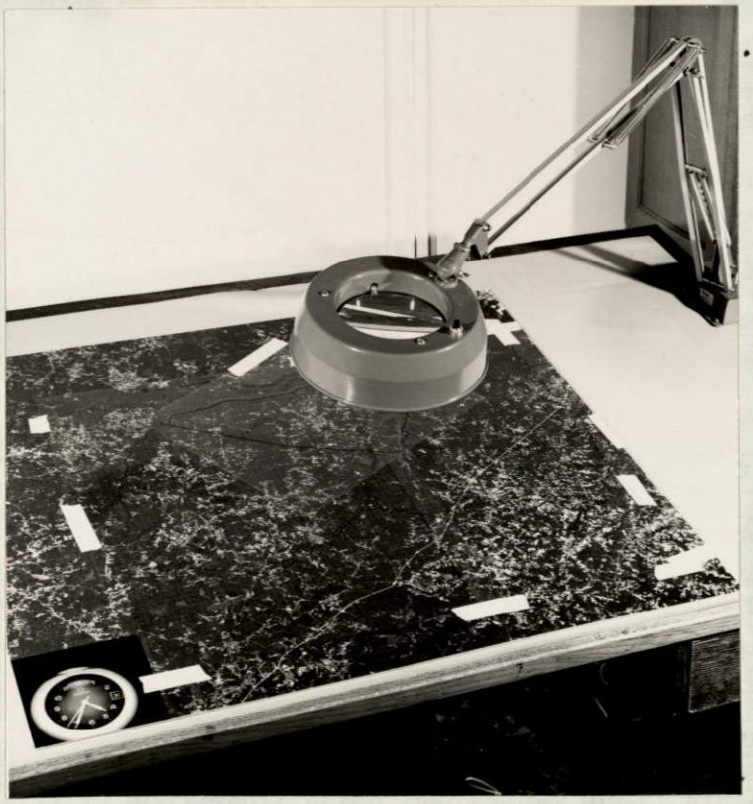

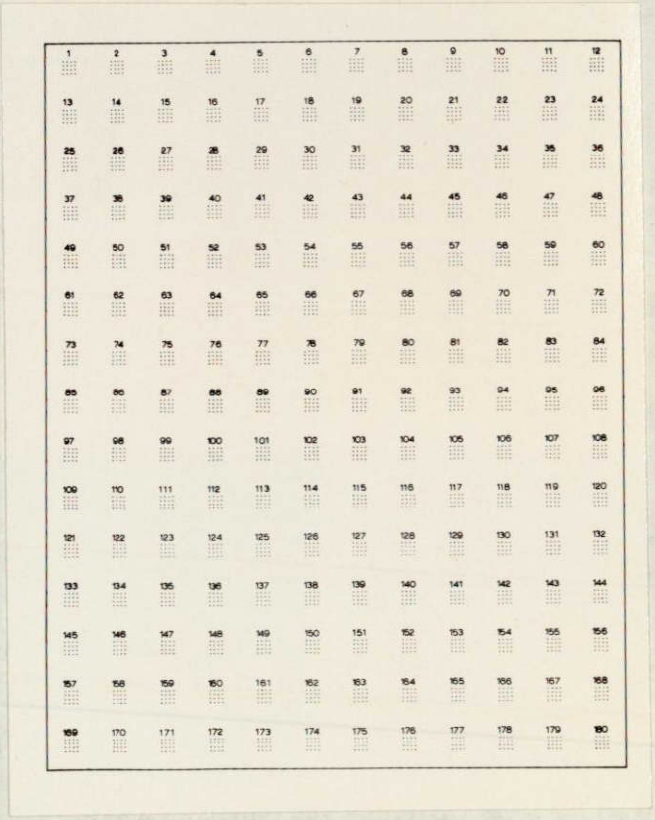

Figure 4.--A Zoom Transfer Scope (top left) was used to interpret and transpose forest and related land-use classes from 1:120,000 CIR photographs to a map control base. This instrument was also used to verify Skylab interpretations on 1:120,000 scale CIR photographs. An Old Delft scanning stereoscope (top right) was used at 4X power to interpret overlapping 1:500,000 scale enlargements of S190B color photographs with stereoscopic effect. A lamp magnifier (bottom left) was used to interpret combined land-use classes on a 16-point cluster grid overlay (bottom right).

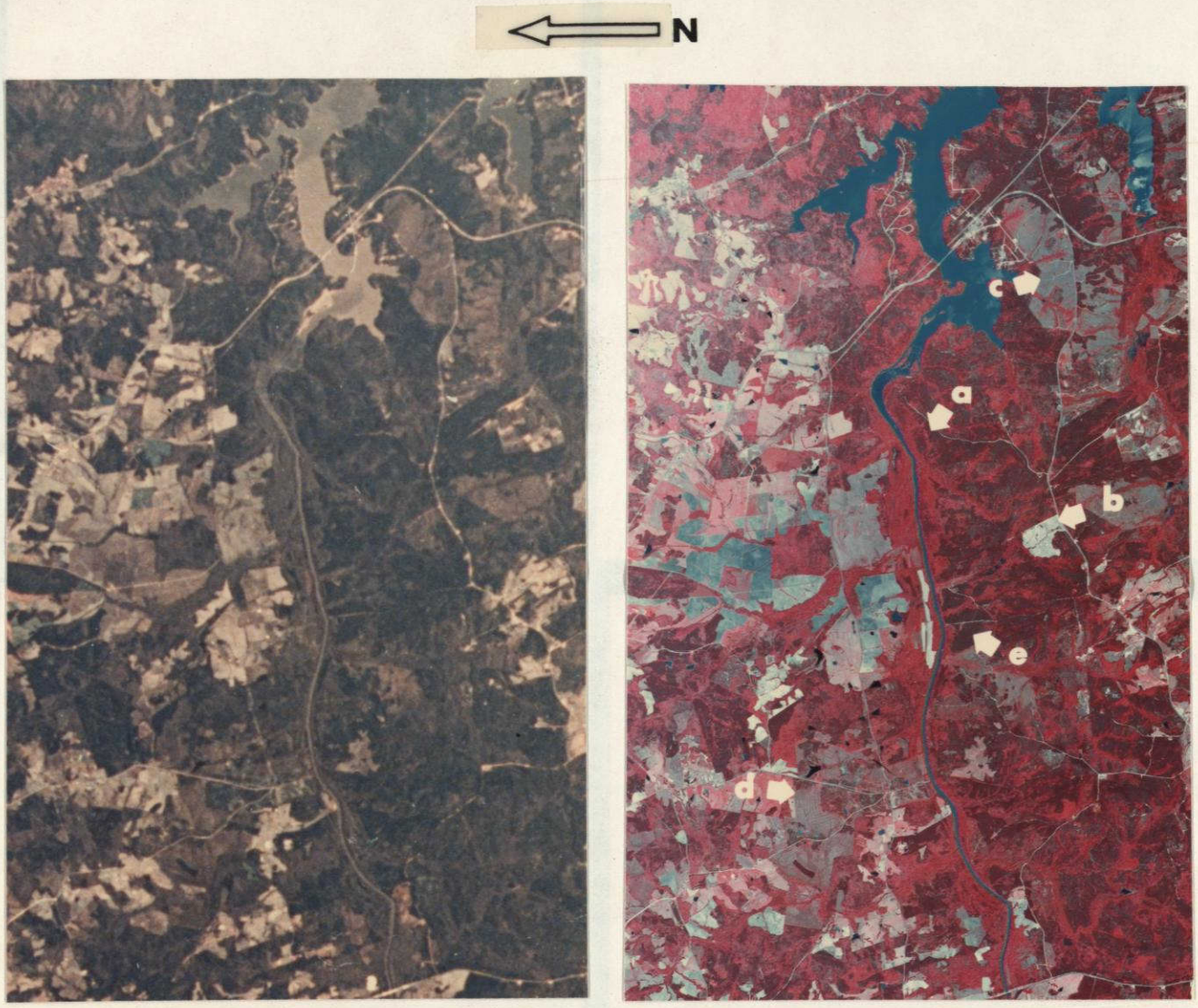

Figure 5.--Forest management and other land-use practices caused variations in image patterns on Skylab photographs. Intensive management of loblolly pine involves pure, even-aged stands. The stand in (a) has an average height of 19.8 meters (65 feet) and a d.b.h. of 22.9 centimeters (9 inches). These stands are the darkest images in the photograph with the exception of water and shadows. The clear-cut area at (b) shows that debris has been windrowed and burned, and the soil harrowed for machine planting. Pioneering weeds and hardwood reproduction have not yet invaded the areas between rows. In (c) the pioneering species have filled in spaces between pine seedlings. Sometimes logging debris is still visible in windrows (d) because sapling-size pines are not large enough to completely cover the ground. Thinning operations before stand maturity remove every other row and appear as in (e).

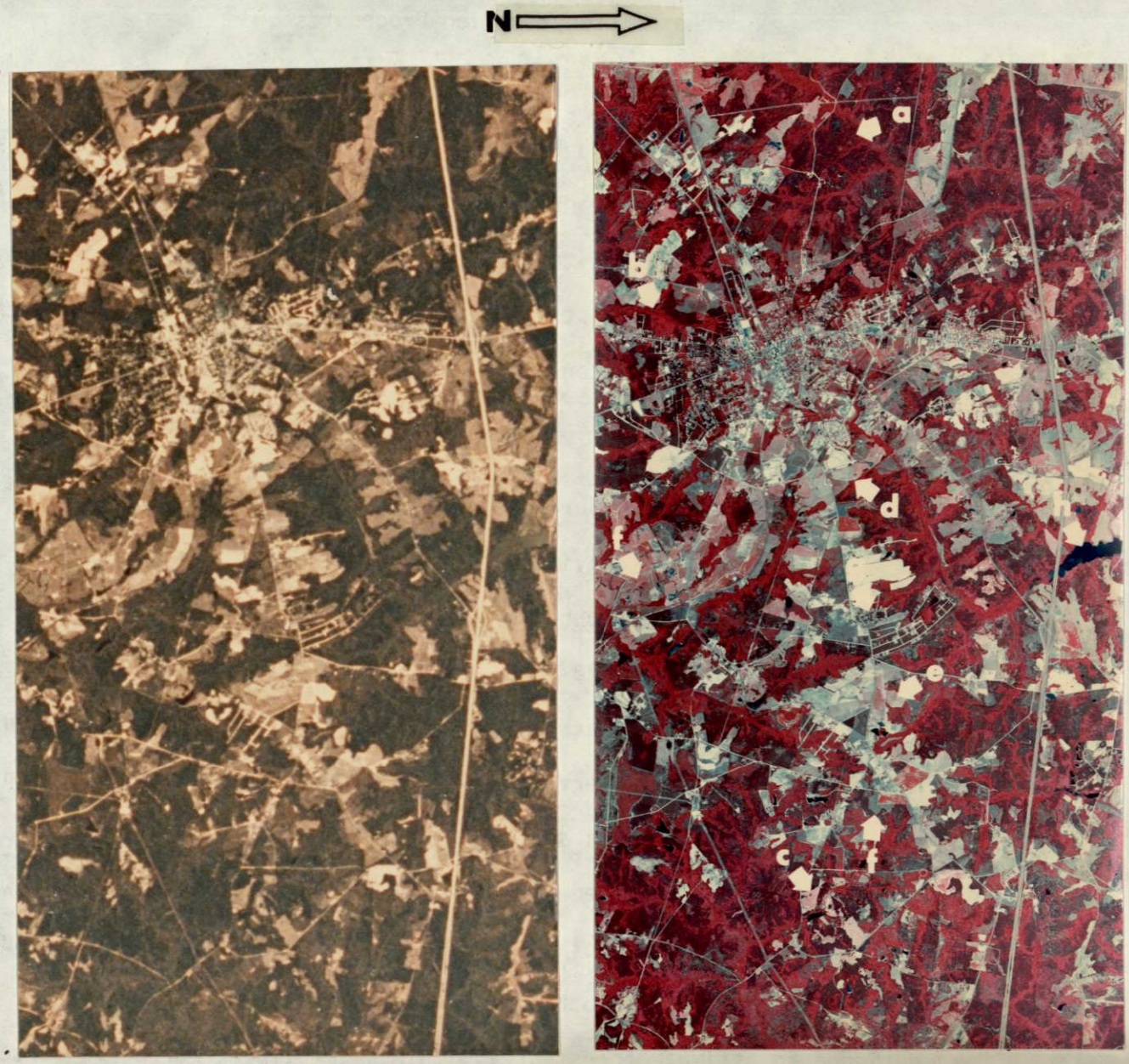

Figure 6.--A Skylab photograph (left) and a 1:120,000 CIR photograph (right) were used in photo interpretation aids to illustrate the forest and related land-use classes: (a) pine forest, (b) hardwood forest, (c) grassland, (d) cropland, (e) bare soil, (f) wild vegetation, (g) urban, and (h) water.

Photo Interpretation Procedures

Procedures used for the forest resource evaluation study and for the sampling design study differed by objectives. The forest resource evaluation study was geared to the current photo procedures used by the Forest Survey in the Southeastern United States.[5] The sampling design study objective was to develop and test computer techniques for sampling digitized remote sensing data recorded on computer-compatible tapes.

Forest Resource Evaluation

The Forest Survey procedure followed in the 1971 inventory of the State of Georgia included solving for regression coefficients for each grouped land-use class in a photo sample. In the procedure, a photo interpreter examined points in a 16-point (4 x 4) cluster design printed on 1:20,000 scale panchromatic aerial photographs purchased from the Agricultural Stabilization and Conservation Service (ASCS)(fig. 7). The design consisted of 25 clusters in a systematic pattern on each photograph. Each point in a cluster represented a circular 0.4-hectare (1-acre) plot and was classified into one of five classes--forest land, urban and other, census water, noncensus water, and other miscellaneous land uses. This sample was designed to estimate forest area within a sampling error of ±3 percent per million acres (404,858 hectares).

After photo interpretation was completed, a subsample of photo clusters was selected for ground examination. Each point in the clusters was

---

[5]Forest Survey Manual for the Southeast, Parts I through V. U. S. Department of Agriculture, Forest Service, Southeastern Forest Experiment Station, Ashville, North Carolina. 1968. Part I, p. 1-6.

Figure 7.--The Forest Survey uses 16-point photo clusters imprinted on ASCS 1:20,000 scale panchromatic photographs to determine land use in each country.

located on the ground with the aid of the photographs and the individual land-use class determined at the time of the inventory (table 1). Since the photographs were taken in 1967, and were 5 years old at the time of the inventory, the subsample provided information that reflected changes that had occurred since the date of photography.

Using the photograph and corresponding ground-cluster classifications, the regression coefficients were computed for each grouped land-use class. The proportion of points in the photo clusters and the corresponding proportion of points in the ground clusters were used as continuous variables in the computation.

To evaluate Skylab photographic imagery as a source of first-level information, we adopted the Forest Survey procedure. All photo subsample clusters located on 1:20,000 ASCS photographs had to be located on Skylab photographs and the points classified by individual land use. This was accomplished using an Old Delft stereoscope, a scaled cluster template, and a photo illuminator (fig. 4).

Three separate evaluations were made. In the first, Lincoln County was used to test three combinations of Skylab photographic data to find the one most suitable for the remaining evaluations. These combinations were:

Combination 1: 1:250,000 enlargement of an S190B color photograph (November 30, 1973) made at PSW and a 1:250,000 enlargement of an S190A false-color combination (September 12, 1973) made at PSW. Interpretation was without stereoscopic effect.

In this evaluation we used all 210 16-point clusters in the four-county area. Interpretation procedures were identical to those described above. Classifications made on ASCS photography, on Skylab imagery, and on the ground were analyzed by both grouped and ungrouped land-use classes.

In the third and final evaluation, Lincoln County was used as a case study to test the hypothesis that Skylab photographic data could be used in the Forest Survey procedure to measure forest area within specified accuracy limits. For this evaluation, a 1:125,000 scale enlargement was made of one Skylab S190B photograph that covered the entire test site. A grid overlay of 16-point clusters was constructed to sample the photograph at an intensity very similar to that used by the Forest Survey Unit. The boundary of Lincoln County was drawn from a 1:250,000 USGS map sheet and an overlay made to the scale of the photo enlargement. Interpretation was completed using a lamp magnifier (fig. 4). The grouped land-use class was recorded for each cluster point. Forest type and disturbances were recorded for the cluster center. Time to complete interpretation was recorded for cost effectiveness analysis.

Using the proportions in each cluster as a continuous variable, computations were made for each combined land-use class in the photo sample (see footnote 5).

Where:

x = proportion of land use in a photo subsample cluster (ASCS).

y = proportion of land use in a ground or Skylab subsample cluster.

p = proportion of land use in the photo sample cluster.

P = adjusted land use proportion in the county.

a = regression constant.

b = regression slope coefficient.

n = number of clusters in subsample.

m = total number of photo clusters.

N = total number of sampling units in the population.

L = adjusted area in land-use class.

A = total area being sampled.

and:

SS_y = corrected sums of squares of y.

$$= \Sigma y^2 - \frac{(\Sigma y)^2}{n}$$

SS_x = corrected sums of squares of x.

$$= \Sigma x^2 - \frac{(\Sigma x)^2}{n}$$

SP_{xy} = corrected sums of squares of the cross products.

$$= \Sigma xy - \frac{(\Sigma x)(\Sigma y)}{n}$$

s_y^2 = variance of y.

$$= \frac{SS_y}{n-1}$$

Computations were made for:

1. The mean proportions for individual land-use classes using ground or Skylab data.

$$\overline{y_j} = \frac{\Sigma_{i=1}^{n} (y_{ij})}{n}$$

where:

y_{ij} = proportion of the i^{th} cluster in land-use class j.

$\overline{y_j}$ = mean proportion in land-use class j.

2. The mean proportions for grouped land-use classes using ASCS, Skylab, and ground data.

$$\overline{y_k} = \frac{\Sigma_{i=1}^{n} (y_{jk})}{n}$$

where:

y_{ik} = proportion of the i^{th} cluster in grouped land-use class k.

$\overline{y_k}$ = mean proportion in grouped land-use k.

3. Regression constant (a) and slope coefficient (b) were computed for (1) the relationship between land-use proportions on ASCS photographs and the corresponding proportions on the ground, (2) the relationship between land-use proportions on the ground and the corresponding proportions on Skylab photography, and (3) the relationship between land-use proportions on ASCS photographs and the corresponding proportions on Skylab photographs. The equation for adjusting land-use proportions took the form:

$$P = a + b\,(\overline{p})$$

4. The squared standard deviation from the regression for each method.

$$s_{y.x}^2 = \frac{SS_y - \frac{(SP_{xy})^2}{SS_x}}{n-2}$$

5. The adjusted area for each combined land use class for each method.

$$L = (P)(A)$$

6. The standard error of the adjusted forest area for each method expressed as a percent.

$$s_P = \sqrt{s_{y.x}^2 \left[\frac{1}{n} + \frac{(\overline{p} - \overline{x})^2}{SS_x}\right]\left[1 - \frac{n}{m}\right] + \frac{s_y^2}{m}\left[1 - \frac{m}{N}\right]}$$

$$SE = \frac{(s_p)}{(P)}\,(100) \quad \text{at the 67-percent level of confidence.}$$

Forest Sampling Designs

McDuffie County, Georgia, is one of four counties in the Augusta test site covered by SL-4 S190B photographs. It was used as a test area to examine the feasibility of using Skylab photographic products as one stratum of data for obtaining Level I and some Level II land-use statistics now obtained for extensive forest inventories without the aid of satellite photography.

To provide a data base on which to evaluate several sampling strategies, a land-use map (fig. 8) of the county was made from interpretation of 1:120,000 scale CIR photography from RB-57 Mission 274. All Level I land-use classes (forest, nonforest, and water) and Level II classes (pine and hardwood) were mapped at a scale of 1:50,000. The mapping interpretation was done using a ZTS. A control base enlarged from the 1:250,000 scale USGS Athens, Georgia, quadrangle was placed on the ZTS mapping table. Class boundaries were interpreted from the CIR photo on the easel and drawn on clear acetate overlaid on the map base. This method eliminated cumulative positional errors.

The photography used allowed rather easy, though time-consuming, interpretation into the four land-use classes. A ground-check which covered nearly 20 percent of the county showed that the only classifications which might cause a problem were those involving a judgment decision between idle farmland and transitional land reverting to forest. The decision is made on the ground on the basis of the density of natural stocking with commercial seedling species. Lands classified as forest using this criteria are often plowed the following season and returned to farmland. Changes back and forth between forest and farmland can be quite rapid in this part of the country.

Figure 8.--Land-use map of McDuffie County, Georgia, produced by photo interpretation of 1:120,000 scale CIR photography. Geometric control obtained by mapping onto a USGS base map.

In addition to the extensive ground sampling as stated above, 6 percent of the county was intensively mapped on the ground directly onto 1:10,000 scale photo prints. The ground data were used to check the accuracy of the land-use classification and correct the map produced from interpretation of high-altitude CIR photography. Thus, the land-use map produced from CIR high-altitude photography is an accurate representation of the actual land use on the ground within the limits of the classification system used.

In order to use this map as a data base on which sampling strategies could be tried, and against which results of microdensitometer scanning of Skylab imagery could be compared, it was necessary to digitize the map.

A dot grid at a frequency of 16 dots per inch, representing approximately 50.3-meter (165-foot) spacing on the ground, was laid over the completed map. Each grid point was classified according to its mapped land-use type and recorded on magnetic tape through a keyboard interface. The position of each data point is known by line number and position within the data string for that line. The resulting data matrix samples the ground area to a resolution of about 0.6 hectare (1.5 acres).

Having the data on magnetic tape allowed a digital display to be generated in color on a tape-controlled plotting device. The output display is seen as Figure 9.

A scanning microdensitometer was used to make optical density measurements on a 9" x 9" (1:500,000) S190B color photograph from SL-4. The microdensitometer was programmed to sample points in the same matrix used to sample the land-use map, i.e., an array of 278 (x) by 539 (y) sample points. The ground positions of the four corners of the land-use

Figure 9.--Land-use map produced by digitizing, at a resolution of 0.6 hectares (1.5 acres), the hand-mapped data shown in Figure 8 and replotting with a computer-controlled plotter. The resolution of this map matches that of the microdensitometer data.

map were located on the S190B photograph and the microdensitometer programmed to scan this area and make measurements at each of the 149,842 points in the array. Density ranges for each of the four land-use types were established by measuring sample areas just prior to the programmed scanning. Density slicing was then used to classify each of the points on the resulting scan data into one of the four land-use types. This is the simplest type of classification and was tried to determine if even this crude classification yielded a stratification which would improve the statistical efficiency. Each microdensitometer point has a counterpart in one of the sample points on the land-use map. Each is located by the same line and column number, and each represents the same point on the ground. The counterpart of each microdensitometer point was located in the land-use map data tape and put in one of the four land-use type strata for sampling purposes. A more powerful classifier which is also being used is linear discriminant analysis using maximum liklihood and Gaussian assumptions. Training sets are chosen from among the data and used to establish the expected spectral statistics for each class. The land-use map is stratified according to the resulting classification and sampling effectiveness compared with random sampling and with systematic sampling.

The effect of sample spacing for systematic sampling of the land-use map was investigated by sampling the data matrix for all possible placements of grid spacing from 50 x 50 to 2 x 2. Descriptive measures are compared for these sample spacings and for the expected values from random sampling.

Automated Land Classification Procedures

A Photo Data Systems (PDS) microdensitometer and companion Model 2300 process computer (fig. 10) were used to scan and record optical density on one S190B color photograph for November 30, 1973. Computer routines necessary to meet the special data formatting problems presented by the Model 2300 computer were already written and operational. It was necessary, however, to update these programs for use with a new Executive 9 operating system on a Univac 1108 computer. The microdensitometer tapes were then rewritten in binary code decimals (BCD) to use with a CDC 7600 computer. Statistical methods and a nearest neighbor classification algorithm developed for LANDSAT data (Heller and others 1974) were modified as necessary. The algorithm was then applied to diffuse densities using the CDC 7600 computer at the University of California Lawrence Berkeley Laboratory. A more complete description of the PSW procedure is in Appendix 1.

Two 10,000-meter-square (6.22-mile-square) study blocks were selected for this experiment. These blocks were purposely selected to satisfy two criteria: (1) each had to have a broad representation of land-use types with a significant amount of forest and nonforest land and (2) the Skylab photo coverage for each site had to be complete. Boundaries of the two study blocks (called block 2 and block 4) were delineated on each of the photographs to be studied. Since annotating directly on the photos was undesirable, templates were made for each photo containing the blocks or parts of the blocks. The template was precisely oriented with the photos and fiducial marks; then major highways and other identifiable features were outlined with a fine drafting pen. These templates were used

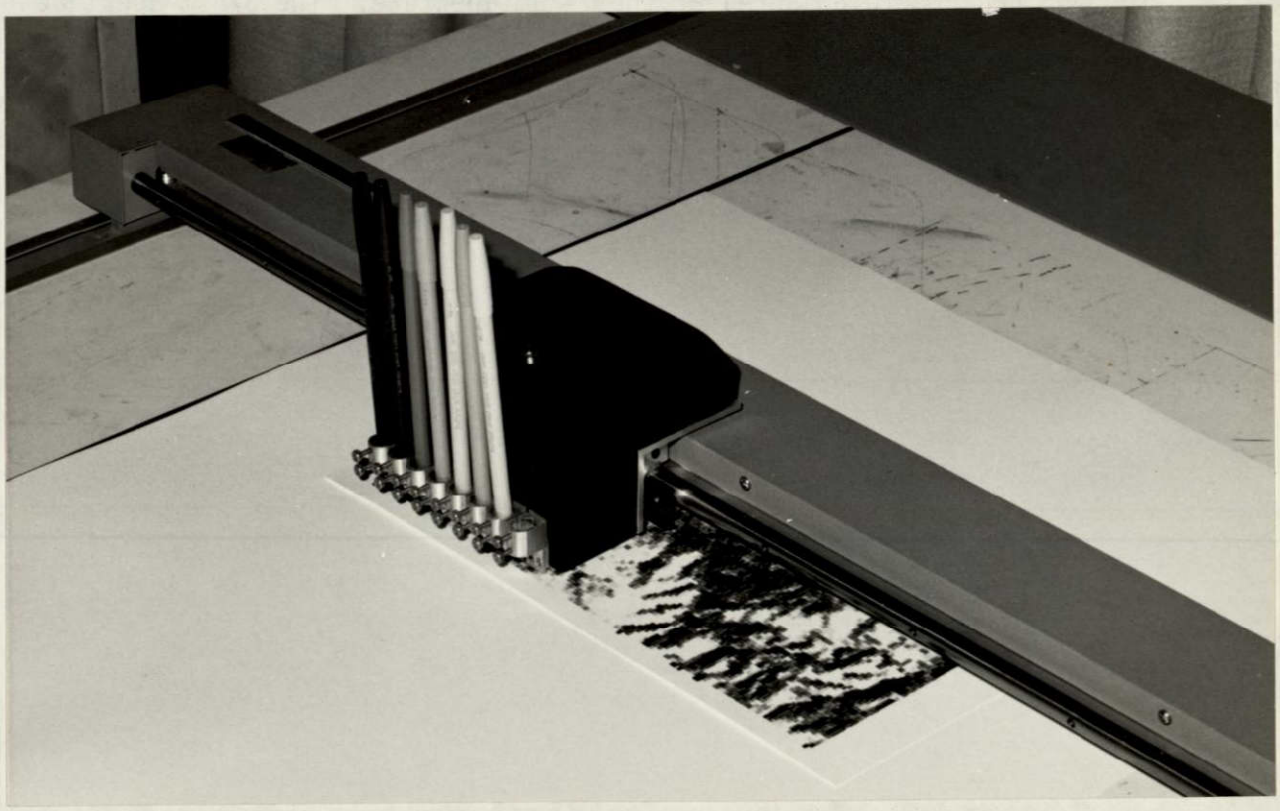

Figure 10.--A Photo Data Systems automatic scanning microdensitometer (top) and companion Model 2300 process computer used to read and record film densities on CCT tapes. The EAI tape-driven plotter (bottom) was used to plot color-coded classification maps.

on the microdensitometer for purposes of orientation only and removed before scanning began.

Block 4 was used to develop training sets and classifiers for 16 Level II and Level III forest and nonforest classes to be recognized in the study (table 2). The S190B color photograph was scanned using four scanning apertures (28 μm, 37 μm, 56 μm, and 74 μm). The microdensitometer was programmed to read densities at an interval approximating the aperture diameter. This procedure avoided excessive data integration and redundancy. The smallest area of interest for our classification purposes was 0.4 hectare (1 acre). With this in mind, the range of aperture settings sampled the 1:900,000 scale photograph in units of approximately 0.05 hectare (0.12 acre) in effective ground area at the 28 μm aperture to 0.35 hectare (0.86 acre) at the 74 μm aperture. The 37 μm aperture sampled approximately 0.09 hectare (one-fifth of an acre).

The microdensitometer was calibrated before each run after the proper aperture setting and optical filter were in position. After each filter run, the filter was changed and the microdensitometer recalibrated. A run for the complete block was made for each aperture setting and for four filter settings--blue (Wratten-94), green (Wratten-93), red (Wratten-92), and clear (no filter)--before continuing to the next aperture. In addition, a step tablet furnished with the SL-4 sensitometry package was scanned before the scanning began and again after the scanning was completed. This made it possible to convert microdensitometer optical density readings to NASA/JSC-PTD diffuse densities. The entire procedure was repeated for each of the four aperture scans.

Originally, we intended to evaluate aperture size by producing an eight-class land-use map from each aperture scan. Time limitations would not allow this, however, and we had to modify the plan. Instead, we produced an eight-level gray-scale map for each aperture scan. By examining the gray-scale maps it was apparent that the 37 μm aperture resulted in a ground resolution that best suited the requirements of this study. Classifiers were then developed for the 16 land-use classes and applied to the diffuse densities for block 4 using a nearest neighbor classification procedure.

A color-coded land-use map was produced on an EAI tape driven plotter for block 4 (fig. 10). The classifiers developed for block 4 were then extended to the data for block 2 and a plotter map produced to determine the operational capability of the classification system.

Accuracy of computer classification was checked in two ways. The first computed the proportional areas in each land-use class and compared them with proportions determined from the ground truth map. A second method checked the positional accuracy. That is, the plotter map was overlaid with a systematic grid of 480 points for which the classification on the ground truth map was known. The classification was recorded and compared with its counterpart on the ground. Plotter maps for both blocks were checked in this way and the number of correct calls determined and analyzed. Points falling in five randomly selected 1,000-meter cells with detailed classifications were checked to explain any discrepancies.

Results and Discussion

Each of the forest inventory studies was carried out independently to meet a separate objective. Thus, comparisons between results in this report must be made intuitively because of differing study conditions.

Forest Resource Evaluation

The choice of a Skylab data combination for conventional photo interpretation had less effect on accuracy than expected. We reached this conclusion by comparing omission and commission errors for land-use classification in one county. Some omission and commission errors are caused by misinterpretation of the photo images. In many instances, however, the errors are the result of chance judgements. For example, a point falling on a boundary line between forest and cropland may be called forest by the interpreter but called cropland by the field man. The field man can make judgement errors, but they are usually ignored because the ground tally is accepted as the truth. In comparing results of the Skylab interpretation with ground truth, this factor should be kept in mind.

Table 4 shows omission and commission errors resulting from the interpretation of three combinations of Skylab data for Lincoln County. The purpose of this comparison was to select the best combination for interpreting first- and second-level information in a four-county survey. At first glance it appears that many omission and commission errors are compensating. This is true for all combinations. Combination 1 had the fewest errors and Combination 2 had the greatest number of errors. Although Combination 3 resulted in a higher number of errors than Combination 1, the resolution was better, stereoscopic viewing was an aid in making borderline decisions, interpretation was faster, the interpreter felt more confident in making

Table 4. Number of points interpreted per hour and number of omission and commission errors for three Skylab data combinations. Data based on 640 observations in Lincoln County, Georgia.

Skylab data combination[1]	Number of PI points per hour	Total hours	Omission errors	Commission errors
1	121	5.3	34	34
2	98	6.5	58	46
3	160	4.0	36	42

[1] Combination 1: 1:250,000 enlargement of an S190B color photograph (PSW) and a 1:250,000 enlargement of an S190A false-color combination (PSW)

Combination 2: 1:500,000 enlargement of an S190B color photograph (NASA) and a 1:500,000 enlargement of an S190A false-color combination (PSW)

Combination 3: 1:500,000 enlargement of an S190B color photograph (NASA) and an overlapping enlargement of an S190B color photograph (NASA) for stereoscopic viewing.

decisions, and there was less eye strain. Based on this evaluation, Combination 3 was used to interpret land use in a four-county survey.

A comparison of individual land-use proportions resulting from a four-county survey shows close correlations between Skylab and ground truth for some classes (table 5). Only in pasture and idle land are the discrepancies much greater than ±1 percent. The differences of -6.61 percent for pasture and +4.34 percent for idle land for the most part represent errors in classification--either on the ground or on the Skylab imagery. These classification errors can be attributed to several causes: (1) borderline judgements where a point falls on or near a field boundary, (2) seasonal differences between the date of the imagery and the date the field crews located the points, and (3) changes that occurred since the ground data were recorded. If pasture and idle land are combined, the difference seems less apparent--0.1801 on the ground as compared to 0.1595 on the Skylab data. Since a major purpose of land-use classification in forest resource surveys is to measure the forest area base, it appears that despite differences in agricultural land use, forest land would be well within the accuracy limit of ±3 percent per million acres of commercial forest land. Increases in urban development during the 2-year span between ground and Skylab data acquisition can account for the increase in urban area (+0.8 percent). Noncensus water measured on Skylab normal-color film is underestimated because small bodies of water cannot be distinguished when background contrast is low. This limitation would be overcome using CIR film.

Land-use proportions listed by individual counties in Table 5 show much greater variation between Skylab and ground data than the grouped county data. The greater variation is due to the smaller sample size and the

Table 5. Summary: Individual land-use class proportions determined by ground examination (1971) and by Skylab photo interpretation (1973).

		Individual counties and combined counties								
			Land use							
Data Source	County	Sample Clusters	Forest	Cropland	Pasture	Idle	Other Ag.	Urban	Census Water	Noncensus Water
			Proportion							
Ground 1971 (July)	Columbia	49	0.6812	0.0293	0.0867	0.0294	0.0128	0.0816	0.0548	0.0242
	Lincoln	40	0.6984	0.0000	0.1062	0.0110	0.0094	0.0313	0.1359	0.0078
	McDuffie	44	0.6932	0.0909	0.0582	0.0356	0.0213	0.0611	0.0241	0.0156
	Wilkes	77	0.7597	0.0130	0.1542	0.0390	0.0008	0.0227	0.0041	0.0065
	Combined Counties	210	0.7158	0.0307	0.1092	0.0307	0.0095	0.0461	0.0452	0.0128
Skylab 1973 (Nov.)	Columbia	49	0.7283	0.0268	0.0166	0.0867	0.0013	0.0689	0.0574	0.0140
	Lincoln	40	0.6812	0.0187	0.0314	0.0578	0.0062	0.0625	0.1391	0.0031
	McDuffie	44	0.7088	0.0639	0.0171	0.0852	0.0071	0.0824	0.0270	0.0085
	Wilkes	77	0.7597	0.0381	0.0811	0.0682	0.0057	0.0422	0.0049	0.0000
	Combined Counties	210	0.7268	0.0372	0.0431	0.0741	0.0051	0.0607	0.0473	0.0057

vagaries of sampling. Normally, if area statistics are required by county they should be based upon a much larger sample.

If agriculture and pasture classes are grouped into the Forest Survey class, "other miscellaneous," much of the problem in separating these classes is overcome (table 6). The data do indicate, however, that either "other miscellaneous" is slightly underestimated or there is a real increase in forest and urban area. This point is explored later in this report.

Four additional classifications would be useful in forest resource evaluations: stand origin, physiographic site, forest type, and treatment class. Attempts to classify these parameters are discussed in the following paragraphs.

Classification of stand origin into two categories, natural and artificial, was unsuccessful. Failure to classify stand origin is attributed to the 20- to 30-meter (66- to 98-feet) ground resolution of the color film. The effect of poor resolution was to make all stands within types (pine type particularly) to look alike.

Physiographic site was classified for 148 forest plots but due to the restricted geographical area within the study site, 90 percent of the plots fell in one category--rolling upland. Ninety-seven percent of these plots were correctly classified. No attempt was made to analyze the remaining data because the observations were too few to be relevant to normal operating conditions. It was observed, however, that to successfully classify physiographic site, stereoscopic coverage is essential.

Forest types in the four-county area were classified correctly on Skylab S190B color only 50 percent of the time. Accuracies ranged from

Table 6. Summary: Agriculture and pasture class proportions grouped into "other miscellaneous."

Data Source	County	Sample Clusters	Other Miscellaneous
			-proportion-
Ground	Columbia	49	0.1582
1971	Lincoln	40	0.1266
(July)	McDuffie	44	0.2060
	Wilkes	77	0.2070
	Combined Counties	210	0.1801
Skylab	Columbia	49	0.1314
1973	Lincoln	40	0.1141
(Nov.)	McDuffie	44	0.1733
	Wilkes	77	0.1931
	Combined Counties	210	0.1595

a low of 16 percent for mixed pine-hardwood to a high of 59 percent for pine. The distribution of 161 plots by Skylab and ground types is shown in Table 7.

Two conclusions can be drawn from this test. One, mixed pine-hardwood cannot be separated from pine and hardwood with sufficient accuracy to be useful in resource surveys. The problem here is that a pine-hardwood classification is based on the decision rule, "Does pine comprise more than 25 percent but less than 50 percent of the stocking?" This rule can be tested by stem counts on the ground. On photographs, however, the decision must be based on crown counts which cannot be accomplished on 20- to 30-meter (66- to 98-feet) resolution imagery. The second conclusion we can draw from the results is that upland and bottomland hardwood cannot be separated on normal-color film except in the most obvious situations. Experience with CIR film, however, indicates that high moisture content in bottomland sites can be detected during late fall, winter, and early spring seasons and would result in higher classification accuracies.

On Skylab S190B color, forest types must be combined to maximize their usefulness. For instance, when pine and pine-hardwood plots are combined in a single pine class, the accuracy of classification would increase to 73 percent--a much more respectable figure. By combining upland and bottomland hardwoods into a single hardwood class, the accuracy improves to 69 percent.

Treatment classes, redefined as disturbance classes for remote sensing, were classified for 40 plots in Lincoln County. To compare relative accuracy at three levels of remote sensing, classifications were made on LANDSAT-1, Skylab S190B, and 1:120,000 CIR photographs. The results are shown in Table 8.

Table 7. Distribution of forest plots by Skylab and ground forest type classes. Photo interpretation was by stereoscopic examination of overlapping S190B photography in a four-county area.

Skylab class	Pine	Pine-hardwood	Upland-hardwood	Bottomland-hardwood	Non-forest	TOTAL
Pine	54	7	5	1	3	70
Pine-hardwood	20	4	1	1	2	28
Upland-hardwood	13	12	13	1	2	41
Bottomland-hardwood	1	2	4	4	0	11
Nonforest	3	0	1	1	6	11
TOTAL	91	25	24	8	13	161

Table 8. Accuracy of detecting disturbances by four methods--Lincoln County, Georgia.

Disturbance class (Ground)	Detection method			
	Ground[1]	RB-57[2]	Skylab[3]	LANDSAT[4]
	--Number of plots correctly classified--			
No disturbance	22	21	21	19
Prescribed burn	1	0	0	0
Cleaning, release, or intermediate cutting	5	4	4	1
High grading	1	0	1	0
Commercial thinning	7	3	2	1
Harvesting with artificial regeneration	1	1	1	1
Clearing of site preparation	1	1	1	1
Natural regeneration on nonforest land	1	1	1	1
Artificial regeneration on nonforest land	1	1	1	1
Total detected	40	32	32	25
	----------Percent ----------			
Detection accuracy	100	80	80	63

[1]July, 1971
[2]April 25, 1974
[3]November 30, 1973
[4]February 17, 1973

As would be expected, detection varies by the ground resolution of the sensors and the level of disturbance. The greater disturbances, such as harvesting with artificial regeneration and clearing or site preparation, are detected on LANDSAT-1 data. However, only 63 percent of the plots were correctly classified on LANDSAT imagery compared with 80 percent on both Skylab and the RB-57 imagery. One possible explanation for not detecting commercial thinnings and the more subtle disturbances might be the 1½- to 3-year time lapse between ground observation and the dates of the imagery.

To evaluate Skylab data in a quasi-operational test, land use was classified for Lincoln County using a cluster overlay that sampled at a slightly higher intensity than the existing Forest Survey design. The overlay, unlike the Forest Survey design (every other photograph in alternate flight lines), covered the entire county area. This eliminated the chance of oversampling some classes and undersampling others. The results in Table 9 show that, according to Skylab, the unadjusted forest proportion is almost 3 percent higher than that obtained on 4-year-old Department of Agriculture (ASCS) photographs. The "other miscellaneous" class decreased, urban increased, and both census water and noncensus water were reduced using Skylab data. These could be real differences detected by the more recent Skylab data and the improved distribution of the photo sample--unfortunately there is no way of checking this because of the time lapse since the data were collected.

A 40-cluster subsample was examined on Skylab and ASCS photographs and on the ground to classify land use in Lincoln County by combined classes. The unadjusted forest proportion computed from Skylab data was almost 2

Table 9. Unadjusted mean land-use proportions from ASCS and Skylab S190B photographs. Computed from intensive photo sample for combined land-use classes--Lincoln County, Georgia.

Data Source	Total Clusters	Forest	Other Misc.	Urban	Census Water	Noncensus Water
		----------proportion----------				
ASCS (1:20,000)	536	0.6472	0.1351	0.0169	0.1725	0.0283
Skylab (1:500,000)	667	0.6747	0.1201	0.0260	0.1636	0.0150
Difference	---	+0.0275	-0.0150	+0.0091	-0.0089	-0.0127

percent lower than the ground check and 3 percent lower than the ASCS photo estimate (table 10). The latter is a complete reversal from the estimate made from the larger photo sample and reflects differences in the two samples. The small subsample apparently sampled areas under development for homes at a greater intensity than the larger photo sample. The larger proportion of the land area estimated in the urban class on both the Skylab photos and the ground seems to indicate this. By interpreting forested areas within residential developments as urban, an overestimate of urban and an underestimate of forest land resulted. Errors of this sort can be avoided by improving the criteria for interpreting urban land.

The 40 subsample clusters were examined on 1:120,000 scale CIR photographs to verify the mean Skylab proportions (table 10). As can be seen, forest proportion is more than 3 percent higher and urban 4 percent lower on the CIR photography than on the Skylab imagery. This seems to substantiate the previous analysis that urban developments within forested areas are overestimated on Skylab. Because the ground estimate of urban is higher than either Skylab or ASCS, it can be assumed that the CIR estimate is low and that the true proportion of urban area is nearer 3 percent.

In the Lincoln County case study, mean forest proportions determined from a large photo sample were adjusted by regression techniques. Unadjusted forest proportions determined from the large area photo sample (table 9) on both Skylab and ASCS photographs, were adjusted using regression equations developed from the small photo subsample checked on the ground. The results are shown in Table 11. Skylab techniques estimated

Table 10. Unadjusted mean land-use proportions from ASCS, Skylab S190B, and high-altitude color infrared photographs, and from ground samples. Computed from small photo subsample for combined land-use classes--Lincoln County, Georgia.

Data Source	Total Clusters	Grouped Land-use				
		Forest	Other Misc.	Urban	Census Water	Noncensus Water
ASCS (1:20,000)	40	0.7094	0.1313	0.0156	0.1375	0.0062
Skylab (1:500,000)	40	0.6812	0.1141	0.0625	0.1391	0.0031
Ground	40	0.6984	0.1266	0.0313	0.1359	0.0078
CIR (1:120,000)	40	0.7141	0.1250	0.0187	0.1391	0.0031

Table 11. Adjusted mean forest proportions, adjusted forest land area, and standard errors of the estimates for Lincoln County, Georgia.

Data Source	Photo Sample Clusters	Sub-sample Clusters	Adjusted Proportion	Adjusted Area	SE of Estimate
				--ha--	
ASCS	536	40	0.63753	42,123	±3.17
Skylab	667	40	0.69229	45,741	±3.53
Difference	--	--	+0.05476	+3,618	--

forest area 3,600 hectares (8,892 acres), or 8.6 percent higher than the ASCS technique. Despite this, the standard error of the adjusted forest area estimate using Skylab data was ±3.53 percent--slightly higher than the adjusted estimate on ASCS photography. The difference in the estimates can be attributed to differences in sampling intensity, sample distribution, and misclassification of urban areas as forest land.

The flow chart in Figure 11 shows the general procedure followed in computing adjusted mean forest proportions, adjusted forested area, and standard errors for Lincoln County.

Forest Sampling Designs

The digitized land-use map for McDuffie County (hereafter called the ground truth map to distinguish from other maps) and the 1971 Forest Survey agree closely when the areas of commercial forest (69.6 percent map, 69 percent Forest Survey) are compared. The Forest Survey data gives no information about the location of commercial forest and other land-use types; therefore, no cross-checks can be made with the ground truth map. The area of noncensus water (defined in Table 1) in the county is less than 2 percent. The mapped area of noncensus water differs from the Forest Survey figure primarily because much of the water was excluded from the land-use map where the northern boundary of the county crosses Clark-Hill Reservoir and could not be accurately located. Noncensus water, therefore, is included with all other nonforest for stratification purposes in this study.

A facsimile gray-scale map was produced on a line-printer from the red-filtered microdensitometer scan of the Skylab S190B color image. Alphabetic characters were used to represent four optical-density ranges

(density slices). Maps produced in this way are stretched in the Y direction due to the greater spacing between rows of characters than between the characters along a row. Using this same procedure with digitized data from the ground truth map, a geometrically similar line-printer facsimile was produced for comparison. The two facsimile maps were compared and the registration appeared to be good. Based on this result, we went to a more powerful classifier using three spectral bands of microdensitometer data.

Training sets for each of the land-use types were identified on the ground truth map and then located in the microdensitometer scan data matrices. Optical densities from the red, green, and blue microdensitometer scans, and generated statistics, were used to develop linear discriminant functions to classify the entire county into land-use types from the Skylab data. A facsimile type-map was generated on a line-printer using this classification procedure. This type-map is compared with the line-printer ground truth map (fig. 12).

The linear discriminant functions used in the classification procedure could not separate pine and hardwood with sufficient accuracy for inventory purposes. Thus, all forest land was aggregated into a single forest type and all nonforest land was aggregated into a single nonforest type for further analysis. The confusion matrix for the training set is shown in Table 12 as both number of points identified and percentages by types. Table 13 is the confusion matrix for the entire population. These classifications were used to test systematic sampling with postsampling stratification in the following discussion.

Having the ground truth map digitized as a regularly spaced grid of data points at 80.5-meter (264-feet) spacing allowed a comparison to be

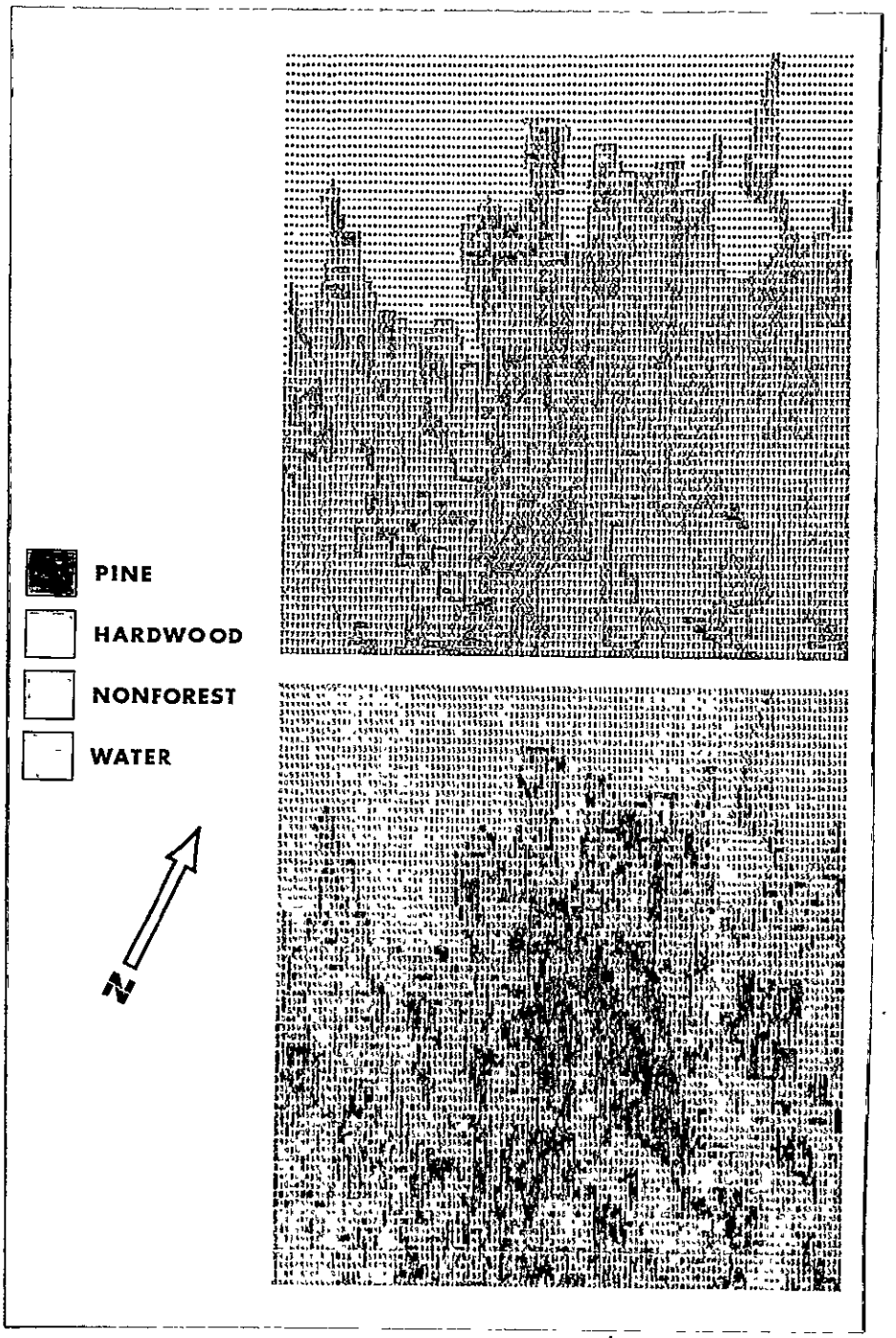

Figure 12.--The northwestern portion of McDuffie County, Georgia, is shown on the land-use maps. The upper map was produced from data digitized from the land-use map shown in Figure 8. The lower map was produced from the classification of microdensitometer scans on an S190B color transparency. Many nonforest areas, mostly roads or road segments which were below the minimum mapping size to separate on the land-use ground truth map (top), are shown on this map.

Table 12. Training set confusion matrix for classification of microdensitometer scan data from Skylab image.

Predicted Type (Skylab)	Actual Type (Ground Truth)	
	Forest	Nonforest
	--------Number of points (percent)-------	
Forest	479 (94.7)	109 (17.7)
Nonforest	27 (5.3)	506 (82.3)

Table 13. Entire population confusion matrix for classification of microdensitometer scan data from Skylab image.

Predicted Type (Skylab)	Actual Type (Ground Truth)	
	Forest	Nonforest
	---------Number of points (percent)------	
Forest	59,783 (80.5)	9,781 (30.0)
Nonforest	14,507 (19.5)	22,570 (70.0)

Table 14. Characteristics of grid sizes used to sample the land-use map data matrix.

Grid Spacing (data elements)	Number Sample Pts.	Ground Spacing		Sample Fraction	Ground Area per Sample Pt.	
		meters	feet	percent	hectares	acres
50	43	4,020	13,189	0.04	1,567	3,873
42	61	3,377	11,078	0.06	1,106	2,733
36	82	2,894	9,496	0.08	813	2,009
25	171	2,010	6,594	0.16	392	969
21	242	1,688	5,539	0.23	277	684
18	329	1,447	4,748	0.31	203	502
14	544	1,126	3,693	0.51	123	304
12	741	965	3,165	0.70	90	223
10	1,066	804	2,638	1.00	63	155
9	1,317	724	2,374	1.24	51	126
7	2,176	563	1,846	2.04	31	76
6	2,962	482	1,583	2.78	23	56
5	4,266	402	1,319	4.00	16	39
4	6,665	322	1,055	6.25	10	25
3	11,849	241	791	11.11	6	14
2	26,660	161	528	25.00	3	6

Table 15. Comparison of bias and variance for forest proportions estimated using simple random sampling (SRS), systematic sampling (SYS), and systematic sampling with postsampling stratification (PSS) for 16 sampling fractions.

Sampling Fraction (proportion)	Grid Spacing -data pts.-	Bias of Forest Proportion -SRS-	-SYS-	-SYS&PSS-	Variance of Forest Proportion -SRS-	-SYS-	-SYS&PSS-
0.0004	50	0	0.0006	0.0008	0.00495	0.00412	0.00334
0.0006	42	0	0.0000	0.0005	0.00350	0.00278	0.00241
0.0008	36	0	0.0002	0.0007	0.00257	0.00231	0.00181
0.0016	25	0	0.0001	0.0003	0.00124	0.00075	0.00074
0.0023	21	0	0.0000	0.0000	0.00087	0.00057	0.00052
0.0031	18	0	0.0000	0.0000	0.00064	0.00035	0.00032
0.0051	14	0	0.0000	0.0000	0.00039	0.00015	0.00018
0.0070	12	0	0.0000	0.0001	0.00029	0.00014	0.00015
0.0100	10	0	0.0000	0.0000	0.00020	0.00011	0.00010
0.0124	9	0	0.0000	0.0000	0.00016	0.00007	0.00008
0.0204	7	0	0.0000	0.0000	0.00010	0.00004	0.00005
0.0278	6	0	0.0000	0.0000	0.00007	0.00003	0.00004
0.0400	5	0	0.0000	0.0000	0.00005	0.00002	0.00002
0.0625	4	0	0.0000	0.0000	0.00003	0.00001	0.00001
0.1111	3	0	0.0000	0.0000	0.00002	0.00001	0.00001
0.2500	2	0	0.0000	0.0000	0.00001	0.00000	0.00001

The study has shown that forest area proportion is more efficiently determined using systematic sampling rather than simple random sampling when applied to an area with forest distribution as in McDuffie County, Georgia. The precision of the estimate is further increased by using postsampling stratification from the computer classification of Skylab S190B microdensitometer data. However, there is no advantage when the sampling fraction is larger than 0.0016. If it had been possible to direct more effort to developing better discriminant functions for the supervised Skylab data classification, an advantage might have been shown for larger sampling fractions. We are planning to continue our efforts to improve the classification in the future.

The classification effort pointed out the difficulty of trying to classify photo data into categories which reflect the intent of land-use rather than actual ground conditions. With the inevitable revision of resource classification systems into a common and aggregative type of inventory system it should be possible to more effectively use unsupervised classification to provide a more useful data stage for future sampling systems.

Automated Land Classification

Optical film densities measured on normal-color film (S190B), and analyzed by the nearest neighbor classification algorithm, showed promise for computer-assisted land classification. Only broad Level I land classes and Level II forest types, however, could be separated with reasonable accuracy (table 16). For instance, in block 4, pine area was 17 percent lower and the hardwood area was 40 percent higher than the ground area.

Table 16. Comparison of percent accuracy of area estimates and sample point classification for PSW computer mapping procedure for two test blocks, Skylab S190B color photograph, November 30, 1973.

Block and land-use class (Levels I & II)	Ground[1] area	Skylab area accuracy	Number of points	Skylab classification accuracy
	--Ha-	---Percent-----		---Percent----
Block 4				
I Forest	6,055	60.55	64.41	290	92
II Pine	4,427	44.27	36.62	217	70
Hardwood	1,628	16.28	22.82	73	68
Cutover	--[2]	--	4.97	0	--
I Nonforest	3,616	36.16	32.14	180	74
II Grassland	1,548	15.48	9.51	78	53
Crops	61	0.61	6.57	2	0
Bare Soil	881	8.81	6.90	52	37
Wild Veg.	441	4.41	4.96	26	27
Urban	685	6.85	4.20	22	14
I Water	329	3.29	3.45	10	20
Block 2[3]				
I Forest	5,151	51.51	53.48	271	93
II Pine	3,327	33.27	26.95	150	83
Hardwood	1,824	18.24	20.84	121	74
Cutover	--[2]	--	5.69	0	--
I Nonforest	4,721	47.21	44.04	204	85
II Grassland	1,473	14.73	8.25	57	54
Crops	151	1.51	5.00	23	35
Bare Soil	700	7.00	22.92	33	67
Wild Veg.	805	8.05	4.41	26	42
Urban	1,592	15.92	3.46	65	17
I Water	128	1.28	2.48	5	80

[1]Areas were determined by dot count on ground truth maps at an intensity of approximately one dot per 0.4 hectare (1 acre).

[2]Cutover land was not classified separately on the ground truth map. This means cutover forest land was placed in the appropriate forest type.

[3]Block 2 is approximately 61 kilometers (38 miles) southeast of Block 4.

The latter figure seems high, but as a percentage of the total area it represents only about 6.5 percent--22.82 percent compared with 16.28 percent on the ground. In block 2, pine area was 19 percent lower and hardwood 14 percent higher than the ground areas. This was true even though block 2 was classified using training sets derived from block 4--61 kilometers (38 miles) away. The total forest area in block 4 was 6 percent higher and in block 2 only 4 percent higher than the ground truth. Pine was always underestimated and hardwood was always overestimated.

Total nonforest area, like total forest area, was estimated within reasonable accuracy--block 4 within 11 percent and block 2 within 7 percent--and both were underestimated. Area estimates by Level II nonforest classes varied considerably from the ground truth and can be explained by seasonal differences between the Skylab data (late November) and the ground truth (late spring). This problem will always be a factor in machine classification unless land classifications are restructured to recognize what is present on the ground rather than trying to interpret what local land managers intend to use the land for. The best time of year to measure the landowner's intent is in the late spring when the fields are plowed or planted and can be separated from grassland and idle land.

Areas of water and urban land estimated in both blocks 4 and 2 in some instances appear to be quite accurate. This is misleading, however, because major bodies of water in both blocks were called bare soil, grassland, and crops. Water was misclassified because high levels of sedimentation created false signatures. Urban areas were misclassified as grassland, bare soil, and crops, because on color film the spectral signatures

are very similar. Roads and utility rights-of-way, passing through forested areas, can be detected by the spatial alignment of pixels but not by their spectral characteristics.

The computer maps shown in Figures 13 and 14 allow a visual comparison to be made with both the Skylab S190B photograph and the ground truth map. The agreement between Level I forest areas and nonforest areas, and between Level II forest types, is quite apparent. A point-by-point comparison was made between points located on the ground truth map and the same points on the computer map. We found that 92 and 93 percent of forest points were correctly classified on the computer map for blocks 4 and 2, respectively (table 16). Of the points in pine type, 70 percent (block 4) and 83 percent (block 2) were correct. Points falling in hardwood were correct 68 and 74 percent of the time for blocks 4 and 2, respectively. Although nonforest points were found accurate 74 percent (block 4) and 85 percent (block 2) of the time, the accuracy for individual Level III classes was extremely poor.

The results show that forest area can be stratified on high-resolution Skylab-quality photographs (20- to 30-meter resolution) with an accuracy of approximately 96 percent. In other words, the forest area can be mapped and an estimate of the area made within limits that can be accomplished using aerial photographs. We also found this to be true in our LANDSAT-1 experiment (Heller and others 1974). However, because of geometric distortions in the LANDSAT image, point-by-point comparisons were correct only 50 percent of the time.

BLOCK 4

GROUND TRUTH (Prepared from 1:120,000 CIR photo, April 1974)

Pine	1	Harvested crop	12	Marshland	23
Pine-hardwood	2	Orchard	13	Alder swamp	24
Upland-hardwood	3	Farmstead	14	Transportation and	
Bottomland-hardwood	4	Plowed field	15	utilities	25
Undisturbed grass	5	Erosion	16	Home developments	26
Disturbed grass	6	Site preparation (urban)	17	Commercial develop-	
Dead grass	7	Rock	18	ments	27
New improved grass	8	Idle land	19	Recreation	28
Immature grain	9	Abandoned land	20	Clear lakes and ponds	29
Immature row crop	10	Transitional	21	Turbid lakes and ponds	30
Mature crop	11	Kudzu	22	Rivers and streams	31

Block 4

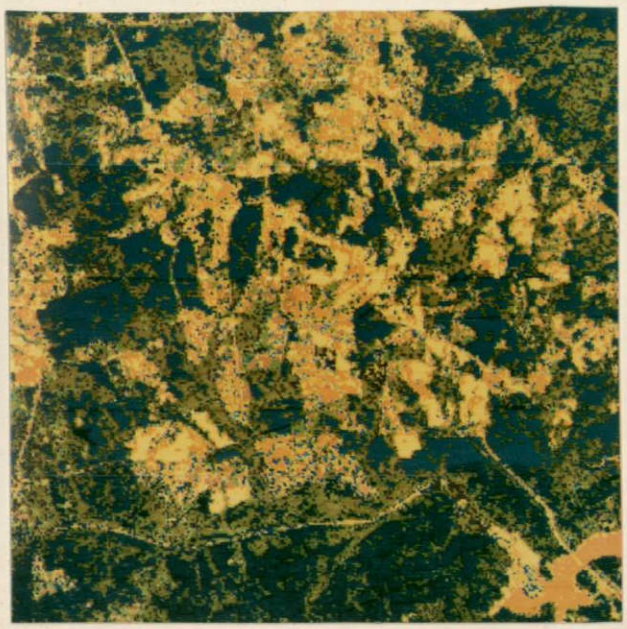

Computer map

Skylab S190B
November 30, 1973

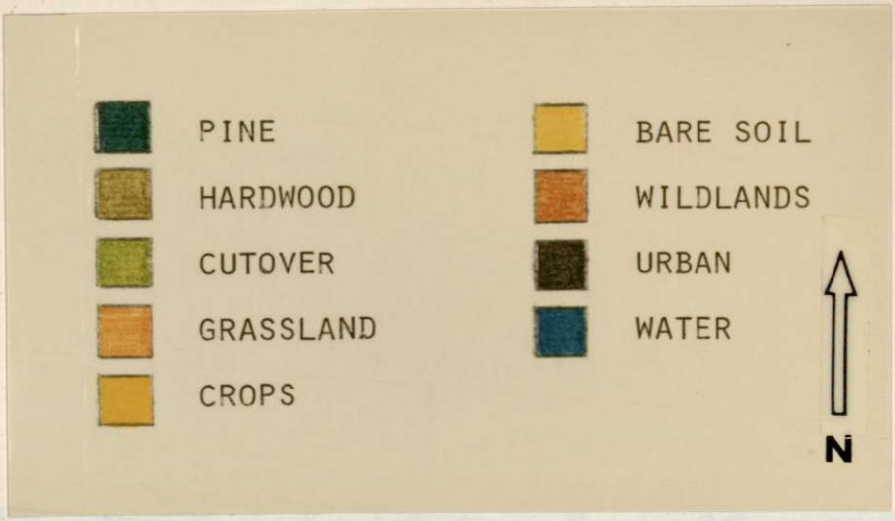

Figure 13.--The computer map (above left) was made using diffuse densities converted from optical densities measured on the S190B photograph (above right). The photograph was scanned with a PDS Microdensitometer and optical densities digitized and recorded on tape. The map was produced by the PSW computer classification system using nearest neighbor theory and an off-line tape-driven plotter with eight colored marking pens. Point-by-point evaluations can be made with the ground truth map (opposite page).

BLOCK 2

GROUND TRUTH (Prepared from 1:120,000 CIR photo, April 1974)

Pine	1	Harvested crop	12	Marshland	23
Pine-hardwood	2	Orchard	13	Alder swamp	24
Upland-hardwood	3	Farmstead	14	Transportation and	
Bottomland-hardwood	4	Plowed field	15	utilities	25
Undisturbed grass	5	Erosion	16	Home developments	26
Disturbed grass	6	Site preparation (urban)	17	Commercial develop-	
Dead grass	7	Rock	18	ments	27
New improved grass	8	Idle land	19	Recreation	28
Immature grain	9	Abandoned land	20	Clear lakes and ponds	29
Immature row crop	10	Transitional	21	Turbid lakes and ponds	30
Mature crop	11	Kudzu	22	Rivers and streams	31

Block 4

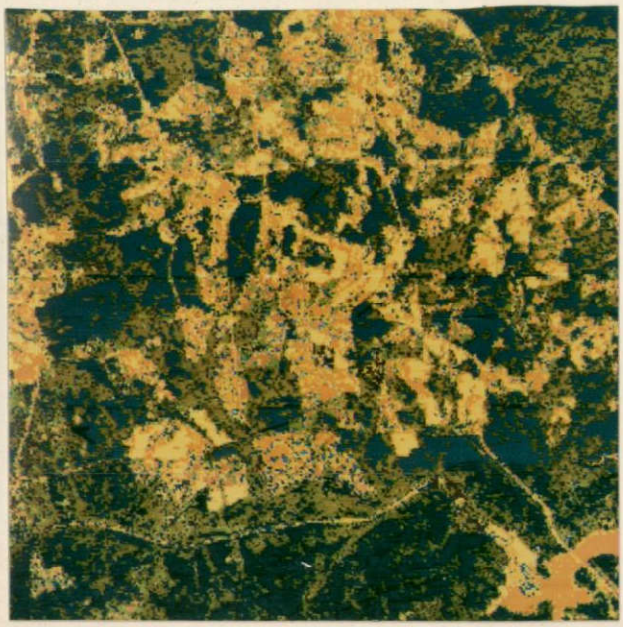

Computer map

Skylab S190B
November 30, 1973

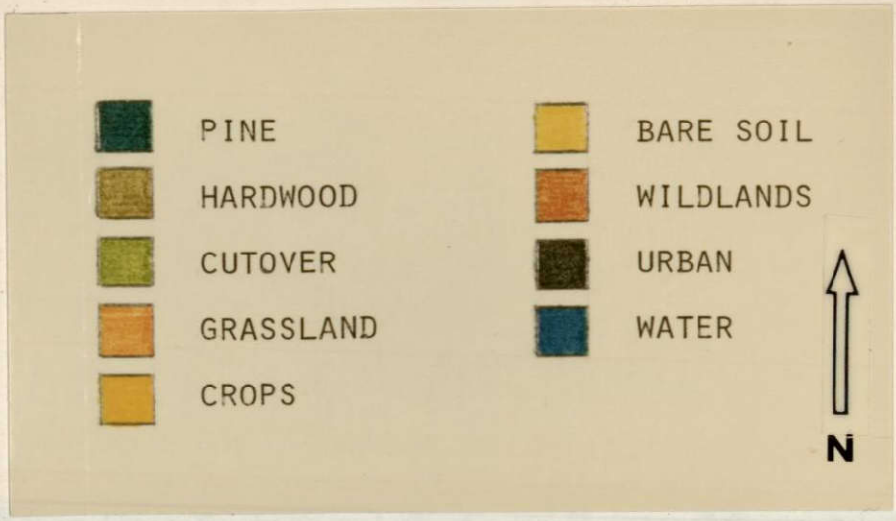

Figure 13.--The computer map (above left) was made using diffuse densities converted from optical densities measured on the S190B photograph (above right). The photograph was scanned with a PDS Microdensitometer and optical densities digitized and recorded on tape. The map was produced by the PSW computer classification system using nearest neighbor theory and an off-line tape-driven plotter with eight colored marking pens. Point-by-point evaluations can be made with the ground truth map (opposite page).

BLOCK 2

GROUND TRUTH (Prepared from 1:120,000 CIR photo, April 1974)

Pine	1	Harvested crop	12	Marshland	23
Pine-hardwood	2	Orchard	13	Alder swamp	24
Upland-hardwood	3	Farmstead	14	Transportation and	
Bottomland-hardwood	4	Plowed field	15	utilities	25
Undisturbed grass	5	Erosion	16	Home developments	26
Disturbed grass	6	Site preparation (urban)	17	Commercial develop-	
Dead grass	7	Rock	18	ments	27
New improved grass	8	Idle land	19	Recreation	28
Immature grain	9	Abandoned land	20	Clear lakes and ponds	29
Immature row crop	10	Transitional	21	Turbid lakes and ponds	30
Mature crop	11	Kudzu	22	Rivers and streams	31

Block 2

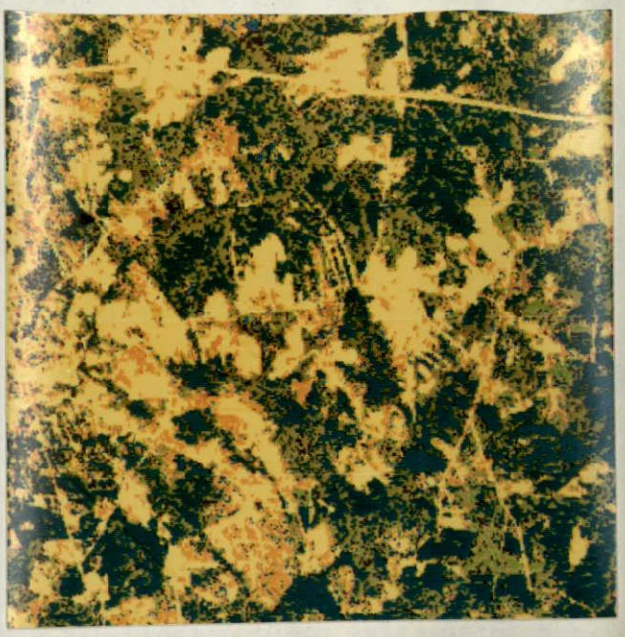

Computer map

Skylab S190B
November 30, 1973

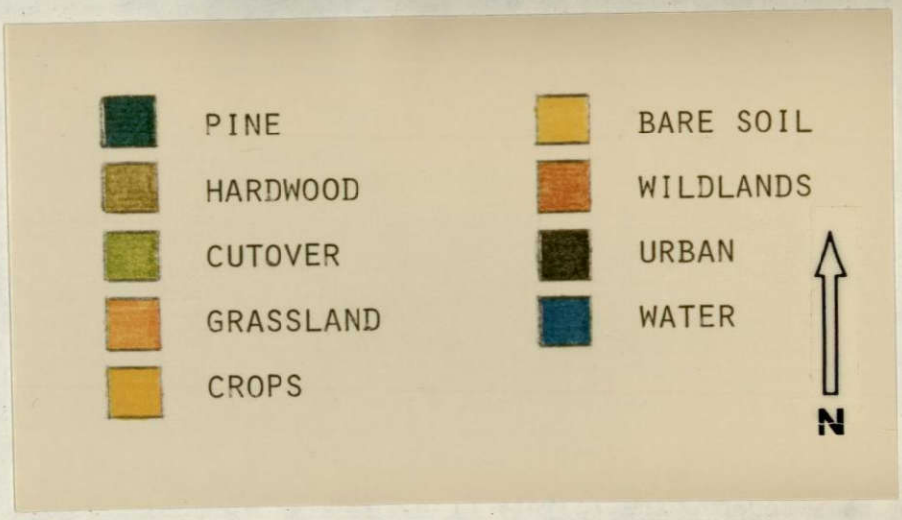

Figure 14.--The computer map (above left) was made using diffuse densities converted from optical densities measured on the S190B photograph (above right). The photograph was scanned with a PDS Microdensitometer and optical densities digitized and recorded on tape. The map was produced by the PSW computer classification system using nearest neighbor theory and an off-line tape-driven plotter with eight colored marking pens. Spectral signatures developed for block 4 were used in this classification without modification. Point-by-point evaluations can be made with the ground truth map (opposite page).

Under certain assumptions, Skylab-quality photographs will provide a data base for Level I and Level II land use and broad forest-type stratifications (as defined in this report) by both human and machine-assisted procedures. The assumptions are that:

1. High-resolution color infrared photography is available.

2. Radiometric measurements by supporting aircraft flights are available within a few days of a satellite pass.

3. A high-speed scanning microdensitometer is available for recording optical film density on computer-compatible tape.

4. An off-line minicomputer and interactive display (CRT) are available for preprocessing remotely sensed data for input to a large non-dedicated high-speed computer for classification mapping or sampling. If a minicomputer is not provided, an interactive display--on-line with a dedicated large, high-speed computer--must be available.

5. A classification system is designed which is based upon land cover rather than land use intent.

In this investigation, normal-color photography taken from orbital altitudes did not allow complete land-use classification even at Level I. In this regard, the failure of both human and automated classification procedures to resolve differences between water, grassland, bare soil, and idle fields was important. However, examples of Skylab CIR photographs for nearby areas indicated that the infrared reflectance and absorption differences for these classes will provide excellent separation. Thus if CIR film is available, both human and computer classification of land use and forest type should be more effective.

land cover to classify use based on the intent of the manager. Using this definition, an area which had been clearcut and prepared for planting would be considered forest although no trees were present. Computer-aided classification would probably classify the area as bare soil. While in some parts of the country it might be inferred that a forest opening of bare soil was a clearcut to be planted, in the Southeast it is just as probable that the area is agricultural land.

There is a much greater probability of high classification accuracy if classification is in terms of present land cover. The spectral signatures of classifications based on present land cover have inherently less variability than classifications based on intended use which may include diverse land cover categories. However, a system based solely on land cover, although appealing from the standpoint of identification from remote sensing data, may not be amenable to aggregation and disaggregation into the classes desired by the data users.

An alternative classification system might be one which utilizes information directly attainable from satellite data and calls for a separate subsample of those classes not well characterized by the land cover. Before the system could be implemented, however, it would be necessary to know the land cover types that can be recognized in a given region. To date, most studies have concentrated on determining the accuracies attainable when classifying land into predetermined categories. Results of these studies have often been discouraging because a satisfactory classification accuracy could not be attained for the predetermined categories. At the same time, the possibilities for further subdivision within easily identified categories went unexplored. We feel that operational applications

of machine-assisted classification will depend on additional research to determine the land cover categories which are, and those which are not, spectrally separable with acceptable accuracy.

Cost Comparisons

The primary advantage of Skylab-quality photography in forest resource surveys is the broad areal coverage within a single frame. In the four counties used in this experiment, it required 183 aerial photographs (1:20,000) to cover an estimated 80 percent of the total area. This was single photographic coverage without the advantages of stereoscopic overlap. A Skylab S190B photograph, on the other hand, will cover these four counties and two to four additional counties as well. Complete county coverage offers better distribution of photo samples and reduces data handling and photo acquisition costs--assuming that only printing and processing costs are involved.

If all other survey costs are considered equal, the costs of Level I and Level II land use and forest stratification would be 49 percent lower on Skylab photographs than on conventional 1:20,000 scale photographs (table 17). The major difference between the two methods is the cost of photographs. Because of the small scale and the use of normal-color film, more time was required to make interpretative decisions on Skylab photographs. However, if color infrared photographs were available on a regular recurring basis, the advantages of up-to-date information far outweigh any additional interpretation time.

Because of variations in system efficiency and effectiveness, it is very difficult to make comparisons between conventional interpretation and computer-assisted classification and mapping techniques. Numerous

Table 17. Comparative cost of land use and forest stratification on Skylab photographs and on 1:20,000 ASCS photographs.

Data Source	Photo handling[1]	Photography cost[2]	Photo Interpretation[3] [4]	Total
	----------dollars----------			
ASCS	140.00	366.00	36.35	542.35
Skylab	125.00	100.00	50.90	275.90

[1]Based on time studies--includes ordering, organizing, and labeling photographs and transferring plots. Rate: $5.00 per hour.

[2]Based on 1974 ASCS price list and cost of one S190B color internegative and one 1:125,000 color print.

[3]Based on time studies--ASCS interpretation at 5 clusters/minute, Skylab interpretation at 3 clusters/minute. Rate: $5.00 per hour.

[4]Based on time studies--ASCS forest type classification at 40 plots/hour, Skylab forest type classification at 30 plots/hour. Rate: $5.00 per hour.

computer classification procedures are now available for resource analysis, but there have been no comparative tests. Computers and accessories vary widely. There are nondedicated computers accessed through terminals on a time-sharing basis, dedicated computers with on-line interactive displays, and complex systems including off-line minicomputers and interactive displays to preprocess data for classification and mapping on large computers. An analysis of the efficiency of one system over another is lacking.

In this study a system was used that included a nearest neighbor classification algorithm and two time-sharing computers. Without an interactive display, two or more iterations of the classifications were required to improve accuracy. This is more time consuming than an interactive display and less efficient. The cost breakdown in Table 18 compares our PSW computer-assisted technique with conventional mapping and transfer procedures on a ZTS. Although the computer technique was more expensive ($177.00 more), it required only one-fourth the man-hours. Thus, when manpower and time are short, the machine-assisted system would be beneficial despite the higher cost.

Table 18. Cost comparison to produce classification map for 40,000-hectare (98,800-acre) area using conventional mapping and computer-assisted techniques.

Method	Task description	Time		Cost	
		Man-hours	Machine time	Man-hours[1]	Machine
				------dollars-------	
Conventional photo interpretation	Map and transfer class boundaries from 1:120,000 CIR to 1:24,000 map base.	100.00	0	617	0
	Total	100.00	0	617	0
Computer-assisted classification	Microdensitometry	2.00	4 hrs[2]	12	240
	Computer classification				
	IHIST-rewrites raw density tape and interleaves scans	0.50	356 sec[3]	3	41
	IGREY-gray-scale printout; area location, training set selection	16.00	560 sec[3]	99	50
	TAPEJOB-rewrite tape from IHIST in BCD	0.25	700 sec[3]	2	63
	PROTO-produces sums of data used in TYPEPIX	2.00	6 sec[4]	12	2
	TYPEPIX-produces classification map (4 parts) on EAI plotter	4.00	389 sec[5]	25	245
	Total	24.75	4.56 hrs	153	641

[1]GS-9, $6.17 per hour rounded to the nearest dollar

[2]Computed at the commercial rate of $60.00 per hour.

[3]Univac 1108; $0.09 per second.

[4]CDC 7600; charged for 34 accounting units (AUS) @ $0.07 per AUS. Averages out at $0.38 per second.

[5]CDC 7600; average for 4 runs = 218 AUS @ $0.07/AUS. Averages $0.63 per second.

RANGE INVENTORY

Classification and Mapping Plant Communities

Richard E. Francis and Richard S. Driscoll

Never in our Nation's history has our natural resource base been under such scrutiny and at the same time been in such great demand. The Nation's forest-range resources are being continuously sought by a demanding, ecologically aware public for various goods and services. These resources, within natural ecosystems that produce or could produce herbaceous and shrubby vegetation, occur on approximately 63 percent of the land area of the 48 contiguous states (Forest-Range Task Force 1972). Natural resource inventories and reinventories are required to assess causes and effects of change to meet multiple resource management decisions.

The initial requisite for forest-range inventory and monitoring is to determine what the resources are, where they are, and how much is present. What they are involves a hierarchy of plant community classification. Where they are involves geographic location. How much is present involves area measurement of the communities and quantification of their parameters. How Skylab data could fulfill this requisite formed the basis for the research reported here.

The primary objective of this research was to determine at what level in a plant community classification hierarchy Skylab photographic products, or their equivalent, can be used for plant community classification in a central Colorado mountainous area. Secondary objectives were (1) to determine the kind of aircraft support photography needed to extend these classifications to other levels in the hierarchy, (2) to determine how both Skylab and aircraft support photography can be used to detect and identify

cultural features of a mountainous landscape that could affect resource management alternatives, and (3) to make quantitative estimates of certain plant community characteristics from large-scale aircraft photography.

Background

This is the latest in a series of studies that began in 1967 to evaluate remote sensing technology for range inventories. The Rocky Mountain Forest and Range Experiment Station, located in the center of a variety of range plant community systems, was a proper focal point for this research.

Initial studies conducted in 1967 investigated large-scale 70-mm color and color infrared (CIR) photographs (1:600 to 1:4,600) for identifying plant species (Driscoll 1969). From this work it was concluded that major rangeland species can be identified most consistently on 1:600 and 1:1,200 scale CIR photographs.

In 1968, the Rocky Mountain Station entered into a 4-year study under the NASA Earth Resources Aircraft Program to evaluate multiband photography and multispectral scanner imagery taken from both aircraft and spacecraft. Results indicated that CIR photographs taken from space (Apollo 9, 100-meter ground resolution) can be used to map general plant community systems (Driscoll and Francis 1972). However, larger scale (1:20,000 to 1:80,000) aircraft photographs with 3- to 10-meter ground resolution were required to determine the areal extent of the individual habitat types. Still larger scale aerial photographs (>1:2,400) were needed to analyze community components. Initial efforts to relate optical film density measured on small-scale CIR photographs to plant communities showed promise.

In 1972, the Rocky Mountain Station and its range inventory research team initiated a study to assess the value of low-resolution (65- to 100-

meter ground resolution) LANDSAT-1 (ERTS-1) MSS data for classifying plant communities (Heller and others 1974). This study showed that LANDSAT imagery acquired in August was best for the Region level (ECOCLASS) classification. Aspen can be reliably separated from conifer only during this time of year (92 percent accuracy). Conifer and grassland, on the other hand, can be classified on June-to-September LANDSAT and high-flight aerial photos with 95 to 99 percent accuracy. Regardless of season, interpreters could not classify to the Series level (ECOCLASS) with acceptable results. An analysis of optical film density measured on LANDSAT photographic color composites showed highly significant differences between all Region level vegetation classes. Thus, automatic scanning of LANDSAT photographic data and computer-assisted classification of Region level vegetation classes seemed possible.

Skylab photographs used in this study have better ground resolution (S190A, 30 to 120 meters; S190B, 20 to 30 meters) than either Apollo 9 or LANDSAT images. An evaluation of this improved data was important for planning future earth resources satellite programs for forest-rangeland assessments.

Study Area

The study area is located between 38°30' and 39°30' north latitude and 104°40' and 106°10' west longitude and includes approximately 14,000 square kilometers (5,400 square miles)(fig. 15). Included within the area is the NASA/Manitou Test Site, No. 242. From 1969 to 1972, considerable work was done there to determine the best aerial photo film, filter, scale, and seasonal combinations to characterize and quantify plant community systems and their components.

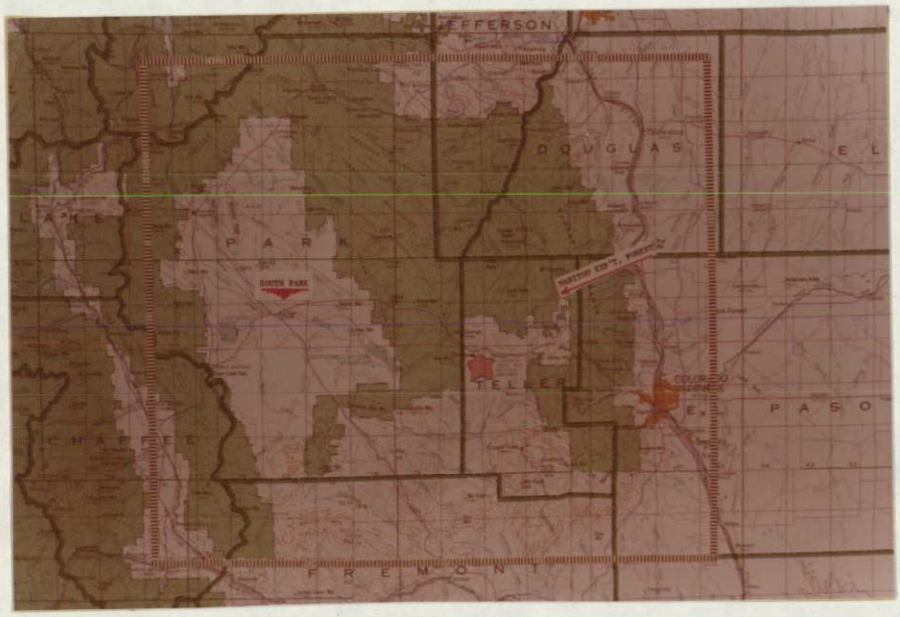

Figure 15.--Geographic location of the mountainous central Colorado study area. The area included approximately 14,000 square kilometers (5,400 square miles). Two intensive test sites can be seen--South Park and the Manitou Experimental Forest. Colorado Springs appears near the SE corner of the area.

This nonurban, nonagricultural area in central Colorado is characterized by extreme diversity in plant community systems and extreme variations in topography. For example, ponderosa pine (Pinus ponderosa Laws.) forests occur mostly on ridges and slopes between 2,000 and 2,700 meters (6,500 and 8,800 feet), but extend below this zone to 1,800 meters (5,900 feet) and above the zone to 3,000 meters (9,800 feet) depending on local environmental conditions. Other community systems vary similarly. In general, however, the vegetation aligns itself to changes in elevation, but frequently terrain slope and aspect compensate for elevation differences.

The vegetation in the area consists of a variety of forests and grasslands. The forests, ranging from approximately 1,900 meters (6,232 feet) above mean sea level to tree line at approximately 3,500 meters (11,480 feet), include: (1) ponderosa pine, (2) Douglas-fir (Pseudotsuga menziesii var. glauca [Beissn.] Franco), (3) lodgepole pine (Pinus contorta var. latifolia Engelm.), and (4) spruce/fir--primarily a mix of Engelmann spruce (Picea engelmanni Parry) and subalpine fir (Abies lasiocarpa [Hook.] Nutt.). Intermingled throughout the area are deciduous forests of quaking aspen (Populus tremuloides Michx.). These forests occur as "pure" types, but frequently there are varying mixtures of species in the ecotones between forest types or as a result of plant succession due to man-caused disturbance. In addition, the forest canopy varies from open to dense. The open tree stands permit the development of an extensive herbaceous and/or shrubby understory; little understory exists within the dense forest stands.

Mountain bunchgrass parks, in which Arizona fescue (Festuca arizonica Vasey) and mountain muhly (Muhlenbergia montana [Nutt.] Hitchc.) were the dominant grasses, occur in the lower elevation areas and are principally

associated with the ponderosa pine forests. These dominants are replaced by other species of fescue (Idaho fescue (F. idahoensis Elmer) and Thurber fescue (F. thurberi Vasey)) and oatgrass (Danthonia parryi Schribn.) at higher elevations. In many instances the gradation from forest to grassland is subtle, and it was difficult even at ground level to establish the line of demarcation between the two systems (fig. 16).

Within the central part of the study area is South Park, a large, nearly treeless area. The vegetation of South Park is generally of low stature in which blue grama (Bouteloua gracilis [H.B.K.] Lag.), slimstem muhley (Muhlenbergia filiculmis Vasey), and several low-growing shrubs and forbs are the most prominent. These and associated species provide the aspect of a shortgrass prairie. Around the fringes of the Park, and in some places within the Park where herbaceous communities interface with the forests, mountain bunchgrass communities become prominent.

Wet meadow and stream bank communities are especially well developed in South Park and occur as occasional narrow strips throughout the entire area. Various species of sedges (Carex L.), rushes (Juncus L.), and bulrush (Scripus L.) predominated either as monospecific or mixed stands in the moist areas. Tufted hairgrass (Deschampsia caespitosa (L.) Beauv.), mixed with species of bluegrass (Poa L.), formed communities in those areas that are less moist. In association with the meadows throughout the study area, there are shrubby communities dominated by species of willow (Salix L.) and shrubby cinquefoil (Potentilla fruticosa L.).

The main portion of the study area varies topographically from 2,100 to 4,300 meters (6,888 to 14,104 feet) above mean sea level. Elevation variations are dramatic--as much as 400 meters per kilometer (2,000 feet

Figure 16.--Ground photo shows the gradation and mixing between and within the forest and grassland vegetation systems. The forest system is a mixture of aspen and spruce/fir. Mountain bunchgrass (on slopes) and a high elevation wet meadow (valley floor) are the grassland systems. Note the extremely dense shadow on the north slope (left center) which affected classification.

per mile) in many places. The average elevation of South Park is 2,750 meters (9,020 feet) above mean sea level.

The eastern portion of the study area is associated geologically with the Pikes Peak and Kenosha batholiths, comprised primarily of granitic mountains and outwash. The mountains in the eastern portion consist of highly intruded sediments; the intrusions are primarily of granite or granite-gneiss material with some schists. Trachytic and andesitic extrusive flows are relatively common, especially in the southwestern part of the area. The western mountains have been highly dissected by glaciation--the outwash conglomerate deposits are common within and around the mountains. The northern end of the area is framed by the Kenosha batholith and other intrusive materials. The southern part of the area is associated with the Arkansas Hills, an ancient volcanic region from which extensive andesitic flows originated. Also associated with the southern portion are geologically old uplifted sediments. Igneous intrusions and flows are abundant through South Park (Weimer and Haun 1960).

Generally, the mountain ranges in the area are oriented on a north-south axis, but many spur-fragments, as well as individual units within the major ranges, are oriented east-west. This presented a complex matrix of various slope-aspect relationships that influences vegetation patterns and adds to the complexity of interpreting the remotely sensed data.

Skylab and Support Data

Only S190A and S190B photographic data from SL-2 (June 11, 1973) and SL-3 (August 4, 1973) were used in this analysis (table 19). Of the S190A Multispectral Camera System products, only color and CIR 70 mm photographs could be used. S190A material was available from both SL-2 and SL-3 but

the overall image quality was only fair. Photographs from the S190B Earth Terrain Camera System were available only from the SL-3 mission. The overall quality of these photographs was very good.

Our initial proposal also called for the analysis of data from both the S191 Infrared Spectrometer and the S192 Multispectral Scanner systems. However, the imagery from both of these systems was excluded from the analysis due to delays in obtaining the rectified data and the workload time constraints that resulted. It should be noted, however, that the sampling design used for testing photographic products in this study was based on the expected resolution of the S191 system (435 meters or 1,427 feet).

Two aircraft missions were flown by the NASA aircraft support program to assist the interpretation of the Skylab products for the defined objectives. MX-239 (June 22, 1973) and MX-248 (August 9, 1973) provided both color and CIR photographic products at three scales (table 19). The overall quality of these photographs was very good. This photography was timed to represent plant phenological conditions on the dates of the Skylab passes. In addition, both color and CIR large-scale 70 mm photography was flown by a U. S. Forest Service aircraft (table 19). These photographs were obtained on August 24, 1973--within three weeks of the SL-3 photographs. Only the CIR was analyzed to estimate specific quantitative grassland plant community parameters. Film quality was poor due to severe reticulation.

Classification System

The hierarchical vegetation classification scheme used to evaluate the effectiveness of the Skylab and supporting aircraft data was

ECOCLASS (Ecosystem Task Force, 1973), which was established according to ecological principles of polyclimax concepts (Daubenmire 1952). This system is in current use by the Forest Service to classify plant communities for land management planning, and is in accord with that established by the International Biological Program for classifying terrestrial communities (Peterken 1970).

The system defines five categories proceeding from the most general to the most specific, as follows:

V. Formation - The most general class of vegetation, characterized by general appearance: Grassland, Coniferous Forest, Deciduous Forest, etc. The basis of this category is continental in scope, i.e., all of the United States, and is controlled by continental climatic differences.

IV. Region - Subdivisions of the formation, associated regionally and therefore determined by subclimates within continental climates: Montane Grassland, Temperate Mesophytic Coniferous Forest, Alpine Grassland, etc.

III. Series - A group of vegetation systems within the Region category, with a common dominant climax species: Ponderosa Pine Forest, Fescue Grassland, Herbaceous Meadow, etc.

II. Habitat Type - Units within a series, each with relatively pure internal biotic and abiotic structure: Ponderosa Pine-Arizona Fescue habitat type, Arizona Fescue-Mountain Muhly habitat type, etc. <u>These are the elemental units of the classification scheme upon which primary management is based</u>. These units are frequently related to climax vegetation or vegetation held in a relatively stable state of high succession by proper management.

I. Community Type - A system that appears relatively stable under

management and may be equivalent to the habitat type. Usually the biotic components are dissimilar, but abiotic components are analogous to habitat type.

The entire study area is considered to be within one general physiographic province, the Central Rocky Mountains, in which three Formation categories occurred: Grasslands, Coniferous Forests, and Deciduous Forests. Within these Formation categories, three Region and eight Series categories were defined for this study:

IV. REGION	III. SERIES
1. Coniferous Forest	1. Ponderosa Pine
	2. Lodgepole Pine
	3. Douglas-fir
	4. Spruce/Fir
2. Deciduous Forest	1. Aspen
3. Grassland	1. Shortgrass
	2. Mountain Bunchgrass
	3. Wet Meadow

Ground Truth

A combination of ground checks and existing maps were used to verify the interpretation of Skylab and underflight photographic data.

Visual and microdensitometer classifications of plant communities were checked with a 10 percent ground sample of the 660 photo samples used in the study. Less than 5 percent of the ground samples were found misclassified. This lead us to believe that the remaining classifications would be acceptable to meet the study objectives.

Vegetation maps prepared from Skylab and underflight photographs were verified against existing Forest Service range and forest vegetation type-maps. To prepare a base vegetation map from Forest Service type-maps, Series level (ECOCLASS) class boundaries were traced directly on the base. However, since the Forest Service type-maps were functionally developed they had to be reorganized on an ecological basis. This meant combining and integrating some of the existing type-groups to meet our objectives. As an example, on the forest type-map, aspen was separated into commercial and noncommercial classes. For our purposes, the two classes were combined.

Foliar estimates made on large-scale color photographs were verified using ground data obtained from two grassland sites within South Park--subsequently referred to as Eleven Mile and Antero. Five plots were established at the Eleven Mile site and four plots at the Antero site. Each plot was 10 meters (32.8 feet) square. Within each plot, four 10-meter (32.8 feet) transects were established and marked with white wooden surveyor stakes laid flat on the ground. The transect locations were marked prior to the photo mission so that they could be located in the subsequent aerial photography.

Estimates of plant species foliar cover, litter, and bare soil were obtained using a line intercept technique (Canfield 1942). The technique was modified to use 10-meter (32.8 feet) transects rather than 100-foot transects as specified by the author.

Photo Interpretation Procedures

Visual Interpretation

Plant Community Classification

Vegetation type-maps, topographic maps, ground reconnaissance, and aerial photographs were used to select and locate sample cells for photo

interpretation of both the Skylab and support aerial photographs. The sample cells were initially selected and plotted on vegetation type-maps and topographic maps to represent an area approximately 500 meters square (1,640 feet square). The size of the data cell was determined by: (1) the expected resolution of the Skylab S191 EREP products which were to be compared with photographic products,[6] (2) the expected positional errors in both the satellite and data collection systems, (3) the plotting errors in transferring sample cells from maps to the Skylab and supporting aircraft photographs, and (4) the need to minimize edge effects of cell-wall lines. There were 660 cells used for training and testing photo interpretation--at least 20 cells were selected in each vegetation class.

Photo interpretation was conducted using: (1) the SL-2 and SL-3 S190A color and color infrared photographic products, (2) the SL-3 S190B color photographic products, and (3) the MX-238 and MX-249 color and color infrared support aircraft photography.

Transparant overlays were constructed for the Skylab photographs which showed the training and test cell locations for the study area (fig. 17). The Universal Transverse Mercator (UTM) coordinates representing the location of each cell were precisely plotted to a scale of 1:100,000 on the overlay. Obvious landmarks were also plotted to assist in positioning the overlays on the Skylab frames. These overlays were then photographically reduced on 0.004 mil clear positive film to the appropriate scale matching the Skylab S190A and S190B formats.

---

[6]Skylab S191 and S192 data were subsequently excluded from any analysis procedures.

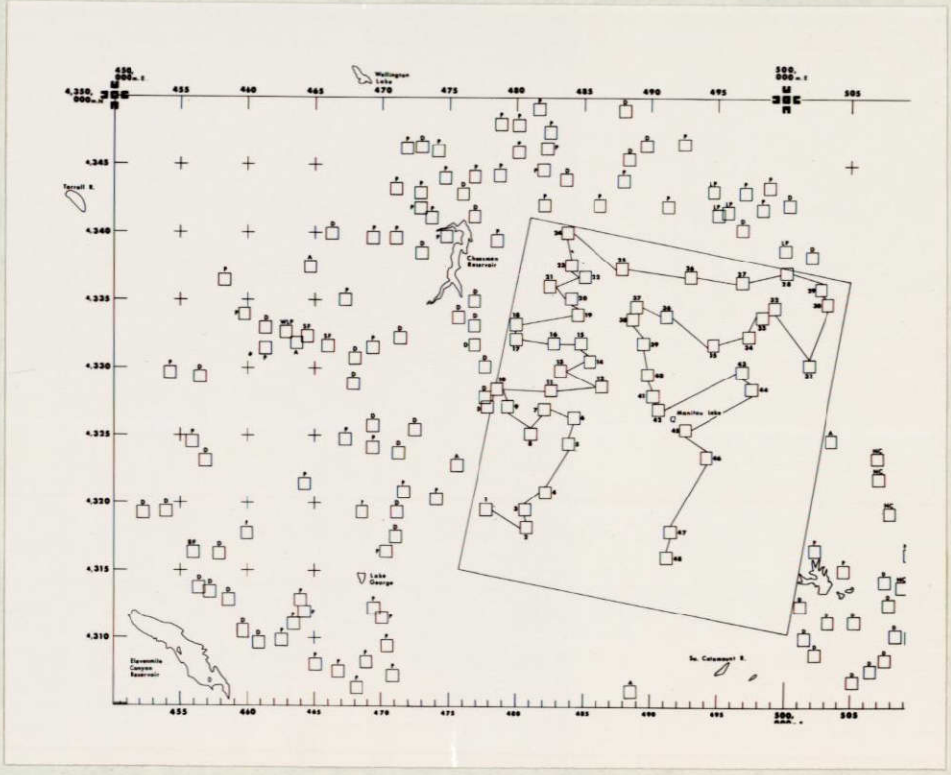

Figure 17.--An example of the transparent overlays used to locate training and testing sample cells. These cells were used for visual and microdensitometer interpretation of the Skylab photographs. Each small square represents an area approximately 500 meters square (1,640 feet square).

The same sample cell locations were used again to interpret the aircraft support photographs. Cell locations were transferred directly from the vegetation and topographic maps to overlays on the aerial photographs.

A factorial design for analysis of variance was used to test for differences between the appropriate factors of film type, photo scale, flight date, photo interpreter, and plant community class. All factors were considered to be fixed effects. The highest order interaction term was used as the error term to obtain the F statistic.

Plant Community Mapping

U. S. Forest Service vegetation type-maps were used as base data to develop both a Region and Series level plant community classification map for areal comparison with maps drawn from Skylab and support aircraft photographs. The base map covered 138 square kilometers (54 square miles) within the Manitou area (fig. 15) and was initially drawn to the Series level. Region level maps were made by consolidating Series classes into the three Region categories of coniferous, deciduous, and grassland.

The photographic products used were: (1) the SL-3 S190A color transparencies and (2) the MX-248 1:100,000 scale CIR transparencies. The two photographic products were not truly comparable film types but were used because they offered the best photographic quality available from the two types of photography. The area to be typed was imaged within one frame of the aircraft photography, thereby reducing interframe differences. Photographs from SL-2 S190A and SL-3 S190B could not be used because of cloud cover over the Manitou area.

Separate and completely independent vegetation maps were made to the Series level from stereoscopic examination of Skylab and underflight

photographs. Once the maps were completed, they were brought to the same scale for comparison using a Bausch and Lomb Zoom Transfer Scope (ZTS).

Areal comparisons between the vegetation base map and the Skylab and underflight vegetation maps were accomplished using planimetric methods.

Cultural Feature Mapping

To examine the possibilities of using Skylab photography to interpret and map cultural features, a 156-square-kilometer (61-square-mile) area was selected within the study site. Within this area cultural features were mapped from Skylab and underflight photographs and compared with cultural features traced from a 1956 USGS quadrangle sheet.

Photo interpretation was carried out on SL-3 S190B photographic products enlarged to twice their original scale (1:500,000) and underflight CIR photos (1:100,000 scale). In attempting to map from the Skylab material, detail could be seen under a zoom stereoscope, but the majority of detail was lost while transferring information to a map under the ZTS. Therefore, an overlay was placed on the Skylab photo and a needle was used to etch the location of road systems into the overlay. Using this technique, the zoom stereoscope could be used and more detail seen and mapped. Once the road system net was etched into the overlay, the etched overlay was put onto the ZTS and enlarged. Using the enlarged road system net overlay as a reference, the other cultural features were mapped by referring back to the original Skylab photos under the zoom stereoscope. Next, a photo-revised cultural feature map was made with additional information obtained by photo interpretation of the underflight photos. The underflight photography offered better resolution than did Skylab; therefore, the road system net was transferred directly to an overlay base map with

the ZTS. Once this was done, the other cultural features were mapped by referring back to the underflight photos under the stereoscope.

Foliar Cover Estimates

Large-scale (1:600) 70 mm CIR photographs taken from a Forest Service aircraft were used to determine the proportionate amounts of live vegetative foliar cover and bare ground for selected grassland sites within the study area. The ultimate intent is to use these kinds of data in quantitative sampling of ground surface characteristics as imaged in the satellite photographs.

Transects measured on the ground were located on the large-scale aerial photographs and foliar cover measured using three methods: (1) a zoom stereoscope, (2) a hand-held measuring micrometer, and (3) image magnification using the viewing screen of a GAF microdensitometer.

Linear regression was used to determine the relationships between image-measured cover estimates and those estimates obtained on the ground.

Microdensitometric Interpretation

A GAF Model 650 microdensitometer (fig. 18) was used to evaluate the Skylab photographic products for classifying plant communities. A microdensitometer measures the optical density of an image on a photographic transparency using a calibrated light source. S190A normal-color photos and CIR photos from SL-2 and SL-3, and normal-color photos from S190B, (SL-3) were used in the evaluation.

All normal-color photographs were examined using a green filter in the optical system; the CIR photos were examined with a red filter. These filters were inserted into the light-beam path for enhancement of the color

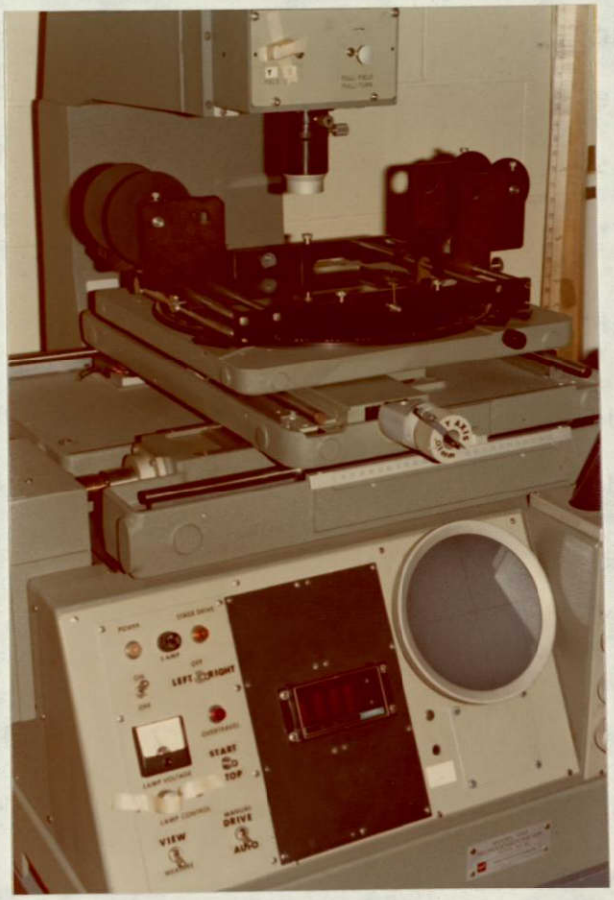

Figure 18.--Photo shows a GAF microdensitometer used to obtain optical image density. The light beam tube and moveable image-holding stage can be seen in the center of the photo. In the lower center of the photo the circular viewing screen can be seen. The viewing screen and stage also aided in the estimation of foliar cover from large-scale photos.

and CIR vegetation signatures. An effective circular aperture covering an image area of 6,640 square microns was used with the S190A material. For the S190B material, an effective circular aperture covering an image area of 41,500 square microns was used. These effective areas provided a circular image with the diameter approximating the side dimensions of the sample cells used for visual interpretation.

The same sample cells used in the photo interpretation test were measured with the microdensitometer. Optical image density measurements were made of each sample cell. The calibrated light beam of the microdensitometer was aligned with the cell location using the sample-cell overlay described under visual interpretation procedures. The apparent optical density of the transparent overlay was compensated for to remove this effect from the apparent image density values. Values from all sample cells were obtained.

A two-tailed t test was used to determine whether there was a significant difference between optical density sample means for both the Series and Region level classifications. It was assumed that the sample variances were equal.

Results and Discussion

Results indicate that Skylab and support aircraft photographic products can be successfully used to classify and map the areal extent of native plant communities to the Region level of classification using visual photo interpretation. Series level classification from these same photo products indicates that the results are dependent on date, scale, and film type. Areal mapping of plant communities at the Series level required formation of class-complexes.

Table 20. Accuracy of visual classification for Region level plant communities by date, scale, and film type.

Data source	Date/Scale	Region classification: Deciduous C[1]	Deciduous CIR[2]	Conifer C	Conifer CIR	Grassland C	Grassland CIR
		- - - - - - - - -percent- - - - - - - - -					
	June 1973						
Aircraft							
RB-57	1:50,000	nd[3]	88.9	nd	99.4	nd	100.0
	1:100,000	58.8	72.2	99.7	98.9	100.0	100.0
	1:400,000	nd	63.9	nd	99.7	nd	98.4
Skylab							
S190B	1:1,000,000	nd	nd	nd	nd	nd	nd
S190A	1:2,800,000	33.4	40.0	100.0	97.3	97.5	89.8
	August 1973						
Aircraft							
RB-57	1:50,000	nd	77.8	nd	98.2	nd	100.0
	1:100,000	44.2	88.1	98.9	96.8	100.0	100.0
	1:400,000	50.0	87.9	98.2	98.6	98.2	98.2
Skylab							
S190B	1:1,000,000	25.0	nd	98.4	nd	95.8	nd
S190A	1:2,800,000	20.6	41.5	99.3	97.9	100.0	95.8

[1]C = color film; mean percent correct for two interpreters

[2]CIR = color infrared film; mean percent correct for two interpreters

[3]nd = no data available

The Deciduous category was date, film-type, and scale dependent; only CIR provided acceptable accuracies (table 20). One acceptable level (88.9 percent) was obtained for the June 1:50,000 scale photos, and the August date provided two acceptable levels from 1:100,000 (88.1 percent) and 1:400,000 (87.9 percent) scale photos. Interpretation accuracy on 1:50,000 scale August photos was only 77.8 percent--not as acceptable as the June 1:50,000 scale photos--probably due to interpreter fatigue or the result of the testing sequence used.

Differences between photo interpreters were generally small and non-significant. However, the photo interpreter most knowledgeable about the physiography and vegetation of the test area provided the greater (although nonsignificant) accuracies.

The majority of commission errors for both color and color infrared film occurred when the Deciduous class was identified as Conifer (table 21). This was due to the heterogeneous mixing of these two classes of vegetation in the Deciduous test cells (fig. 19) and the difficulty of the interpreters to make a decision as to Deciduous dominance within a test cell. Very few of the Conifer class were committed to the Deciduous class, however, because most of the Conifer test cells were obvious in their homogeneous Conifer dominance. Those test cells that were correctly identified as Deciduous were homogeneous (fig. 19). The June and August dates, using CIR film, had significantly ($p = 0.99$) fewer commission errors of the Deciduous class to Conifer than when using color film. Also with CIR film, the August date had significantly ($p = 0.90$) less Deciduous class commission errors to Conifer than did the June date. This was due to the greater separability between Deciduous and Conifer using CIR, and that an even greater separation occurred at the August date due to the beginning

Table 21. Visual classification accuracy and commission errors for Region plant communities from Skylab and aircraft photos by date and film type.

Data source	Date/Region classification	Correct classification[1]		Commission errors					
				Deciduous		Conifer		Grassland	
		C[2]	CIR[3]	C	CIR	C	CIR	C	CIR
		- - - - - - - - - -		-percent-		- - - - - - - - - -			
	June 1973								
Aircraft									
	Deciduous	58.8	75.0	X	X	41.2	24.1	0	0.9
	Conifer	99.7	99.3	0	0.4	X	X	0.3	0.3
	Grassland	100.0	99.5	0	0.5	0	0	X	X
Skylab									
	Deciduous	33.4	40.0	X	X	59.9	56.7	6.7	3.3
	Conifer	100.0	97.3	0	1.4	X	X	0	1.3
	Grassland	97.5	89.8	0	2.5	2.5	10.3	X	X
	August 1973								
Aircraft									
	Deciduous	47.1	84.6	X	X	52.9	15.4	0	0
	Conifer	98.6	97.9	0.9	1.7	X	X	0.5	0.4
	Grassland	99.1	99.4	0.9	0.6	0	0	X	X
Skylab									
	Deciduous	20.6	41.5	X	X	72.3	51.5	7.1	7.0
	Conifer	99.3	97.9	0	2.1	X	X	0.7	0
	Grassland	100.0	95.8	0	0	0	4.2	X	X

[1]Mean percent of three scales from aircraft photos and two scales from Skylab photos; two interpreters

[2]C = color film

[3]CIR = color infrared film

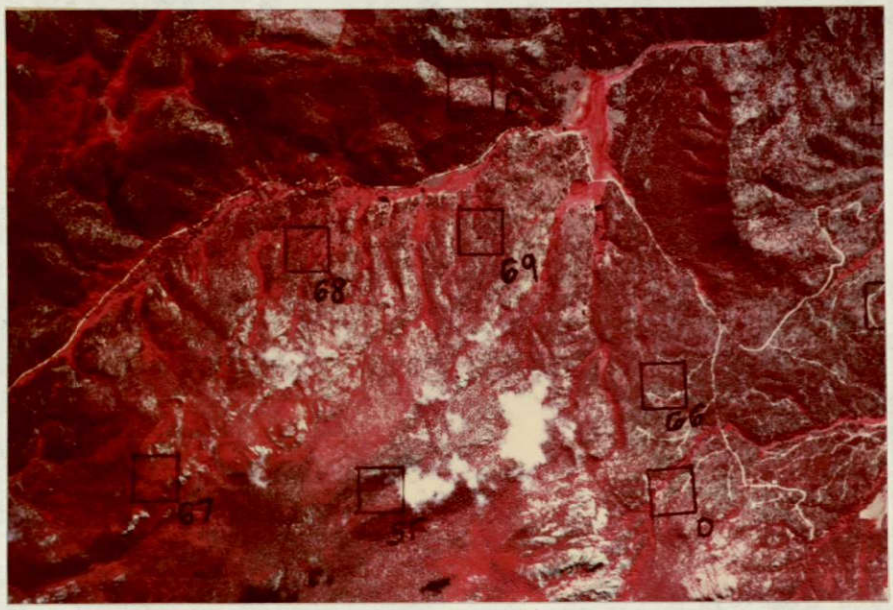

Figure 19.--An example of 1:50,000 scale CIR late-season (August) aircraft photography. Squares are training and test cells used to visually classify native plant communities from Skylab and aircraft photos. Each cell represented an area on the ground of approximately 500 meters square (1,640 feet square). In this example, training cells are labeled SF (Spruce/Fir) and D (Douglas-fir). Test cells are labeled 67 (Aspen) and 66, 68, and 69 (Ponderosa Pine). Interpreters classified each test cell to the Region and Series level. Note the Deciduous/Conifer (Aspen/Ponderosa Pine) mixing in cell 68, the variability within and between the Ponderosa Pine cells, and the similarity between the Spruce/Fir (SF) and Ponderosa Pine cell (69).

of leaf-color change of the Deciduous class. Deciduous leaves at the June date were only 1/2 to 2/3 developed and gave a low IR reflectance relative to the sensor altitude. Therefore, deciduous foliage was difficult to separate when mixed with conifers.

Commission errors of the Deciduous class to the Grassland class type resulted most often on the Skylab photographs (table 21). This was due to the extremely small scale and resultant difficulty of the interpreters to separate these two classes in ecotonal situations. This was further complicated by the subtle color difference between the Deciduous class and some members of the Grassland class in both the June and August photographs regardless of film type. Another factor involved in commission errors was the lack of topographic (stereo) relief near the mountain/grassland interface. Some misclassification was due to the positional accuracy of the photo overlay.

There were a small number of Conifer and Grassland commission errors for both film types (table 21)--the majority of them committed on Skylab photographs due to class mixing and misregistration of the sample location overlay.

Series Level - In general, of the five tree categories included, only Aspen was consistently classified with an acceptable level of accuracy and then only for the August CIR aircraft photos (table 22). The 1:50,000 scale approached an acceptable level with 77.8 percent while the 1:100,000 and 1:400,000 scales both exceeded the 80 percent accuracy level. The satellite photos had no acceptable levels for the Aspen Series class.

The Douglas-fir, Lodgepole Pine, Ponderosa Pine, and Spruce/Fir classes were occasionally classified with accuracies of 80 percent or greater, and then usually with the early-season smaller photo scales (table 22).

Table 22. Accuracy of visual classification for tree Series plant communities by date, scale, and film type.

Data source	Date/Scale	Tree Series classification: Aspen		Douglas-fir		Lodgepole Pine		Ponderosa Pine		Spruce/Fir	
		C[1]	CIR[2]	C	CIR	C	CIR	C	CIR	C	CIR
		- -percent -									
	June 1973										
Aircraft											
RB-57	1:50,000	nd[3]	88.9	nd	46.2	nd	21.5	nd	71.8	nd	86.1
	1:100,000	58.8	72.2	40.7	49.1	58.9	58.4	77.5	79.1	82.5	75.7
	1:400,000	nd	63.9	nd	45.4	nd	45.2	nd	79.1	nd	77.8
Skylab											
S190B	1:1,000,000	nd	nd	nd	nd	nd	nd	nd	nd	nd	nd
S190A	1:2,800,000	33.4	40.0	78.2	81.3	80.0	70.0	80.3	68.2	75.0	60.7
	August 1973										
Aircraft											
RB-57	1:50,000	nd	77.8	nd	48.0	nd	33.4	nd	73.2	nd	69.4
	1:100,000	44.2	88.1	56.9	59.1	52.3	48.4	69.9	70.7	78.3	77.3
	1:400,000	50.0	87.9	43.6	39.2	42.9	54.8	73.1	75.1	83.8	66.8
Skylab											
S190B	1:1,000,000	25.0	nd	76.3	nd	66.7	nd	75.7	nd	75.0	nd
S190A	1:2,800,000	20.6	41.5	65.9	65.8	72.9	66.7	73.2	82.6	70.0	48.6

[1]C = color film; mean percent for two interpreters
[2]CIR = color infrared film; mean percent for two interpreters
[3]nd = no data available

The greater accuracy at smaller scales was due to the blending of species mixtures into a more apparent homogeneous unit with the dominant species signature predominating. The decreased resolution at these smaller scales allowed the photo interpreter to classify the dominant characteristics with greater ease. However, some classification difficulty was still encountered due to species mixing and somewhat broad color signatures.

These classification difficulties resulted in commission errors for all the tree categories. Aspen was generally confused with Spruce/Fir regardless of date, scale, or film type due to their overlapping geographic range. The smallest commission error (5.9 percent), Aspen to Spruce/Fir, was obtained from the August CIR aircraft photos (table 23). At this date, CIR provided the necessary separation between the fall foliage coloration of Aspen and the dark green foliage of Spruce/Fir. Douglas-fir and Ponderosa Pine were most often confused with each other for all film types, dates, and scales. Generally, both Douglas-fir and Ponderosa Pine had the least commission errors (15.4 percent) on early-season (June) color and CIR satellite photography. At the same date, and on both color and CIR, commission errors were the greatest on the underflight aircraft photos (26.7 percent) and were essentially the same (nonsignificant differences) on the late-season (August) photography. The large number of commission errors on underflight aircraft photographs resulted because the Ponderosa Pine and Douglas-fir overlap and occupy the same geographic range but different physiographic positions in the landscape. Douglas-fir generally occurs on north and east slopes while Ponderosa Pine, within the same geographic range, generally occurs on south and west slopes. There is a topographic position, however, depending on the degree of slope and aspect, where the two species form a heterogeneous mixture. These facts cause severe problems in mountainous

Table 23. Visual classification accuracy and commission errors for Series level plant communities from Skylab and aircraft photos--August 1973, CIR.

Series class	Photo type	Correct classification[1]	A[2]	D-f[2]	LP[2]	PP[2]	SF[2]	MBG[2]	SG[2]	WM[2]
		- - - - - - - - - - - -percent - - - - - - - - - - - -								
Tree										
Aspen	U[3]	84.6	X	1.9	2.0	5.7	5.9			
	S[4]	41.5	X	17.2		10.0	24.3	7.2		
Douglas-fir	U	48.9	1.3	X	7.2	30.5	12.1			
	S	65.8	2.4	X	2.4	23.0	6.5			
Lodgepole Pine	U	45.2	0.8	15.7	X	14.0	24.3			
	S	66.7	8.4	16.7	X	8.4				
Ponderosa Pine	U	72.9	0.6	24.6	1.8	X				
	S	82.6	1.3	14.8		X	1.3			
Spruce/Fir	U	78.8	4.3	1.5	10.8	2.7	X	1.5		0.5
	S	52.5		10.0	25.0	12.5	X			
Grassland										
Mountain Bunch-grass	U	80.4	1.7					X	17.9	
	S	20.0				20.0		X	60.0	
Shortgrass	U	98.6						1.4	X	
	S	100.0							X	
Wet Meadow	U	100.0								X
	S	87.5						12.5		X

[1]Mean percent; see [3] and [4]

[2]A = Aspen
D-f = Douglas-fir
LP = Lodgepole Pine
PP = Ponderosa Pine
SF = Spruce/Fir
MBG = Mountain Bunchgrass
SG = Shortgrass
WM = Wet Meadow

[3]U = aircraft photos; mean percent for three scales, two interpreters

[4]S = Skylab photos; mean percent for two scales, two interpreters

terrain: (1) where the two species mix, separation is difficult and (2) in heavy shadows on north-facing slopes, it is difficult to determine where Ponderosa Pine forests terminate and Douglas-fir forests begin. Therefore, commission errors occur, from one species to the other, on the larger scale photos. The difficulty also arises when the photo interpreter makes a decision to call one type or the other based on crown density. His estimate may in fact be accurate, but the vegetation base maps used to establish the correctness of the classification may not be entirely accurate. The base maps differ in the way they were originally derived and their original intent, which was based upon merchantable timber and not necessarily cover-type dominance. Also, the smaller scale (satellite) photos allowed a greater synoptic view with less resolution, thereby providing the use of inference based on dominant color signature and topographic aspect for easier separation of community Series.

Interpretations of the Lodgepole Pine and Spruce/Fir community Series were also often confused. In general, the late-season (August) satellite photos, regardless of film type, provided fewer commission errors (9.9 percent) between the two Series classes. One exception was the lower commission error from Spruce/Fir to Lodgepole Pine on late-season CIR underflight photos (table 23).

The confusion between the Spruce/Fir and Lodgepole Pine classes most frequently occurred within ecotonal areas, and similar physiographic areas, where the geographic range of the two classes overlapped. Within these areas, especially on shadowed north slopes, the color signatures and image texture of the two classes were difficult to separate. Also, due to less resolution on the satellite photos and the synoptic view, fewer commission errors resulted between classes. Improvement in classification of the

Spruce/Fir class, however, resulted from interpretation of the underflight photos regardless of date (season) or film type. The Lodgepole Pine class was more correctly identified from the satellite photos. The accuracy of Lodgepole Pine and Spruce/Fir classes was the result of commission errors going to classes other than Lodgepole Pine or Spruce/Fir. This was due to the area overlap of some of the other tree Series or the lack of orientation and vegetation knowledge of the photo interpreter. In general, the photo interpreter with the most knowledge of the study area classified the tree Series more accurately by using inference and deductive reasoning as well as image signatures.

The three grassland Series classes (fig. 20) were correctly classified with mean accuracies of 80 percent or better from the underflight photos regardless of film type or season (table 24).

In both underflight and satellite photos, most of the commission errors occurred between the Mountain Bunchgrass and Shortgrass classes and between the Wet Meadow and Mountain Bunchgrass classes (table 23). Mountain Bunchgrass was most often classified as Shortgrass due to the ecotonal situation that exists between them. The two classes form a continuum and were difficult to classify especially on the satellite photos. The underflight photos, especially the 1:50,000 scale with improved resolution, provided a better estimate of the Series class "boundaries" and therefore fewer commission errors. Even though the satellite photos provided a greater synoptic view, the reduced resolution did not allow Series separation. The greater synoptic view and reduced resolution appear to be a disadvantage when compared to the tree Series classification which was more accurate due to the blending of color signatures which produced a dominant response.

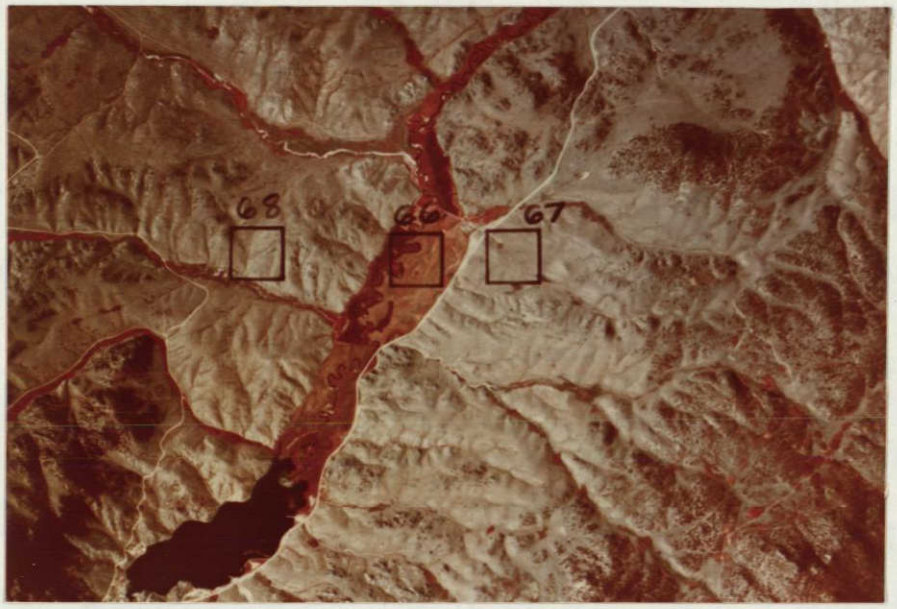

Figure 20.--An example of 1:50,000 scale CIR early-season (June) aircraft photography. Squares represent test cells used to visually classify native plant communities from Skylab and aircraft photos. Each cell represented approximately 500 meters square (1,640 feet square) on the ground. Cells show the three Grassland communities classified: Wet Meadow (66), Shortgrass (67), and Mountain Bunchgrass (68). In this example, there is maximum distinction between the three Series classes. However, cell 68 approaches the ecotone between Mountain Bunchgrass and Shortgrass. Interpreters classified the cells to both the Region and Series level.

The Wet Meadow Series was generally classified with an accuracy level of 80 percent or greater from both underflight and satellite photos (table 24). However, the underflight photos provided the most consistent results and were not date or film-type dependent. Few commission errors (2.7 percent) occurred for this Series class using underflight photos. Commission errors that averaged 21 percent did occur using the satellite photos. In both cases, the classification errors went to the Mountain Bunchgrass class. This was due primarily to the natural mixing of the two classes near mountain slopes. High density Mountain Bunchgrass provided the same color signature as lower density Wet Meadows on the very small-scale satellite photos.

Plant Community Mapping

Late-season (SL-3) S190A Skylab color photos and late-season (MX-248) underflight CIR photos were used to determine vegetation boundaries and estimate their areal extent within a 138-square-kilometer (54-square-mile) area of the Manitou site. These two film types were not totally comparable, but were chosen because they offered the best photographic quality needed to establish vegetation boundaries. U. S. Forest Service timber and range type-maps, reconstructed into a vegetation base map, were used as the basis for ground truth.

Region Level - The Skylab and underflight photos were both successfully used (accuracy > 80 percent) to map the areal extent of the Conifer and Grassland Region classes (table 25). Considering only these two classes, the greatest difference occurred between the vegetation base map and the Skylab map within the Grassland Region. The difference was due to the extremely small scale of the Skylab material and lower resolution.

Table 25. Comparison of base map areas with areas from underflight and Skylab maps for Region and Series classification levels.

Classification level	Classification type	Base map (Ground truth) Area (A)	Underflight map[1] Area (A)	Underflight map[1] Percent of base	Skylab map[2] Area (A)	Skylab map[2] Percent of base
Region	Deciduous (Aspen)	786	285	36.3	none	0
	Conifer	27,687	28,202	101.9	28,923	104.5
	Grassland (w/lake)	2,690	2,676	99.6	2,240	83.3
	TOTAL	31,163	31,163	---	31,163	---
Series	Aspen	786	285	36.3	none	0
	Ponderosa Pine	15,729	7,744	49.2	4,887	31.1
	Douglas-fir	10,269	8,630	84.0	6,546	63.7
	PP/D-f Complex[3]	25,998	26,707	102.7	25,788	99.2
	Lodgepole Pine	1,434	---	---	---	---
	Spruce/Fir	163	---	---	---	---
	LP/SF Complex[4]	1,597	1,495	93.6	3,135	196.3
	Grassland	2,397	2,092	87.3	2,240	93.5
	Wet Meadow	277	566	204.3	none	0
	Lake	16	18	112.5	---	---
	TOTAL	31,163	31,163	---	31,163	---

[1]Late season, CIR, 1:100,000 scale

[2]Late season, color, S190A

[3]Ponderosa Pine/Douglas-fir complex

[4]Lodgepole Pine/Spruce/Fir complex

The result was a reduction of about 17 percent in the Grassland class which, at the Manitou site, occurred in long narrow stringers between the tree stands. Manitou Lake was distinguishable in the Skylab photos, but it occurred within one of these narrow stringers and was too small to be measured planimetrically. Therefore, it was included with the Grassland class in all three Region maps.

The Deciduous (Aspen) class was not successfully mapped from either the underflight or the Skylab photos (table 25). This was due to small stand sizes and class mixing between it and the Conifer class. No deciduous class areas were mapped from the Skylab photos because of small stand size and scale and resolution restrictions of the imagery.

Small areal differences (about 2 percent) between the three maps were attributed to the mapping procedure, planimetric error, and nearly 20 years difference between the original source base map compilation and the current mapping attempts.

Series Level - The Mountain Bunchgrass and Shortgrass Series classes could not be distinguished well enough in the Skylab photos to be mapped separately. Therefore, they were combined into a single grassland Series class--the grassland Series class differs from the Grassland Region class in that the Region class includes Wet Meadows and Manitou Lake. With this Series combination, both the underflight and Skylab photos were used successfully (> 80 percent accuracy) to map the grassland areas (table 25).

The Wet Meadow class was overestimated from the underflight photos when compared with the vegetation base map (table 25). However, the map made from the aerial photographs provided a better estimate of the

ground condition than the base map; the base map was known to underestimate the classes. This was due to the difference in criteria used to identify Wet Meadows in the development of the base maps. For instance, the original timber-type base maps had no Wet Meadow category, and the range type-maps had a very limited Wet Meadow category which did not correspond with ground information from the Manitou site. Therefore, artificial Wet Meadow class boundaries were determined from the original type-maps and ground information. Furthermore, because the Wet Meadow class occurred as long narrow stringers, both within the grasslands and intermingled with the tree classes, the decreased resolution of the Skylab photographs would not permit mapping any of the Wet Meadow class (fig. 21).

The Douglas-fir Series was the only conifer class mapped successfully (> 80 percent accuracy) that was mapped from the underflight photos (table 25). Attempts were made to map the Lodgepole Pine and the Spruce/Fir Series but, due to the extreme difficulty in class separation, no area figures are given in Table 25.

In order to obtain successful mapping accuracies for all the tree Series classes, two class-complexes were formed: (1) Ponderosa Pine/Douglas-fir, and (2) Lodgepole Pine/Spruce/Fir. These complexes were necessary due to species mixing at ecotones, and slope/aspect relationships within these groups. Once the classes were combined, successful mapping was accomplished (table 25). The Ponderosa Pine/Douglas-fir complex was mapped within 1 to 3 percent of the base map estimates from both underflight and Skylab photos. The Lodgepole Pine/Spruce/Fir complex was mapped with 8 percent of the base map estimates from underflight photos, but was overestimated by nearly 100 percent from the Skylab photos. The smaller differences can be explained by mapping and planimetric error. The larger (100 percent)

(A) Base map

(B) Underflight map

(C) Skylab map

Figure 21.--Series level plant communities mapped by visual interpretation from a 138-square-kilometer (54-square-mile) area within the Manitou site. Original maps were scaled to approximately 1:50,000 using a ZTS. Copies here represent: (A) base map (facing page) compiled from U. S. Forest Service timber and range vegetation type-maps, (B) underflight map (facing page) compiled from late-season, 1:100,000 scale CIR aircraft photos, and (C) Skylab map compiled from late-season (SL-3) S190A color photos.

difference was also due to mapping error caused by including Aspen and Wet Meadow classes which were not discernible in the Skylab photos. The planimetric error was due to an increase in areal measurement error with smaller size mapping units.

The Aspen Series class could not be mapped from either the underflight or Skylab photos at the Manitou site (see Region Level-Deciduous class for details).

Manitou Lake was successfully mapped from the underflight photos and was distinguishable in the Skylab photos--however, it was too small to be measured planimetrically (table 25). Manitou Lake was not included with the grassland or Wet Meadow Series classes (as in the Region Level). Thus, a more representative areal estimate was obtained for these two classes at the Series level. The difference between the base map area for the lake and the area obtained from the underflight photos was due to the water level difference between the two map compilation dates.

The three resultant Series type-maps (ground truth base, underflight, and Skylab) can be compared in Figure 21.

Cultural Feature Mapping

Skylab S190B color photographs (August 4, 1973) enlarged two times and underflight CIR 1:100,000 scale photos (August 9, 1973) were used to update a cultural-feature inventory map. Ground truth information was obtained from the most recent (1956) USGS quadrangle and revised using the 1973 underflight photography (fig. 22). The cultural features found within the 156-square-kilometer (61-square-mile) area and a qualitative assessment of their interpretability is shown in Table 26 and discussed below.

Table 26. Qualitative assessment of Skylab and aircraft photographs for interpreting cultural features.

Photo type	Cultural feature[1]											
	Paved highway	Gravel road	Dirt road	Jeep trail	Utility corridor <10 yrs.	Utility corridor >10 yrs.	Buildings groups	Buildings single	Excavations general	Excavations specific	Wind mills	Cemetery
Skylab (1:500,000)	E	E	D-N	N	U-D	N	U	D	U	N	N	N
Aircraft (1:100,000)	E	E	U-D	D	E-U	U	E	U	E	U	D	N

[1]E = Cultural feature easily identified
U = Cultural feature usually identified
D = Cultural feature difficultly identified
N = Cultural feature not identified

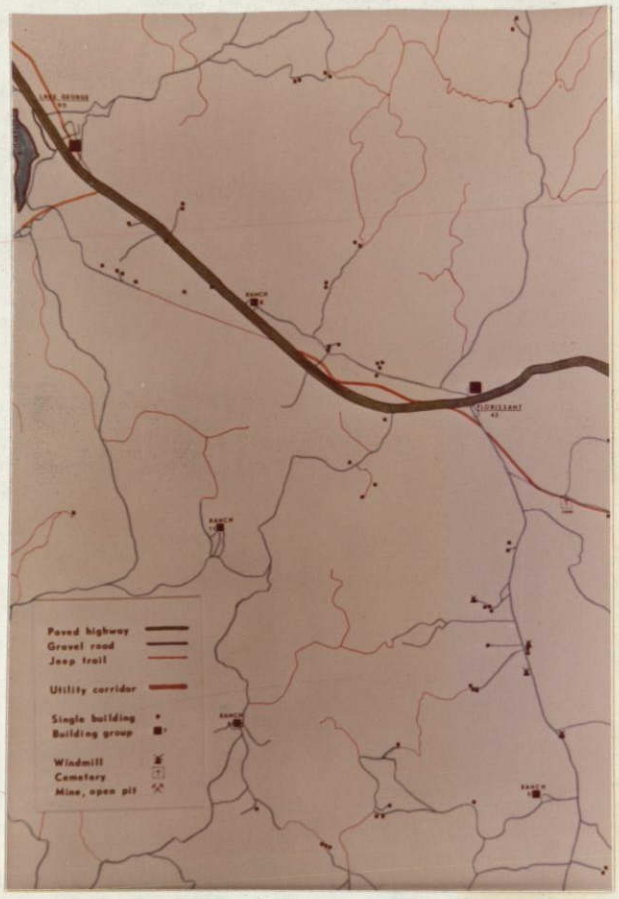

(A) Base map

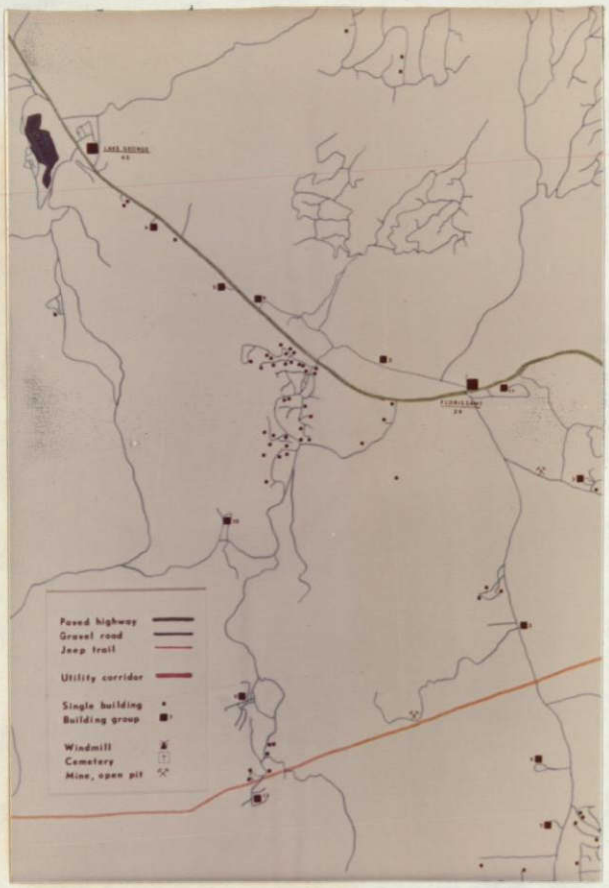

(B) Underflight map

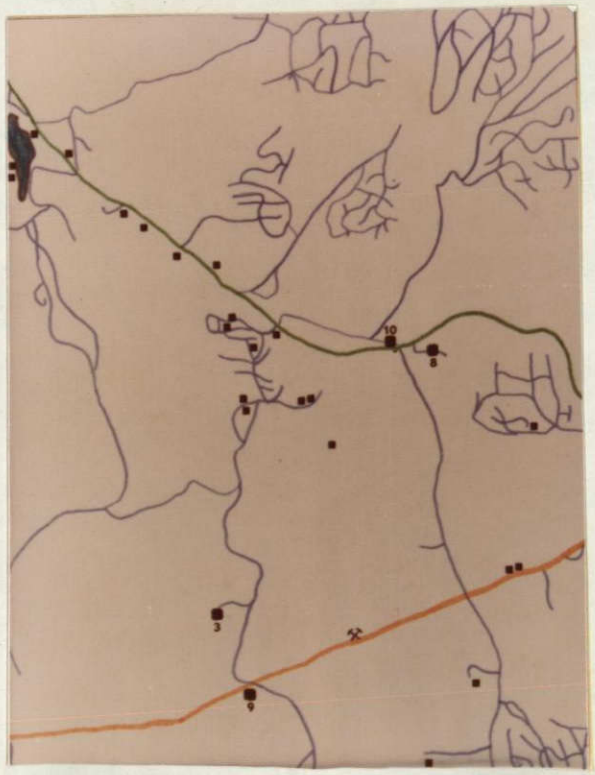

(C) Skylab map

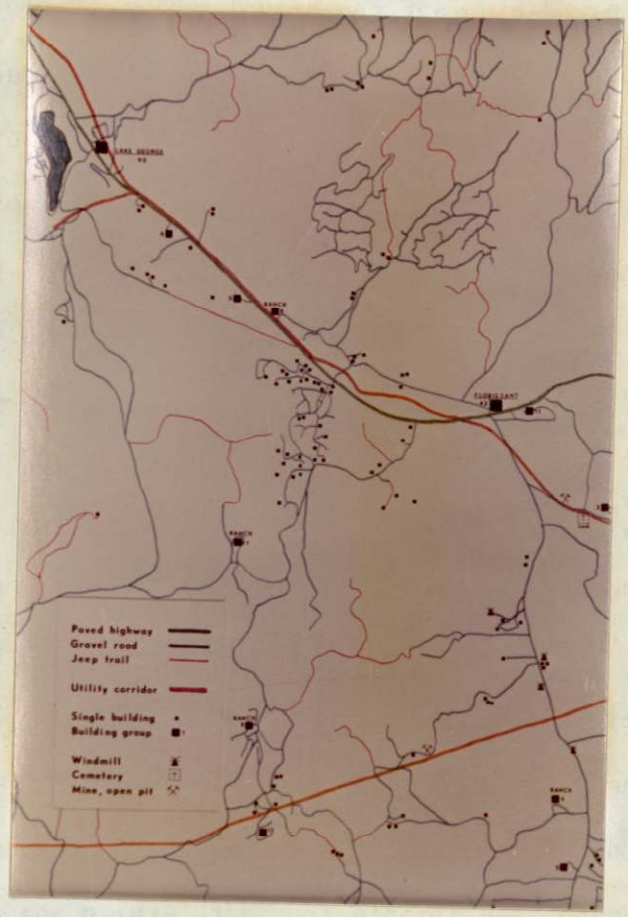

(D) Photo-revised map

Figure 22.--Cultural features mapped by visual interpretation from a 156-square-kilometer (61-square-mile) area within the study site. Original maps were scaled to 1:24,000 using a ZTS. The illustrations on the facing page represent a USGS quadrangle (1956) used as the base map (A), an underflight map compiled from 1:100,000 scale CIR aircraft photos (B), and a Skylab map compiled from 1:500,000 S190B photos (2X)(C). A photo-revised map compiled using the 1956 USGS quadrangle and the 1973 aircraft photos is shown above (D). The buildings grouped near the reservoir (upper left) in (C) were identified as single buildings in (B) and (D), but due to the large number they were grouped and totaled with the building complex at Lake George (upper left in (B) and (D)). Legends within (A), (B), and (D) also apply to (C).

Those features most easily identified from both satellite and underflight photos were paved highways and gravel roads. However, small segments of gravel roads that passed under tree canopies or across treeless areas could not be differentiated due to lack of scene contrast in open areas. This was especially evident in the satellite photos. The same problem existed when using the underflight photos but the problem was not as severe. The majority of the gravel road systems could be aligned on the underflight photos due to the larger scale, better resolution, and occasional openings in tree canopies which allowed at least partial viewing.

Infrequently used dirt roads or jeep trails could not be distinguished on the satellite photos and distinguished only with great difficulty on the underflight photos. These roads and trails have the inherent problems of canopy cover and related shadows, low scene contrast, and lack of resolution due to their narrow track width.

Utility corridors through forested areas, and those constructed within the past 10 years, were identifiable from both Skylab and underflight photos. The kind of utility corridor could not be determined from Skylab photos, but could generally be determined as either pipeline easement or power line from the underflight photos. Corridors older than 10 years usually could not be detected from Skylab photos due to vegetation regrowth, but generally could be detected and identified from underflight photos.

Earth excavation activities, including underground mining evidenced by refuse dumps, open stone quarries, and sand or gravel pits, could be identified as a group but not as to specific activity from the satellite photos. The specific activity could usually be identified from the larger

scale underflight photos. None of these excavations was shown on the USGS base map used as ground truth. Difficulties in identifying the specific activity from Skylab photos were due to lack of scene contrast and lower resolution.

Few individual residential or smaller commercial-sized buildings were detectable from Skylab photos, whereas most of these same structures were detectable from the underflight photos. Structures that were detectable from Skylab photos could not be differentiated as to kind, except the larger industrial facilities. Most individual buildings could be differentiated from underflight photos, except those in close proximity to one another or those that occurred near gravel and paved areas. In general, identification was based on the color and reflectivity of the roofing material, building size, and the scene contrast between the building and its surrounding environment. Buildings with bright-colored and/or highly reflective roofs (metal), located on grassy areas, were the easiest to identify or at least to detect.

Cemeteries could not be differentiated on either Skylab or underflight photos, even though they were generally located in treeless areas and the grassland vegetation was dissimilar inside and outside the cemetery sites.

Windmills could not be identified in either Skylab or underflight photos. However, areas could be detected which appeared to be windmill sites on the underflight photos. These areas had either more lush vegetation than surrounding areas, due to water seepage and little animal use, or they were more denuded due to cattle concentrations. The mills themselves could not be seen due to their small size.

In cultural-feature detection, convergent and divergent inferences can be made to aid identification and differentiation of particular

features by well-trained, knowledgeable photo interpreters. The resultant cultural feature maps (base, underflight, Skylab, and photo-revised) can be compared in Figure 23.

Foliar Cover Estimates

Large-scale (1:600) CIR 70 mm aerial photographs were used to obtain estimates of plant foliar cover, bare soil, and litter from two grassland sites (Antero and Eleven Mile) in the South Park portion of the study area. Aerial photo estimates were compared with ground estimates made prior to the overflight. Linear regression techniques were used to make the comparisons. Only correlation coefficients of 0.75 or greater were considered valuable.

Data were obtained for three cover type classes from the aerial photos: (1) shrubs, (2) herbaceous vegetation and litter, and (3) bare soil. Attempts were made to estimate foliar cover by plant species; however, due to strong vignetting at the photo edges and extreme emulsion reticulation, only the above three classes could be estimated.

Three interpretation techniques were used to estimate ground cover from the large-scale photographs: (1) a zoom stereoscope at 20X with monocular optics and a micrometer scale with 0.1 mm divisions, (2) same as above except stereo-optics were substituted for use with stereo photo pairs, and (3) a microdensitometer (MDT) with a moveable stage and a viewing screen (10X) with crosshairs to align the on-ground transect markers with the photo images.

The stereoscope and measuring micrometer with monocular optics provided only two correlation coefficients of 0.75 or greater for the three cover type classes at the two sites. Using the stereoscope and micrometer with stereo

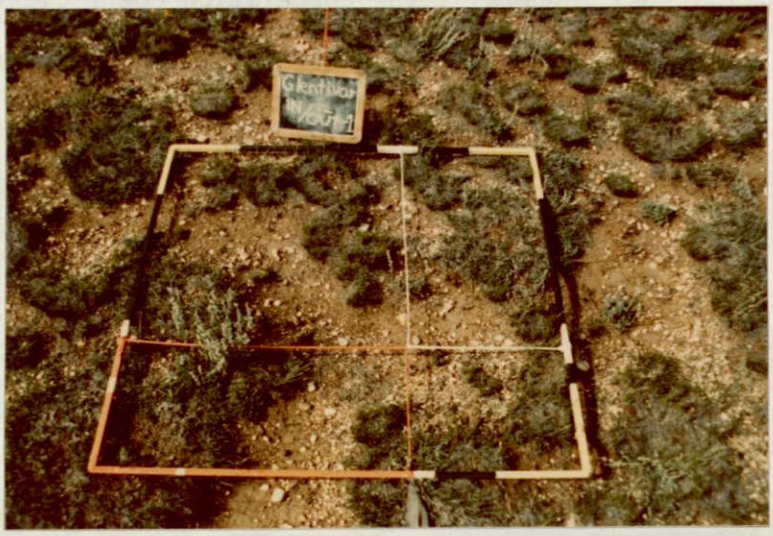

A

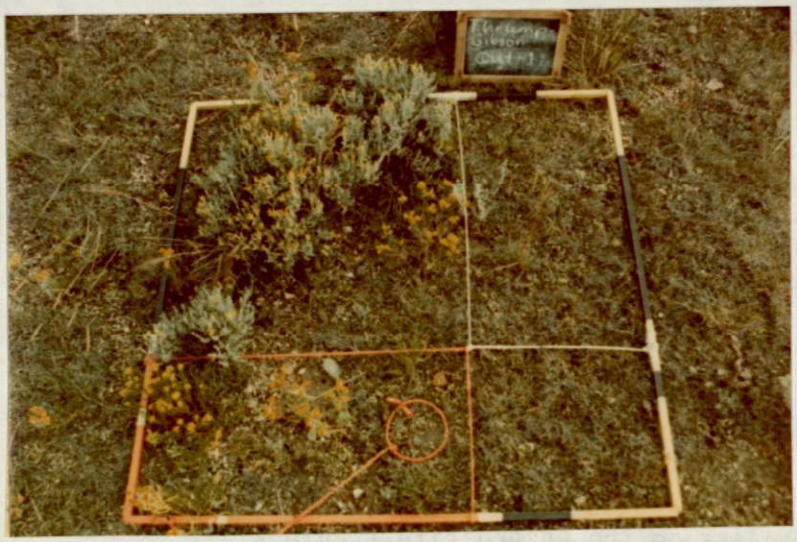

B

Figure 23.--Ground-photo comparison of the vegetation associations at two grassland sites within the South Park portion of the study area. These two sites were used to compare on-ground and aerial photo estimates of plant foliar cover. The vegetation at the Eleven Mile site (A) was less diverse, lacked shrubs, and was of a lower stature than that of the Antero site (B). The plot frame pictured represents 1 meter square (3.28 feet square).

photos, however, provided three correlation coefficients greater than 0.75 for the cover classes. Generally the correlation coefficients were higher for all other cover classes within both sites using this technique (table 27).

It was felt that the micrometer used with the stereoscope was a source of error for two reasons. First, the micrometer was difficult to align with the imaged transect location markers, and once aligned it was difficult to maintain the alignment. The smallest movement of the instrument caused misalignment and repeatability was difficult, if not impossible. Secondly, the micrometer increments became so large under 20X magnification that it was difficult to "see beyond" the markings onto the image even using stereo pairs.

The MDT, used as a viewing and scanning device, proved to be the most convenient and precise. The MDT allowed the transect location markers to be aligned precisely with the viewing screen crosshairs under 10X magnification. The alignment and measurements were also repeatable. The viewing screen also allowed for smaller incremental measurements (0.0001 mm). The major disadvantage was a lack of stereo coverage capability. Three correlation coefficients were significantly improved by this technique--the bare soil and litter/herbaceous classes on the Eleven Mile site and the bare soil class on the Antero site (table 27).

An outstanding fact became apparent from the results of this test. The correlation coefficients for the three classes were generally higher for the Eleven Mile site than the Antero site, regardless of the techniques used. This was difficult to understand because the photographs for both sites were taken on the same day (within an hour of each other), the photographs were of the same quality (although somewhat poor due to

vignetting and reticulation), and both sets of photographs were interpreted using the same techniques. Apparently the difference was due to the spatial arrangement, stature, and amount of vegetation at the two sites. Generally, the vegetation at the Eleven Mile site was less complex, less diverse, essentially lacking shrubs, and of lower stature than that of the Antero site (fig.23). The simplistic nature of the vegegation at the Eleven Mile site allowed a more precise estimate of the ground-cover classes. That is, the majority of the vegetative association was matte-forming blue grama and fringed sagebrush (Artemisia frigida Willd.), interspersed with definite areas of bare soil and litter. The fringed sagebrush and bare areas were readily interpretable, which left the remainder in the herbaceous/litter class. At the Antero site, fringed sagebrush was scarce and rabbitbrush (Chrysothamnus spp. Nutt.) and Actinea (Hymenoxys spp. Cass.) were the taller components of the system. These taller shrub and half-shrub components cast shadows which made interpretation difficult for those lower growing herbaceous plants which formed the understory. It was therefore relatively easy to differentiate the shrubby components, but quite difficult to differentiate the bare soil and herbaceous plant components in the shrub shadows.

Another factor affecting the cover class correlations was the fact that the mean bare soil estimates between the two sites were not significantly different ($p = 0.95$), but the range in bare soil percentages between transects within sites was significantly different ($p = 0.99$). The Eleven Mile and Antero sites had mean bare soil on-ground estimates of 24.9 and 25.4 percent, respectively, while individual transect estimates ranged from 10 to 54 percent at the Eleven Mile site and 15 to 45 percent at the Antero site.

Indications from these results are that bare soil, shrubs, and total vegetative cover can be estimated from large-scale photos in two-dimensional space avoiding plant shadows. Also, more accurate and precise estimates could be made by using photography that is not vignetted nor severely reticulated.

Microdensitometric Interpretation

An MDT was used to point-sample the optical image density of vegetation sample cells of established vegetation classes imaged on Skylab photographs. Standard t tests for unpaired plots and unequal sample sizes were used to determine whether there was a significant ($p \geq 0.95$) difference between optical density sample means for the Region and Series level vegetation classes.

Region Level - The optical density means for the Region level vegetation classes were significantly different except for the Deciduous (Aspen) versus Conifer class which was film-type dependent (table 28). The two classes were not significantly different from each other on CIR film from either the early- or late-season photos. This lack of separation was primarily due to the fact that even though the Deciduous and Conifer classes had dissimilar visual color signatures, they had similar optical densities on CIR film. There was also a class-mixing effect due to ecotonal situations between the individual type classes within these two broader classes. Therefore, the mean optical density seemed to be more dependent upon the mixture than the photo date. However, the Deciduous and Conifer classes were separable using color film even though it was somewhat date dependent. This film type provided a greater separation

Table 28. Mean optical density and the significance of differences between Region level plant communities from Skylab photographs by date, scale, and film type.

Region class	Mean optical density					
	June, S190A		August, S190A		August, S190B	
	C[1]	CIR[2]	C	CIR	C	CIR
Deciduous	3.32	3.86	4.08	2.06	3.90	no data
vs.	**	ns	*	ns	**	
Conifer	3.45	3.94	3.88	2.23	3.63	
Deciduous	3.32	3.86	4.08	2.06	3.90	no data
vs.	**	**	**	*	**	
Grassland	3.01	3.42	3.36	1.79	3.21	
Conifer	3.45	3.94	3.88	2.23	3.63	no data
vs.	**	**	**	**	**	
Grassland	3.01	3.42	3.36	1.79	3.21	

[1]C = color film

[2]CIR = color infrared film

ns = nonsignificant difference at p = 0.95

* = significant difference at p = 0.95

** = significant difference at p = 0.99

when the June S190A photos (p = 0.99) were compared with the August S190A photos (p = 0.95). The greater separation was probably due to the fact that the Deciduous class was in the midleaf to full-leaf stage at the early date and the leaves produced a very strong "light green" reflectance due to their active growth. The color of the lush new deciduous leaves provided less optical density than the darker needles of the Conifer class. The late-season Deciduous provided a darker density due to mature leaves, cessation of leaf activity, and some leaf drop at higher elevations. Therefore, its optical density was nearly as dense as that of the conifers and somewhat less separable.

Series Level - The MDT interpretation results for classification to the Series level were varied. For the three grassland Series tested, there was a significant (p = 0.99) difference between optical density mean values for all three Series classes from the late-season S190A color photos. There was also a significant (p = 0.99) difference between the Mountain Bunchgrass versus Wet Meadow and Shortgrass versus Wet Meadow Series class from both the early- and late-season normal-color photos (table 29). Lack of separation between the Mountain Bunchgrass/Shortgrass Series classes was probably due to their very close physiographic proximity. In most cases, they grow in a very pronounced ecotonal situation within South Park and are frequently difficult to separate on the ground. The two classes actually form a broad ecotone where the Mountain Bunchgrass communities gradually blend into the relative flat terrain Shortgrass communities within the Park (fig. 24); both classes are short statured within the ecotone.

The CIR film type from the early-season S190A photos provided no significant differences between the three grassland Series classes

Table 29. Mean optical density and the significance of differences between grassland Series plant communities from Skylab photographs by date, scale, film type.

Series class	Mean optical density					
	June, S190A		August, S190A		August, S190B	
	C[1]	CIR[2]	C	CIR	C	CIR
Mountain Bunchgrass	2.98	3.47	3.38	1.86	3.15	no data
vs.	ns	ns	**	**	ns	
Shortgrass	2.99	3.42	3.21	1.75	3.13	
Mountain Bunchgrass	2.98	3.47	3.38	1.86	3.15	no data
vs	**	ns	**	ns	**	
Wet Meadow	3.12	3.38	3.77	1.81	3.63	
Shortgrass	2.99	3.42	3.21	1.75	3.13	no data
vs	**	ns	**	ns	**	
Wet Meadow	3.12	3.38	3.77	1.81	3.63	

[1]C = color film

[2]CIR = color infrared film

ns = nonsignificant difference at p = 0.95

* = significant difference at p = 0.95

** = significant difference at p = 0.99

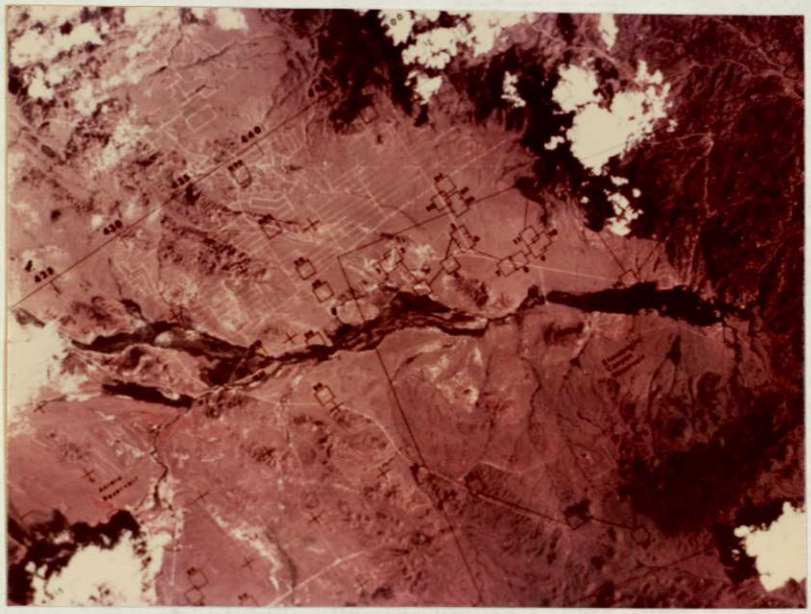

Figure 24.--An example of August 1973 Skylab color photography; original scale was approximately 1:900,000 (SL-3, S190B). The small squares represented 500 meters square (1,640 feet square) on the ground and were used for both visual interpretation and microdensitometric point-sampling of plant communities at the Region and Series level of classification. Note the difficulty in discriminating between square number 1 and 2 (center). Number 1 was ground validated as Shortgrass and number 2 was validated as Mountain Bunchgrass. The overlap between the two squares forms an ecotone between the two classes along a ridge. Number 39 (lower center) is a typical Mountain Bunchgrass site at a higher elevation. Two Wet Meadow sites (WM) can be seen left of center. The area imaged is South Park.

(table 29). However, the CIR late-season S190A photos did provide a significant ($p = 0.99$) difference between the Mountain Bunchgrass/Shortgrass Series classes. The lack of separation was due in part to the ecotonal situation between classes and the aggravation of that situation by the positional accuracy of plot overlays on the very small-scale S190A photographs. Failure to separate the three grassland Series classes was also due to the time of year and poor film quality. The vegetation was in the primary stages of growth and little vigorous foliage was present to provide a strong infrared reflectance for discrimination by mean optical density. In addition, the film was of very poor quality with a strong blue color saturation predominating. Film quality was not considered a factor in the color S190A photographs from the same date (early season) which, as previously mentioned, provided for differences between two of the three grassland Series classes.

Within the tree Series classes, Ponderosa Pine was the only class that had a mean optical density that was significantly different ($p = 0.99$) from the other four tree classes at any one time; that difference was obtained from the late-season S190A and S190B color photos (table 30). Ponderosa Pine was also the only single class consistently separable ($p \geq 0.95$) from the other three conifers regardless of date, film type, or scale. The results in the above two examples do not mean that the other four tree classes were separable from each other within the same date, film type, and scale combinations. For instance, in the second example above, Ponderosa Pine was separable from Douglas-fir, Lodgepole Pine, and Spruce/Fir regardless of date, film type, or scale. However, Spruce/Fir was not separable from Lodgepole Pine at any date, film type, or scale.

Mean optical density differences between Aspen and the Conifer classes were not consistent and were date, film-type, and scale dependent (table 30). For example, Aspen was separable ($p = 0.99$) from Lodgepole Pine in the early-season but not in the late-season S190A color and CIR photos. Aspen was also separable ($p \geq 0.95$) from Spruce/Fir in both the early- and late-season CIR photos, but only separable ($p = 0.99$) in the early-season color photos. The Ponderosa Pine and Aspen Series classes were separable ($p = 0.99$) on the late-season S190A and S190B color photos as mentioned previously. However, Aspen and Ponderosa Pine were not separable on early-season S190A color and CIR photos.

Another example of dependency was within the Douglas-fir Series class. This class was separable ($p \geq 0.95$) from the other three Conifer classes in both the early-season CIR and late-season color S190A photos (table 30). But as can be seen, Douglas-fir was not consistently separated from the other conifers by any one film type and season combination.

It is not completely understood why these separation inconsistencies occurred, but it is believed that the major factors were the phenological stage of development and Series class mixing in both econtonal and overlapping site situations. As an example, Lodgepole Pine and Aspen frequently grow together on the same site, or in ecotones. On early-season photographs the two classes were separable on color and CIR S190A photos, but in the S190A late-season photos the classes were not separable. The early-season Aspen was in the 1/2 to 2/3 leaf development stage which provided increased discrimination (optical density) from Lodgepole Pine. However, later season Aspen with mature leaves was not separable from Lodgepole Pine because of their similar dark reflectance (optical density). Another

example is the fact that Lodgepole Pine was not separable from Spruce/Fir at any date. This was due to class mixing and overlapping of the physiographic range of the two classes; both classes grow in the same area and had similar optical densities. It is believed that most of the inconsistent Conifer class separation was due to that fact. Where the Conifer classes were separable, it could be partly attributed to differences in crown foliar cover and the homogeneity of the stands.

Applications

Some applications of Skylab photographic products for range surveys in mountainous terrain have already been alluded to in this report. Areal plant community mapping on an extensive basis appears to have a high degree of success at the Region level. Intensive plant community mapping at the Series level appears to be applicable if the land manager realizes the constraints imposed by mountainous terrain and the necessity to form community complexes in some areas. The necessity to form community complexes results from natural mixing of dominant species, terrain slope, and aspect.

Plant community mapping involves rangeland and forested areas as well as grasslands and shrublands where trees are not dominant or are absent. This type of information can be useful to update existing vegetation maps, most of which are over 10 years old and are outdated due to changing management schemes, catastrophic events, or changes in land-use patterns.

Extensive cultural feature mapping and monitoring can also be accomplished using Skylab-type photographic products. Depending on the mapping objectives, cultural mapping, however, can require supplementary aircraft photography at larger scales. For instance, an aircraft photographic scale of 1:100,000 proved highly successful for most of the cultural

features mapped in this study. Some features will require either larger scale photos or the use of inference in making interpretative decisions. These decisions require skilled photo interpreters trained in ecological principles. One example of applied cultural feature mapping was a dirt road system being developed within the Manitou area. These roads are to be used for access to a mountain home development and were discernible on the S190B color photos; the roads are about 6.1 meters (20 feet) wide. This type of information will show a land manager the size and extent of developing areas--information not now readily available for large tracts of land, but required for total land management.

In areas where vegetation has not been mapped or only mapped superficially--e.g., South Park--Skylab-type photographs can be useful as a first level of stratification for both mapping and multistage sampling of natural vegetation resources. Stratification was especially successful with vegetation units that display a high scene contrast--e.g., wet meadows within a grassland system--provided those units do not occur in narrow stringers as ecotones and are large enough to be resolved on Skylab-type photographic products.

Skylab-type photographs, coupled with aircraft underflights, can provide a base for multistage sampling schemes. Multistage sampling schemes can be used to stratify and quantify specific plant community systems through the estimation of plant community parameters--when ground based data is used as a final stage. In this study, large-scale (1:600) aircraft photos and ground measurements were used to sample areas delineated on high-altitude aircraft and Skylab photographs to estimate foliar cover of plants and shrubs. Success appears to be dependent upon plant community diversity in relation to the parameters measured.

Descriptive and dichotomous keys may also be an aid to the land manager using aircraft and Skylab-type photographic products. These keys can be compiled at various levels of classification to characterize the appearance of plant communities (table 31). The plant community characteristics can be used as an aid to stratify plant community units at various classification levels for area measurements and to delineate boundaries for sampling with very large-scale aircraft photos to quantify foliar cover by individual species. Keys can be used effectively provided the user is aware of their constraints within mountainous terrain--especially using smaller scale photographs which provide synoptic landscape views. Descriptive characteristics, especially image color signature and texture, are affected by terrain slope and aspect (shadows), degree of plant species mixing, ecotones, and general "condition" of the plant community or species. It must also be recognized that image characteristics represent both plant and soil components.

The research on plant community classification and quantification of plant foliar cover was not replicated sufficiently to fully evaluate the experimental results. Therefore, the tests should be repeated in the same area, or similar area, using the same procedures before the results can be applied in an operational framework. Continued research is also needed to measure the effects of terrain features, amounts of live vegetative cover, plant litter, and bare soil on the spectral response of specific targets in relation to sun azimuth and elevation.

Table 31. Descriptive key of plant community characteristics imaged on early-season (June) 1:400,000 scale CIR aircraft photos. Image characteristics were determined from known (training) sample cells used for visual interpretation.

Plant Community	Descriptive characteristics					
	Color[1]	Aspect	Crown or foliar cover density	Distribution[2]	Texture	Apparent height[3]
Forest						
Aspen	very red (11) or deep red (13)	all; drainages	60-90 percent; med.-high	uniform to clumped; often in stringers	even or rough	rare if clumped
Douglas-fir	very deep red (14) deep red brown (41)	generally N, E	50-80 percent; med.-high	generally uniform when pure	even or mottled	no--a mass
Lodgepole Pine	deep red brown (41) dark gray olive (111)	all; in saddles	70-90 percent; med.-high	generally uniform when pure	smooth or slightly mottled	no
Ponderosa Pine	dark olive brown (96) deep red brown (41)	all; but usually not N	10-60 percent; low-med.	random, not uniform	slightly mottled	rarely
Spruce/Fir	deep red brown (41) dark red brown (44)	all; commonly N	50-90 percent; med.-high	generally uniform	slightly mottled	no
Grassland						
Mountain Bunchgrass	very light bluish green (162)	all slopes to nearly flat	30-70 percent; low-med.	varied with terrain; uniform	smooth	no
Shortgrass	pale purple pink (252) blue white (189)	flat	10-50 percent; low-med.	uniform if pure	smooth to mottled	no
Wet Meadow	deep red (13) dark pink (6)	flat or drainages	30-70 percent; low-high	uniform; near water	smooth or broken	no

[1]Color notation standardized using National Bureau of Standards ISCC-NBS system of color designation. Overlap in colors due to natural mixing of species and terrain slope and aspect.

[2]Apparent pattern (distribution) of the dominant plant species within the sample cell.

[3]Apparent height and resolution of individual dominant species within the sample cell.

FOREST STRESS DETECTION

Ponderosa Pine Mortality from Mountain Pine Beetle

Frederick P. Weber

The detection of stress in our Nation's wildlands and forests is a large multiagency task for which several millions of dollars are spent each year conducting aerial and ground surveys. Stress detection in the National Forest System as well as on State and private lands usually means the detection of insect or disease damage and the evaluation of impact in terms of counting the number of killed or damaged trees. The detection of damage caused by forest pests at the earliest possible time in the development of the pest buildup is important to rapid and effective remedial action. Early and reliable detection methods are required where damage or threat of damage from insects and diseases extends over large areas and involves many ownerships.

The purpose of this part of the Skylab research program was to assess the usefulness and comparative effectiveness of data products from three separate systems of the Earth Resources Experiment Package. In terms of detecting forest stress, data analyses were made to determine the benefits of high spatial resolution (S190B) in comparison to improved spectral discrimination (S190A and S192) and automatic classification (S192) compared to manual interpretation (S190A and S190B). We established the experimental hypothesis that Skylab could not be used to detect stress in forests, and then attempted to disprove it. The Black Hills National Forest and surrounding lands were chosen for the site of the forest stress detection investigation, where an 8-year cooperative research effort in detection and impact evaluation of damage by the mountain pine beetle had been carried on.

Background

The mountain pine beetle (Dendroctonus ponderosae Hopk.) is a threat to ponderosa pine (Pinus ponderosa Laws.) throughout the central Rocky Mountain region and the Black Hills in particular. Aircraft have been used since the mid-1920's to detect and appraise damage caused by the mountain pine beetle. The first remote sensing research to improve aerial detection and appraisal of mountain pine beetle damage in the Black Hills was established in 1952 (Heller and others 1959). During an epidemic outbreak of the mountain pine beetle in the northern Black Hills in 1963-64, the Forest Service Remote Sensing Research Work Unit took aerial color photographs at a scale of 1:7,920 over the northern Black Hills. The resulting high-resolution color transparencies were used to train forest resource managers to locate infestation spots and to count dead trees. In 1965 a formal agreement between NASA and the Department of Agriculture launched the Remote Sensing Research Work Unit on 8 years of stress detection research. This work provided invaluable experience in the requirements for insect damage detection and evaluation of impact on resources.

Detailed studies established guidelines for aerial photography and also identified complex physiological and environmental relationships affecting interpretation of multispectral data (Weber 1969; Weber and Polcyn 1972; Weber and others 1973).

Beginning in 1972, a LANDSAT-1 (ERTS-1) experiment was conducted in the Black Hills to determine the potential usefulness of low-resolution satellite systems to detect and monitor forest stress and map vegetation cover types.

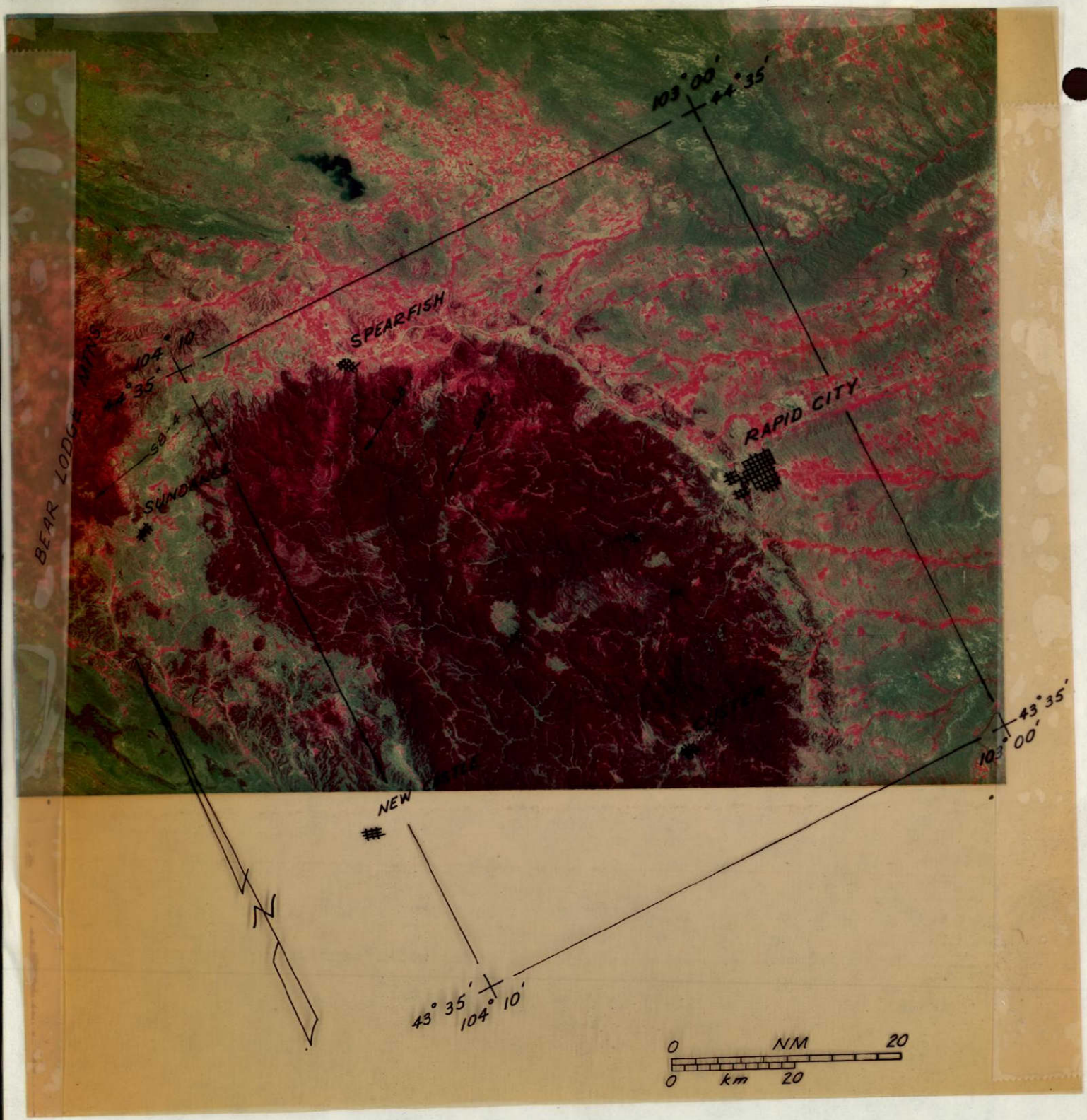

Figure 25.--The Black Hills National Forest test site is outlined on the simulated color infrared composite photograph taken with the S190A multispectral camera system on June 9, 1973. Shown within the test site are intensive study sub blocks 1 and 2 as well as sub block 4 in the Bear Lodge Mountains.

The results of the experiment indicate that the usefulness of LANDSAT-1 (ERTS-1) imagery is limited to providing information for broad area planning and not for providing specific unit estimates of cover-type acreages. The level of classification for which satisfactory accuracies were obtained has questionable utility for the land planner and resource manager. We speculated that the best quantitative application for LANDSAT-1 (ERTS-1) data was in providing the first broad level of stratification of land-use and cover-type classes, i.e., acres of deciduous vegetation, acres of coniferous vegetation, and so forth.

Stress detection was a failure in spite of our best efforts. Neither computer-assisted processing of digital tapes nor manual photo interpretation with special optical viewers was a successful technique for detecting stress.

Study Area

The Black Hills test site (fig. 25) is an area of 10,200 km^2 (3,938 square miles) in western South Dakota and eastern Wyoming. The focus of the site is an elliptical dome extending over 0.75 million hectares (1.85 million acres). The most important tree species, providing more than 95 percent of the total commercial sawtimber volume, is ponderosa pine. Geologically, the Black Hills National Forest portion of the test site is an exposed crystalline core surrounded by sedimentary formations. The central formation, at an elevation between 1,200 and 2,150 meters (4,000 and 7,000 feet), is highly dissected, with large areas of exposed soil and surface rock. Surrounding the central core are sedimentary formations of Paleozoic limestone. The topography here is

gently rolling, especially in the northwestern Black Hills, where the limestone forms a plateau generally above 1,800 meters (5,900 feet). The eastern part of the Black Hills contains the same formations but generally at lower elevations. The radial-dendritic drainage pattern of the permanent east-flowing streams in this area is strongly evident on satellite imagery. Immediately outside the ponderosa pine zone, which surrounds the Black Hills, is a circular valley formed from reddish Triassic and Permian soft shale and sandstone. The "red valley," as it is called locally, is highly visible on Skylab SL-2 photography.

Our primary investigation area covers 653 km^2 (252 square miles) surrounding the gold-mining town of Lead, South Dakota. Two sub blocks were chosen within the area--one called Savoy, with an area of 3,949 hectares (9,759 acres), the other called Englewood, with an area of 4,142 hectares (10,235 acres). During the SL-3 mission in September 1973, a third sub block called Warren Peaks was established outside the primary area in the Bear Lodge Mountains of eastern Wyoming, northwest of the Black Hills. The Warren Peaks sub block, although never surveyed on the ground, was established from aerial reconnaissance surveys and newly acquired aerial color photography. The area of this sub block was 4,144 hectares (10,240 acres).

The Englewood sub block (fig. 26) contains many moderate- and small-sized mountain pine beetle infestations and is important as a transitional area where little beetle activity is noticeable during endemic conditions. This area is first affected, however, during an expanding bark beetle population and thus is a good barometer area for an impending epidemic outbreak. The Savoy sub block (fig. 26) is on the west side

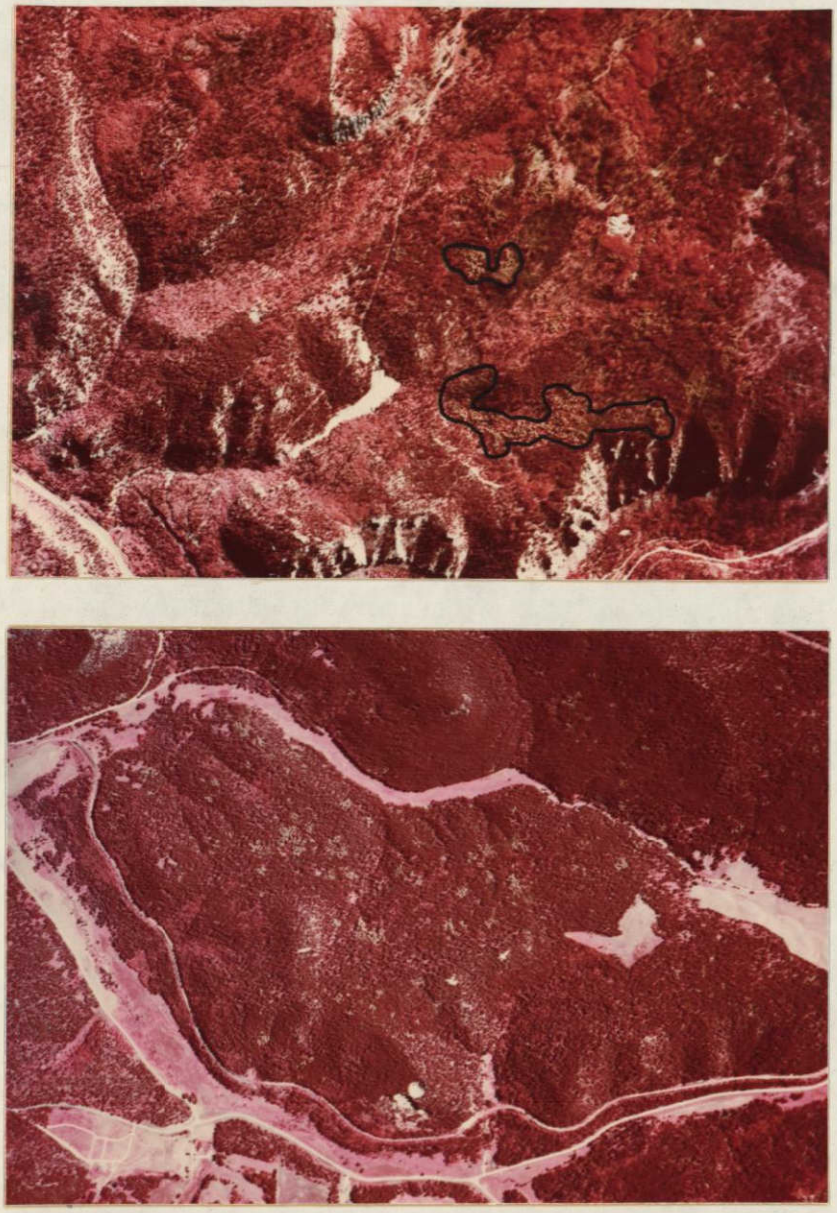

Figure 26.--Infestation spots on the two intensive study sites were identified on September 1972 color infrared aerial photographs, scale 1:32,000. Sub block 1 (Savoy) contained 14 infestation spots greater than 50 meters (164 feet) in the longest dimension. Two of the largest spots were in the southwest corner of the sub block (top). Sub block 2 (Englewood) contained 56 identifiable spots--most of them less than 50 meters long. Some of these are shown in the photo (bottom) of the southwest corner of the sub block. The 1973 photography showed aggregation of many of these small spots into infestations more than 50 meters long.

Intentionally left blank.

Table 32. Black Hills National Forest classification hierarchy for remote sensing imagery.[1]

I Forest

II Conifer

III Dead ponderosa pine
Pine, healthy, < 50% crown closure
Pine, healthy, > 50% crown closure
Spruce

II Deciduous[2]

III Pure hardwood
Predominantly hardwood

I Nonforest

II Grassland[2]

III Wet pasture, on water course
Dry pasture, well drained

II Bare soil[2]

III Rock outcrop
Gravel quarry
Mine tailings

II Transition

III Logging clear-cut
Burn area
Soil, rock, sparse vegetation
Infestation area
Other disturbance

II Urban

III Town
Isolated building(s)
Utilities
Improved highway
Forest road

I Water

II Water

III Lakes and ponds
Reservoirs
Streams and creeks

---

[1]Classes used in computer-assisted mapping are underscored.
[2]Included rock outcrop for computer mapping.

For multispectral scanner data analysis using computer-assisted techniques, a somewhat modified classification system was required (table 33). Although the major Level III categories in Table 32 remain intact, variations in sunlight caused primarily by topography had to be accounted for.

A system for classifying mountain pine beetle infestations by size class was also devised. Prior to the earth resources satellite experiments, the Remote Sensing Research Work Unit had classified infestations into photo strata based on the number of trees identified in an infestation spot. For microscale photography and satellite imagery, however, spot size in meters was a more useful measure. The spot size strata in Table 34 were used in this study. In the sub blocks, however, only those spots greater than 50 meters (165 feet) in the longest dimension were classified.

Skylab Data

Because of the decision not to activate EREP sensors on the SL-3 overhead pass of September 18, 1973, we were left without satisfactory Skylab data to use in the forest stress experiments. September was identified in the original research proposal and data requests as the only satisfactory time (SL-3 mission) to collect data for our studies. With extensive cloud cover obscuring the Black Hills on the September 13 pass and because data were not collected on the September 18 pass, we elected to go ahead with our research program on a restricted basis with available data.

An excellent and complete data set was received from the SL-2 overpass of the Black Hills test site on June 9, 1973 (table 35). We knew, however, that although the imagery was of exceptional quality, June is perhaps the worst possible time of year to detect forest stress resulting from mountain pine beetle damage. Any dead trees in the site had died the previous summer and most of their discolored foliage had dropped to the ground during the winter time.

Table 33. Computer-assisted classification categories, abbreviations, and descriptions used for the Savoy and Englewood sub blocks.

	Category Abbreviation	Category Symbol Number	Description
SAVOY			
	T-Su	1	Transition-sunlit
	BS-R	2	Bare soil-rock
	BS-S	3	Bare soil-sand
	C1-Su	4	Type 1 conifers-sunlit
	C1-Sh	5	Type 1 conifers-shaded
	C2-Su	6	Type 2 conifers-sunlit
	H-Su	7	Hardwoods-sunlit
	Dead	8	Dead pine
ENGLEWOOD			
	P-W	1	Wet pasture
	P-D	2	Dry pasture
	C1-Su	3	Type 1 conifers-sunlit
	C1-Sh	4	Type 1 conifers-shaded
	C2-Su	5	Type 2 conifers-sunlit
	T-Su	6	Transition-sunlit

Table 34. Classification of infestation by average spot size (longest dimension).

Infestation class (meters)	Average number of trees
Less than 10	1 to 3
10 to 25	4 to 10
26 to 50	11 to 20
51 to 100	21 to 50
101 to 300	51 to 100
More than 300	100+

Table 35. Photographic data products from SL-2 mission used in the forest stress experiment.

Photo ID	System	Product	Scale	Area Examined
10-121	S190A	Color	1:2,850,000	Black Hills
09-121	S190A	Color IR	1:2,850,000	Black Hills
12-121	S190A	B&W(0.5-0.6 μm)	1:2,850,000	Black Hills
11-121	S190A	B&W(0.6-0.7 μm)	1:2,850,000	Black Hills
07-121	S190A	B&W(0.7-0.8 μm)	1:2,850,000	Black Hills
08-121	S190A	B&W(0.8-0.9 μm)	1:2,850,000	Black Hills
07, 08, 11, 12-121	S190A	Color composite	1:100,000	Savoy-Englewood
07, 08, 11, 12-121	S190A	False-color composite	1:100,000	Savoy-Englewood
81-157	S190B	Color	1:950,000	Black Hills
81-157	S190B	Color	1:475,000	Savoy-Englewood

Although western South Dakota was obscured by cloud cover during the September 13, 1973, pass, the earth terrain camera and the multispectral cameras were activated. The result was one good frame of S190B color photography with only a wisp of clouds over the Bear Lodge Mountains and one poorly exposed frame of color and color infrared (S190A) photography (table 36). The S190A frame covered the westernmost piece of the Black Hills test site but was badly underexposed and most of the test site was obscured by clouds. In addition, the S190A frame covered the Bear Lodge Mountains but, again, was poorly exposed over the forest. A special processing effort by the photographic laboratories at Johnson Space Center improved the interpretability of the multispectral images.

On January 18, 1974, the SL-4 mission passed over the northern tip of the Black Hills test site and obtained coverage of the Savoy and Englewood sub blocks (table 37) with the multispectral camera. Although the test area was clear of clouds, the ground was snow covered. As a result, the forest vegetation was underexposed on both the color and color infrared film. The test site was not covered by the S190B nor S192 systems.

Ground Truth

The trend and spread of the mountain pine beetle in the northern Black Hills, which included the Englewood and Savoy sub blocks, was monitored with 1:32,000 scale color infrared (CIR) aerial photography. These photographs were taken in late August or in early September 1972 and 1973 by the Remote Sensing Research Work Unit (table 38). The infestations were delineated and recorded by spot size to test detection by satellite

Table 36. Photographic data products from SL-3 mission used in the forest stress experiment.

Photo ID	System	Product	Scale	Area Examined
40-212	S190A	Color	1:2,850,000	Warren Peaks-Savoy
40-212	S190A	Color	1:712,500	Warren Peaks-Savoy
39-212	S190A	Color IR	1:2,850,000	Warren Peaks-Savoy
39-212	S190A	Color IR	1:712,500	Warren Peaks-Savoy
37, 38, 41, 42-212	S190A	Color composite	1:100,000	Warren Peaks
37, 38, 41, 42-212	S190A	False-color composite	1:100,000	Warren Peaks
37, 38, 41, 42-212	S190A	Color composite	1:100,000	Savoy
37, 38, 41, 42-212	S190A	False-color composite	1:100,000	Savoy
88-021	S190B	Color	1:950,000	Warren Peaks
88-021	S190B	Color	1:475,000	Warren Peaks

Table 37. Photographic data products from SL-4 mission used in the forest stress experiment.

Photo ID	System	Product	Scale	Area Examined
70-146	S190A	Color	1:2,850,000	No. Black Hills
69-146	S190A	Color IR	1:2,850,000	No. Black Hills
69, 70-146	S190A	False-color composite	1:100,000	Savoy-Englewood

Table 38. Supporting aerial photography used in the Skylab, Black Hills forest stress experiment.

Date	Scale	Film Type	Aircraft	Source
Sept. 1972	1:32,000	CIR	AC-500B	USFS
Sept. 1972	1:110,000	CIR	RB-57	NASA
Sept. 1972	1:110,000	Color	RB-57	NASA
Sept. 1972	1:50,000	CIR	RB-57	NASA
Aug. 1973	1:32,000	CIR	AC-500B	USFS
Aug. 1973	1:15,840	Color	B18H	USFS
Feb. 1974	1:110,000	Color	RB-57	NASA

and aircraft sensors (table 39). Other yearly surveys were conducted by the Forest Service Rocky Mountain Region.[7] These annual surveys provided estimates of bark beetle damage for the entire Black Hills National Forest and were useful in this study.

Forest Service resource photographs for the Bear Lodge Mountains (at a scale of 1:15,840) were used to establish ground truth in the Warren Peaks sub block. We were fortunate that these photographs were in color and taken near the date of the SL-3 photography of the Bear Lodge Mountains.

Tree mortality counts within the Englewood and Savoy sub blocks for 1972 and 1973 are shown in Table 39. These data encompass the period of the Skylab experiment, but only the 1972 mortality could be used in the test of SL-2 data. Trees which were identified as dead on the August 1973 CIR photography had not yet begun to exhibit discoloration at the time of the SL-2 mission. Table 39 also shows the mortality counts for the Warren Peaks sub block which were obtained from the August 1973 color 1:15,840 resource photography (table 38).

An expanding epidemic is evident by comparing the mortality totals in Table 39. Whereas the Savoy sub block had high mortality counts for both 1972 and 1973, a threefold increase in mortality is seen in the Englewood sub block from 1972 to 1973. The mortality counts in the Englewood sub block for 1973 are conservative--many faded trees were removed by salvage logging during July and August 1973 before the photographs were taken.

---

[7]Information on file, Forest Service Rocky Mountain Region, Division of Timber Management.

Table 39. Tree mortality caused by mountain pine beetle for the years 1972 and 1973, sub blocks 1, 2, and 4.[1]

Infestation size class (meters)	Total number of dead trees					
	Englewood Sub block 1		Savoy Sub block 2		Warren Peaks Sub block 4	
	1972	1973	1972	1973	1972	1973
Less than 10	-	148	-	276	-	236
10 to 25	2,702	2,653	2,552	6,811	-	399
26 to 50	1,198	1,207	252	3,060	-	308
51 to 100	1,079	435	-	870	-	445
101 to 300	715	845	-	325	-	582
More than 300	-	1,050	-	-	-	-
TOTAL	5,694	6,338	2,804	11,342	-	1,970
Ratio, 1972-1973	1.11/1		4.04/1		-	

[1]Area of sub block 1: 3,949.2 ha (9,758.6 acres), 2: 4,142.0 ha (10,235.1 acres), 4: 4,187.2 ha (10,342.2 acres).

Infestations varied greatly between the Savoy and Englewood sub blocks (fig. 26). In the Savoy sub block there was considerable aggregation of smaller prior infestations into several very large infestation centers in both 1972 and 1973. By contrast, most of the numerous infestation spots in the Englewood sub block were less than 50 meters (165 feet) in size in 1972. With an expanding epidemic in this area, the 1973 resource photography revealed considerable aggregation of smaller spots and the creation of many infestations over 50 meters in size (table 39).

From the CIR photography for 1972, 439 sample points representing each of nine cover-type classes shown in Table 32 were selected from the entire test site for the Skylab photo interpretation test. Sample point choice was based on the availability of the sample area for ground check, distribution of the samples throughout the study area, and distinctiveness of the sample point with respect to the surrounding landscape. A map was prepared in the form of an acetate overlay showing the sample points as microdots.

To evaluate the maps created from S192 data tapes by computer-assisted mapping, a type map (fig. 27) was drawn using the nine cover-type classes (table 32). The type maps for the three sub blocks were first drawn on acetate overlays using the 1:32,000 scale CIR resource photographs. Distortions in the original type map were rectified by superimposing a 1:110,000 scale color infrared transparency, taken by NASA on September 14, 1972, onto the acetate overlays using the Zoom Transfer Scope with appropriate adjustments; a second acetate overlay type map was thus drawn having good geometric fidelity and positional accuracy.

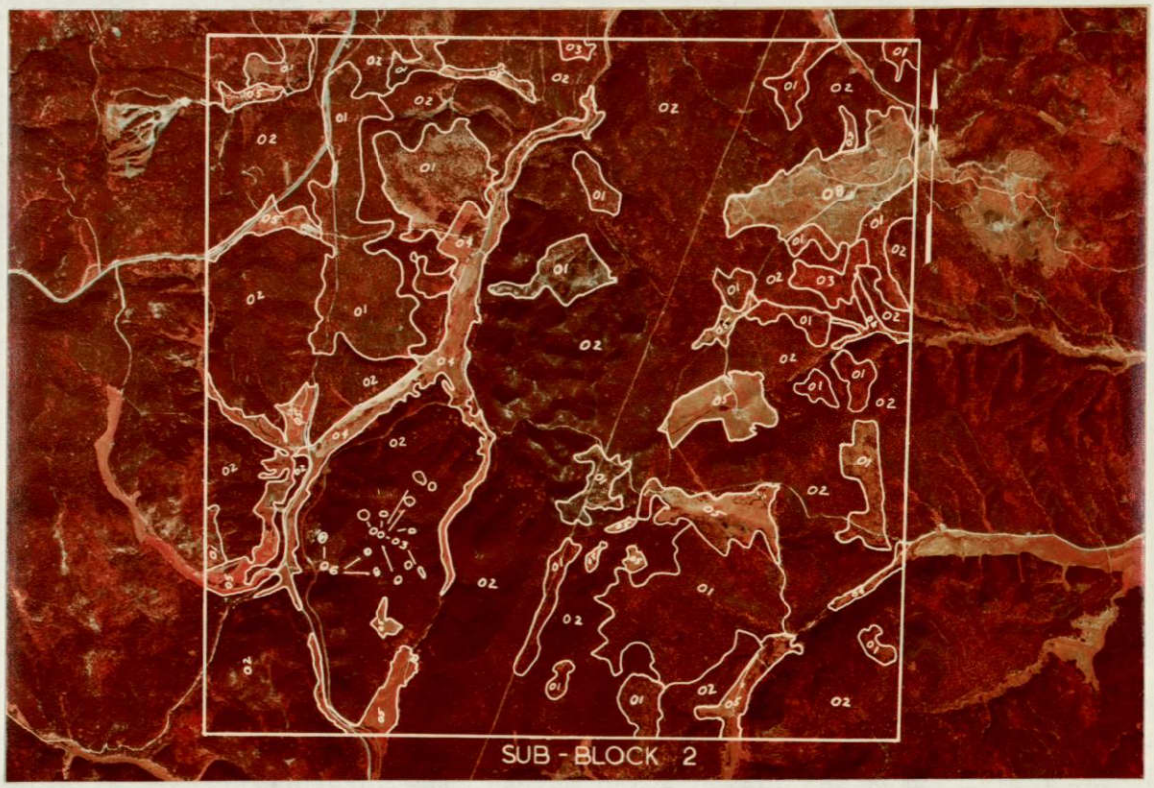

Figure 27.--A cover type map was drawn for sub block 2 (Englewood) using 1:32,000 color infrared resource photographs for classification and 1:110,000 color photographs for geometric rectification. Scale is 1:70,000.

Photo Interpretation Procedures

Prior to the photo interpretation job, all sub block boundaries were marked on the Skylab photographs. Three photo interpretation methods were used to detect and map forest stress on the Skylab photographic products. For the first method, photographs were examined on a Richards MIM 3 light table using a Bausch and Lomb 240 Zoom stereomicroscope. Stereo and zoom optics were changed to provide four separate viewing magnifications. All photo products were viewed in the order shown below. By interpreting the photographic scales in ascending order, we reduced the possibility of interpreter bias.

1:500,000

1:100,000

1:50,000

1:25,000

For the second interpretation method, the same Skylab photographic products were viewed in the same way as above but the stereo optics were replaced with monocular optics. The same four viewing scales were achieved with the zoom feature on the Bausch and Lomb scope.

In the third and last viewing method, the interpreter used a Variscan rear-projection viewer to scan the image at a magnification ratio of 12:1. As areas of interest were identified, the magnification ratio was changed to 29.5:1 which provided the largest interpretation scale. Viewing scales associated with Skylab photographic products were as follows:

The geographic location of the S192 multispectral scanner data, with respect to the Black Hills test site, is as follows:

Location	Latitude	Longitude
First line from	44°59'28"	103°55'01"
to	44°05'28"	104°21'14"
Last line from	44°38'04"	102°56'56"
to	44°03'58"	103°23'39"

The scanner assembly of the S192 multispectral scanner system is constructed in such a way that the path of a scan line on the Earth's surface is not a straight line but a circular arc. This arises from the fact that the scanner is not pointed directly below the spacecraft but at an angle of 5.53° from nadir (84.47° elevation). Machine processing of the circular arc scan line would normally not cause problems. However, the geometric distortion introduced by displaying the circular arc as a straight line hinders the location and identification of landmarks and ground truth. Therefore, before processing the MSS data, geometric distortions were removed by a unique algorithm developed by the University of Kansas. The mathematical details of the scan line-straightening algorithm are described in Appendix 2.

KANDIDATS (KANsas Digital Image DATa System) refers to the entire interactive image processing facility at the Remote Sensing Laboratory, University of Kansas. KANDIDATS is an interactive/batch-mode digital multi-image pattern recognition system designed to facilitate the man-machine interface between the user and the computer complex consisting of a PDP-15, IDECS, IBM 7094 II. The system operates in a standard digital image data. The major processing subsystems include:

(1) image data compression

(2) textural feature extraction

(3) Bayesian classification

(4) spatial clustering algorithms

(5) image utility functions.

The details of the Kansas Digital Image Data System are presented in Appendix 2.

The initial step in the computer processing and analysis of the SL-2 multispectral scanner data was to generate histogram information for each classification category by every spectral band. There was a total of 14 classification categories for the two-sub block and five-spectral-band array, hence, a total of 70 histograms was generated.

The unique nature of the Kansas approach to image processing is derived from the nonparametric statistics of the Bayes decision rule, and the Table Look-up approach of equal probability quantization to the original digitized gray levels which are convolved to 28 levels for classification. The details of the Table Look-up approach are discussed in Appendix 2. The KANDIDATS multi-image files used in computer processing and the presentation of results in contingency tables are as follows:

(1) Englewood sub block = QSG1S2DNV

(2) Savoy sub block = QSG2S2CNV

Results and Discussion

Photo Interpretation

Cursory examination of all Skylab photographic products received significantly reduced the actual number of frames that were subjected to quantitative interpretation. Monocular and Variscan interpretations were performed only on S190B color photos SL2-81-157 (fig. 28), SL2-09-120, SL2-10-120, and SL3-88-021 (fig. 29). Stereoscopic interpretations were performed on S190B color photos SL2-81-156/157, SL2-09-120/121, and SL2-10-120/121. The remainder of the photographic products examined did not reveal evidence of dead trees, forest stress, or bark beetle infestations.

It is important to note at the outset that positive results for the identification of mountain pine beetle infestations with S190 photographic products relate to the identification of infestation spots and in no way indicate ability to count individual dead trees. Results, then, are in terms of infestation spots counted within sub block study areas. It was further resolved that no infestation spots were identified on color or color infrared products from the multispectral camera system. Therefore, all identifications were made on normal-color products from the earth terrain camera (S190B).

A comparison of photo interpretation results for the Savoy study area revealed the benefit of stereoscopic viewing, both in terms of high number of identified infestations and fewer commission errors:

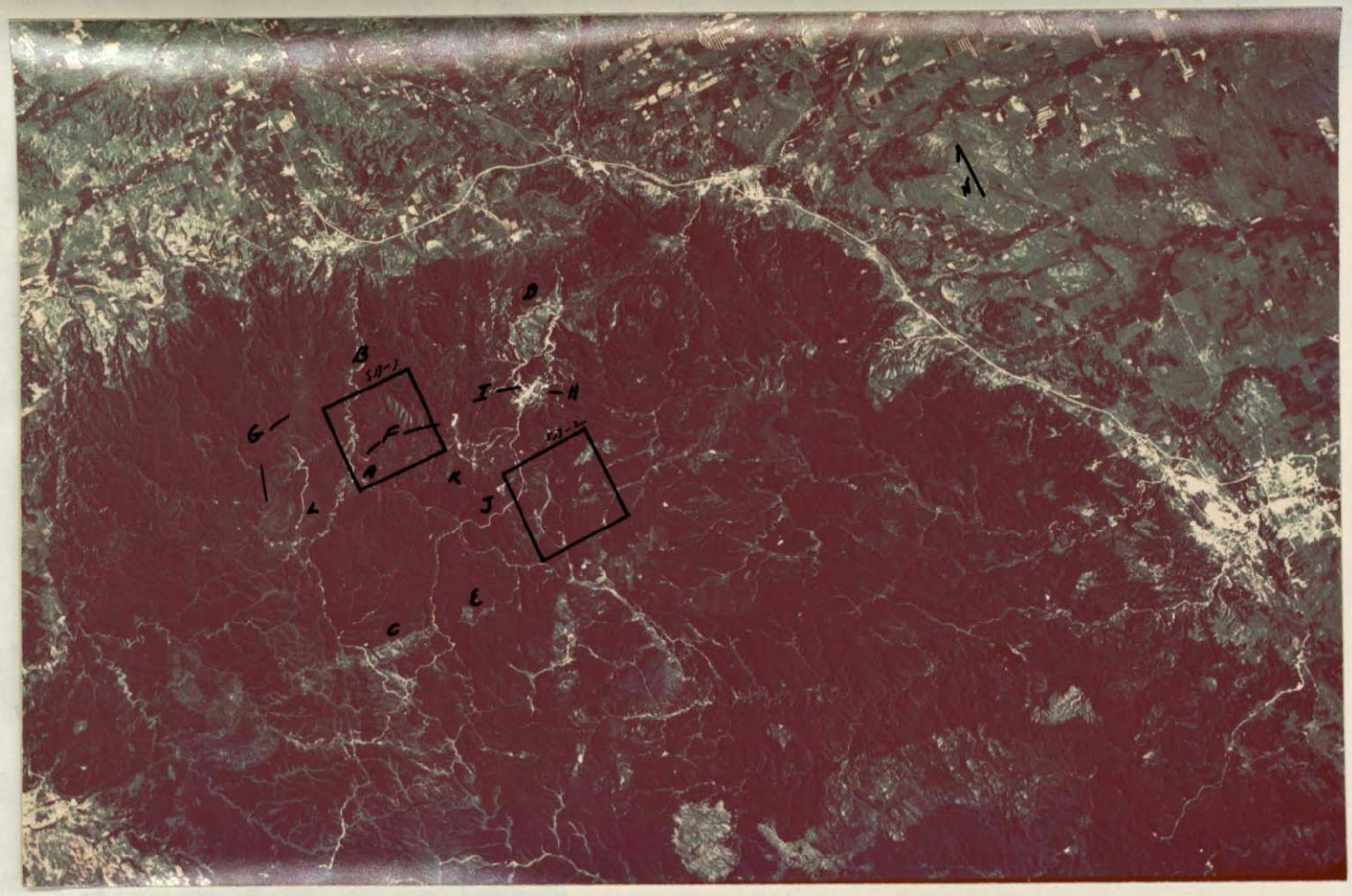

LEGEND

A Infestation area
B Spearfish Canyon
C Tornado path (1962)
D Deadwood burn (1959)
E Dry lake burn
F Mine tailings
G Hardwood forest
H Town of Lead, SD
I Open pit gold mine
J New ski area
K Recreation housing area
L New gravel forest road

Figure 28.--A 1:500,000 scale (1.9X) enlargement of the earth terrain camera color photograph, SL2-81-157, shows the location of two Black Hills National Forest intensive study sub blocks. This June 9, 1973, high-resolution photo (15 meters or 49 feet) was excellent as an earth resource analysis tool when viewed in stereo but was not adequate (because of poor timing) for detecting or counting dead trees.

Figure 29.--Sub block 4 in the Bear Lodge Mountains near Sundance, Wyoming, was photographed (nonstero) with the earth terrain camera on SL-3 pass of September 13, 1973 (SL3-88-021). Adverse atmospheric conditions reduced ground resolution 2½ to 3 times with the result that only the three infestations of dead trees exceeding 100 meters (328 feet) in the longest dimension were positively identified. Photo scale is approximately 1:500,000.

Viewing scale	Number of Infestations			
	Monocular		Stereo	
	Counted	Correct	Counted	Correct
1:500,000	0	0	4	4
1:100,000	13	12	17	17
1:50,000	18	12	12	12
1:25,000	1	1	3	3

All of the correct identifications were made from the group of 40 infestations larger than 50 meters (164 feet) in the longest dimension mapped from ground truth. In every case, all nine infestations in the ground truth which were larger than 100 meters (328 feet) in the longest dimension were located.

Identification within the Englewood study area showed similar results:

Viewing scale	Number of infestations			
	Monocular		Stereo	
	Counted	Correct	Counted	Correct
1:500,000	0	0	1	1
1:100,000	19	14	19	18
1:50,000	22	13	14	14
1:25,000	8	5	4	4

All correct identifications within the Englewood study area were made from a group of 26 infestations in the ground truth which were larger than 26 meters (85 feet) but less than 50 meters (164 feet) in the longest dimension.

The optimum viewing scale, using either monocular or stereo optics on the Zoom 240 microscope, was about 1:75,000 (fig. 30). This scale was the best compromise between magnification and the loss of reasonably sharp image definition. It is important to note that identification of the dead ponderosa pine in the S190B color film was primarily by

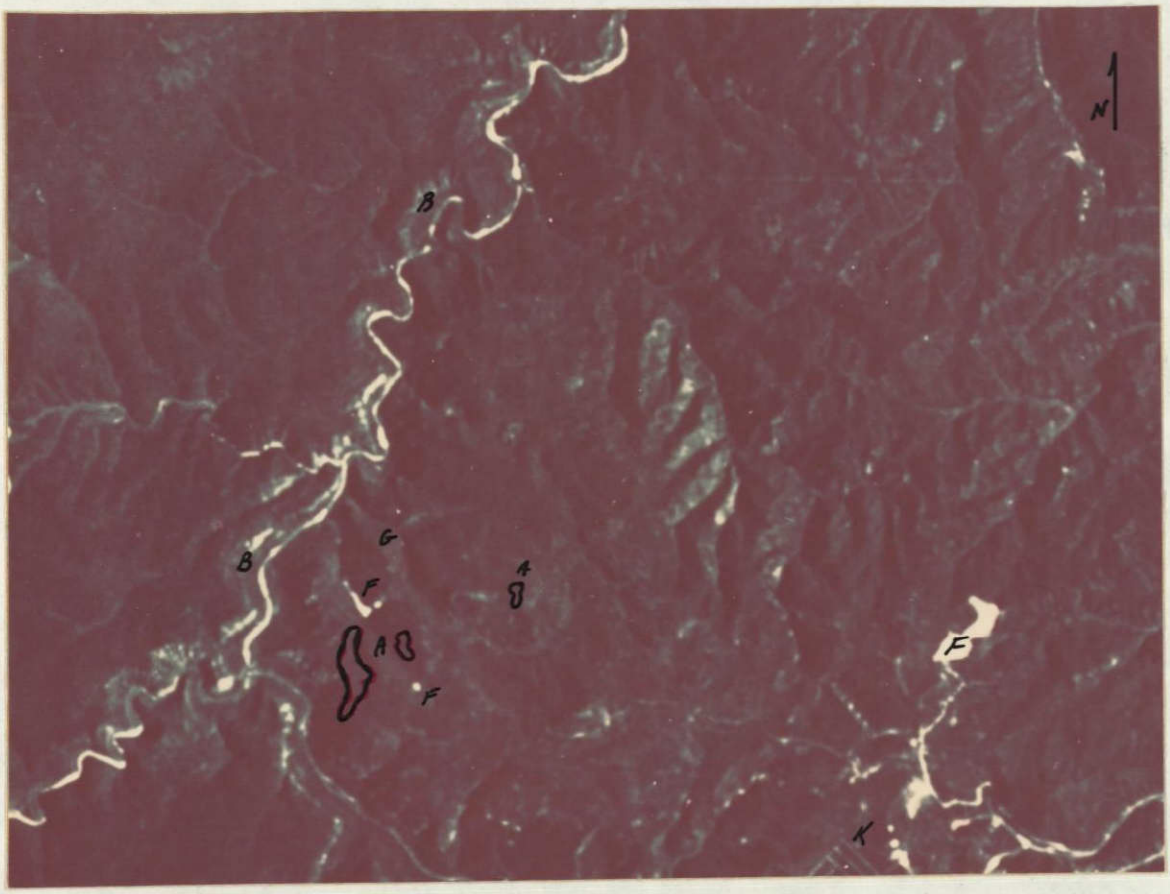

Figure 30.--A photographic interpretation scale of 1:75,000 was determined to be most effective for resource evaluation including the detection of dead ponderosa pine. While photo SL2-81-157 was generally considered to represent the best possible with the earth terrain camera, its resolution of 15+ meters was not good enough to resolve individual trees or small groups of dead trees as would be required for a standing dead timber inventory. Photo scale is approximately 1:100,000.

the bright reddish orange color rather than recognition of any textural difference from the healthy pine. The sparse dead foliage remaining on the trees at the time of the June 9, 1973, pass, 10 months after the time when the dead and dying trees first became visible, undoubtedly prevented much more spectacular results (fig. 31). Furthermore, the SL-2 pass resulted in the photography being exposed early in the morning with a low sun angle. In steep terrain of the Black Hills, most infestations on west- and north-facing slopes were in shadow and were not visible.

The comparison of monocular versus stereoscopic viewing revealed a definite interpreter preference for stereo. The most tangible benefit of stereo viewing was a lesser tendency to make commission errors in the interpretation of dead tree groups. Most of the commission errors resulted from calling patches of bare soil or exposed forest floor (in sunlight) infestation spots.

Results of interpretation with the Variscan viewer indicated this technique was inferior to microscopic viewing of transparencies on a good-quality light table. For example, with the Variscan, 1:80,000 scale was the best viewing scale with eight correct identifications within the Savoy study area and one for Englewood.

Based on our experience with earlier Skylab photographic products, it was unfortunate that during the SL-3 mission (1) stereo S190B color coverage was <u>not</u> obtained for the Bear Lodge Mountains, and (2) opportunity was not taken to image the Black Hills test site on the September 18, 1973, pass when the entire area was clear of clouds. Based on monocular viewing of the earth terrain camera photo of the Warren Peaks area (September 13, 1973, SL3-88-021), the following results were obtained:

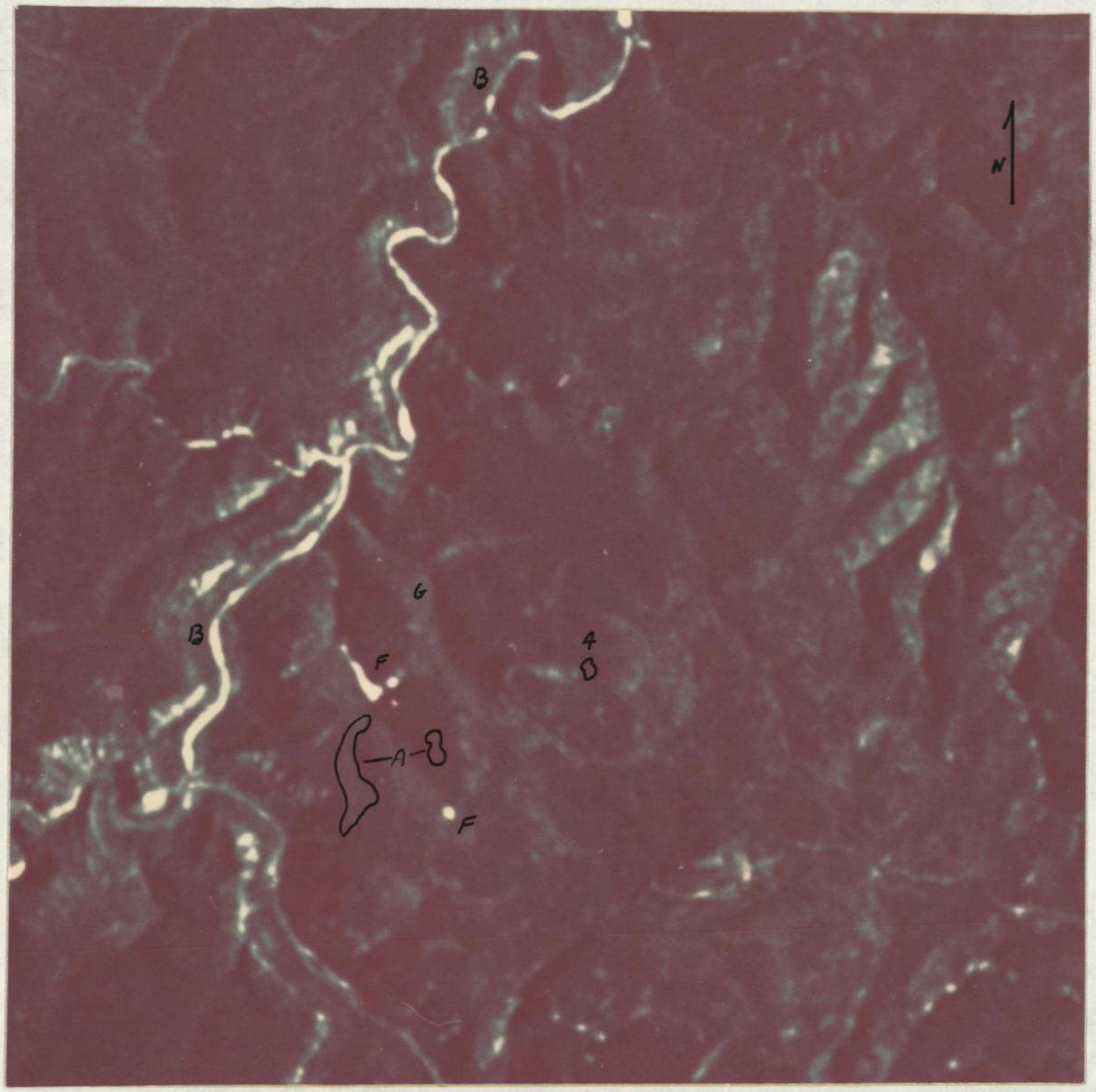

Figure 31.--A 1:50,000 scale (19X) enlargement of SL2-81-157 shows some of the interpreted resource details of the Savoy area (sub block 1). Infestation areas identified as "A" were difficult to discover because few of the reddish orange needles, which make dead beetle-killed pine easy to detect in the fall, remained on the trees at the time of this June 9, 1973, photograph.

Ponderosa pine trees killed by the mountain pine beetle were not detected nor classified by the KANDIDATS processing. In addition to the aforementioned problems, the five usable MSS bands did not accurately register one to another. Table 40 shows the results of one misregistration analysis. With these results, an attempt was made to re-register data through a warp correction algorithm. In several cases classification was improved but still beetle-killed trees were not identified.

Contingency tables were constructed with the classification results from the June 9, 1973, data set of the Black Hills. A large number of tables resulted from different data convolutions, spectral band pairs, and table look-up thresholds used in an effort to optimize classification results. In addition to the above parameters, the contingency tables showed classification results by five error types:

1. Total classification error
2. Equal weighted missed
3. Equal weighted false
4. Poorest individual missed
5. Poorest individual false.

Because of space limitations, the contingency tables are not included in this report.[9] However, the following discussion summarizes the results and indicates how poorly the KANDIDATS processing system classified land use and forest types.

---

[9]The contingency tables may be examined by contacting the author.

Table 40. The registration of the five S192 multispectral scanner bands used in the Black Hills classification was checked by a manual overlay technique using ground control points which could be identified on all MSS bands. The band-by-band misregistrations are shown as ok, up, down, left, or right.[1]

Top scanner band	Bottom scanner band 1	2	3	4	5
1	--	1 U 1 L	OK	1 U 1 L	1 R
2	1 D 1 R	--	1 D 1 R	OK	2 R 1 D
3	OK	1 U 1 L	--	1 U	OK
4	1 D 1 R	OK	1 D	--	1 D 1 R
5	1 L	2 L 1 U	OK	1 U 1 L	--

[1]Prefix 1 or 2 refer to number of resolution cells from the true control point position.

1. Using band pairs (1, 2) and (3, 4) and table look-up thresholds of $(\alpha, \beta) = (0.35, 0.0245)$[10] for the Englewood sub block, a classified image (QSG1S2C73) was created. About 8,300 resolution cells (30 percent) were not classified (reserved decision). Using the training data, the poorest misidentification rate was 20 percent for the wet pasture category. The average misidentification percentage for all classes was 12 percent. Using the test data, the poorest misidentification rate was 35 percent for the conifer type 2 category. The average misidentification percentage was 15 percent.

Filling the unassigned resolution cells of the classified image (QSG1S2C73) by a propogation process resulted in a new classified image (QSG1S2F73). Again using the training data, the poorest misidentification rate was 28 percent for the wet pasture category. The average misidentification percentage was 17 percent. Using the test data, the poorest misidentification rate was 38 percent for the conifer type 2 category. The average misidentification rate was 21 percent.

2. Using band pairs (2, 3) and (4, 5) and table look-up thresholds of $(\alpha, \beta) = (0.30, 0.021)$ on the Savoy sub block, a classified image (QSG2SC81) was created. About 7,000 resolution cells (28 percent) were not classified (reserved decision). The misidentification rate was 45 percent on the training data and 92 percent

---

[10] Alpha (α) and Beta (β) define the process by which a set of categories is assigned by pairs, i.e., a pair of data values from a pair of spectral values (see Glossary).

on the test data. Using the propogation process to fill the unassigned resolution cells, a new classified image (QSG2S2F81) was created. On this new image the misidentification rate was 49 percent on the training data and 90 percent on the test data.

Using band pairs (2, 3) and (2, 4) and table look-up thresholds of (α, β) = (0.30, 0.021) on the Savoy sub block, a classified image (QSG2S2C75) was created. About 5,100 resolution cells (20 percent) were not classified (reserve decision). The misidentification rate was 46 percent on the training data and 95 percent on the test data. Using the propogation process to fill the unassigned resolution cells, a new classified image (QSG2S2F75) was created. On this image the misidentification rate was 48 percent on the training data and 94 percent on the test data.

Several attempts were made to improve these classification results by employing different combinations of convolutions, band pairs, and modified ground truth sets. In one set of experiments, overall classification accuracy was improved by removing the dead tree category, combining all conifer categories, and improving the training set for the transition category. The results were better but, because of the misregistration problem, there remained an unavoidable trade-off between calling hardwoods bare soil and rock or calling bare soil and rock hardwoods. The data in this experiment were analyzed with three different convolutions and by both the set-intersection and majority-vote table look-up decision rules. An effort was made to resolve the conflict between hardwoods and bare soil and rock by modifying the category priors shown in Table 41.

Table 41. File numbers and probability thresholds are given for the five-category set processed using three different convolutions quantized to 28 levels. In the course of processing, different decision rules, band pairs, and priors were used.

File category	Band pairs	Convolution window 1 x 1	2 x 2	3 x 3	Priors[1]
		File number and probability threshold-			
Intersection	(1, 2)	KSG2S3T06	KSG2S3T20	KSG2S3T30	HDWD = 0.19
	(2, 3)	0.021, 0.3	0.021, 0.3	0.021, 0.3	TRAN = 0.20
Majority	(1, 2)(1, 5)	KSG2S3M01	KSG2S3M20	KSG2S3M30	BRSLR = 0.21
	(2, 3)(4, 5)	0.01, 0.14	0.01, 0.14	0.01, 0.14	BRSLS = 0.20
Intersection	(1, 2)(1, 5)	KSG2S3M03	KSG2S3M21	KSG2S3M31	CNFR = 0.20
	(2, 3)(4, 5)	0.021, 0.3	0.021, 0.3	0.021, 0.3	
Majority	(1, 2)	KSG2S3T03			HDWD = 0.20
	(2, 3)	0.021, 0.3			TRAN = 0.20
Intersection	(1, 2)(1, 5)	KSG2S3M02			BRSLR = 0.20
	(2, 3)(4, 5)	0.01, 0.14			BRSLS = 0.20
					CNFR = 0.20

[1]HDWD - hardwood
TRAN - transitional
BRSLR - bare soil and rock
BRSLS - bare soils
CNFR - conifer

The set-intersection rule makes reserve decisions and results in two contingency tables for each image created. In one contingency table the reserve decisions appear. In the other table the decisions are the result of a spatial region growing process. Two iterations of the classification procedure completely fill all resolution cells in the image. The majority-vote decision rule does not modify the test set so that results of the tests are based upon the same training and test sets. Although the results of these different combinations of techniques and processing parameters are quite variable, the best classification showed only about 70 percent of the 439 sample points correctly identified (table 42). This statement is made using the most conservative considerations.

Applications

Of all the various EREP systems, color photography obtained in stereoscopic coverage with the S190B earth terrain camera was best for the location and appraisal of dead ponderosa pine killed by the mountain pine beetle. However, orbital coverage, like aircraft photography, should be optimized by obtaining the photography in late August or early September during the peak spectral reflectance difference between healthy and dying trees. In steep terrain like the Black Hills, where infestations occur independent of slope or aspect, satellite photography obtained in late summer should be planned for midday exposure when the higher sun angles occur. Based on comparisons of S190B color photography, with a ground resolution approximating 15 to 20 meters (49 to 66 feet), and higher resolution photographic systems (as for example photography obtained

Table 42. A composite of 11 contingency tables shows the classification results for five different error types.

File number	Error type: Total classification	Equal weighted missed	Equal weighted false	Poorest individual missed	Poorest individual false
	-percent error				
KSG2S3T20	27	29	33	54	46
KSG2S3M20	28	30	35	55	49
KSG2S3M21	28	27	33	43	54
KSG2S3T20	24	23	27	40	47
KSG2S3M30	24	26	26	53	46
KSG2S3M31	24	24	28	42	44
KSG2S3M02	29	31	37	69	63
KSG2S3T03	29	42	39	64	60
KSG2S3M03	28	27	35	55	58
KSG2S3M01	27	35	36	55	50
KSG2S3T06	28	29	27	44	41

from the U-2 high-flight aircraft), satellite photography having a resolution of 1 to 2 meters (3.27 to 6.54 feet) ground-resolved distance would be ideal for detection and impact appraisal of stress in forests. Photographic emulsions could be either high-resolution color or color infrared, although the former is preferred.

While photography from the multispectral camera (S190A) was of no use for stress detection in the Black Hills, both the multiband capability and large area coverage were useful to forest planners and resource managers. Their preference was for a 28.5X enlargement (1:100,000 scale) of the color infrared band from the multispectral camera system. As a working tool, the CIR print was used to aid in updating existing type-maps, nonsystem road inventory, and planning timber sales. All the resource managers and forest planners convased in the Black Hills agreed that an updated color infrared photo print at 1:100,000 scale received once each year would be effective in carrying out their work. The kinds of ancillary interpretative aids desired to enhance utility of the photograph would be easy to develop. These include such items as a template overlay showing administrative boundary locations, a geographic coordinate grid overlay, and ownership boundaries. Although no effort was made to create type-maps with Skylab photo products, they were used successfully to check the type at point locations which is the way resource managers frequently use photography.

The results of the University of Kansas computer-assisted analysis of S192 multispectral scanner data of the Black Hills showed only limited utility for resource analysis. We recognize that the S192 system was an experimental package, perhaps best thought of as a prototype of a future

shuttle scanner. Regardless, the scanner performance and resulting image products did not measure up to expectation. While on one hand the gross classification results were reasonable (about 80 percent for most classes), many significant land-use classes could not be identified and others had unacceptable errors in point-by-point classification. While the pursuit of optimum computer-assisted classification was exhaustive, the rewards were minimal. A direct comparison of LANDSAT (ERTS) MSS and S192 MSS imagery for the same study blocks was not performed. However, it is assumed from earlier studies that the classification results would have been similar. Due to the poor quality of band 13 data (thermal IR) it remains unresolved as to whether the benefits of moderate resolution thermal imagery from space adds significantly to either (1) the detection of stress in forests or (2) the multispectral classification of land use. Analysis of only the two good-quality bands of MSS data was not adequate for our purposes. Detection and classification accuracy suffered because of (1) misregistration of data between bands, (2) inadequate spatial resolution of MSS imagery, and (3) too few bands of usable MSS data for a full and complete analysis.

During the 2½ years since the Skylab launch, we have had the opportunity to test EREP data for several applications not connected with the Black Hills study objectives:

1. Enlargements of S190B color and color infrared photography have been used on the east coast of the United States to obtain baseline data from sample locations approved for the national Forestry Incentives Program (FIP). Location and examination of FIP sites has in many instances provided information, which was otherwise unavailable, on the condition of practice sites

before the program was initiated. Although S190B resolution was adequate for some examinations, it was inadequate for others. Again, 1- to 2-meter (3.27- to 6.54-feet) resolution with color infrared film would have been ideal.

2. Stereoscopic enlargements of color photos from the earth terrain camera of standing dead Engelman spruce (Picea engelmannii Parry) in the Jemez Mountains northwest of Los Alamos, New Mexico, proved useful for forest managers. Because of the lack of other resource photography, the Skylab photography could be used for planning timber sales utilizing large areas of standing dead timber which were accessible from existing roads.

3. Black Hills National Forest planners and resource managers used 1:100,000 enlargements of color infrared photos from the multispectral camera system. The enlargement prints were used for updating cover type-maps, nonsystems road inventory, and planning timber sale layout. All users agreed that availability and continued use of the satellite photos would produce new and cost-effective applications. To maximize utility, new space photos should be available once a year or, at the most, once each 3 years. Furthermore, most all requirements for remote sensing data could be met with space-acquired color infrared photography having a resolution of 1 to 2 meters (3.27 to 6.54 feet) ground-resolved distance. User preference was for a stereo pair covering a minimum of 240,000 hectares (592,800 acres).

Intentionally left blank.

MEASUREMENT OF FOREST TERRAIN REFLECTANCE

Determination of Solar and Atmospheric Effects on Satellite Imagery

Robert W. Dana

A practical method of correcting satellite radiance data to account for changes in solar irradiance and atmospheric effects is a continuing need. Such a method would be useful for a number of reasons. One is to permit the comparison of spectral signatures of different targets at different sites. Another is to allow accurate measures of spectral variations caused by temporal changes in vegetation and water quality. The final reason is to improve the extension of spectral signatures in computer-aided classification of satellite imagery.

One approach to the problem of obtaining normalization coefficients to correct for solar and atmospheric effects is to study the sensor's response to targets of known reflectance. In the simplest description, the satellite-acquired radiance (N_s) is assumed proportional to terrain reflectance (ρ), with a multiplicative coefficient representing the product of total irradiance and atmospheric transmittance. The radiance data also include an additive term representing the path radiance (N_p) of upward scattered radiation. Specifically, the equation takes this form, assuming the reflector is Lambertian:

$$N_s = \frac{H\tau}{\pi} \rho + N_p , \qquad (1)$$

where H = irradiance and τ = beam transmittance.

Reflectance values of two or more areas that vary greatly in brightness when plotted against their corresponding satellite radiance values yield a first-order measure of atmospheric effects at the time of the satellite overflight.

The reflectance measurement technique has an advantage not present in some methods in that the data acquisition need not be temporally coincident with the satellite overflight. This technique does not probe the atmosphere but studies the reflection properties of the terrain. During some seasonal periods, terrain reflectance probably does not vary over time. Therefore, the reflectance data might be acceptable if acquired within a week or two of the satellite overflight. An important consideration would be the stability of important target aspects such as plant phenology, soil moisture, and water turbidity. Of course, it is advisable to work under the same solar irradiation conditions that the satellite sensor experiences (same time of day and similar cloud and haze conditions) --particularly if the targets are non-Lambertian.

This paper reports results of the analysis of one set of Skylab (EREP) photos and one scene of ERTS-1 (LANDSAT-1) multispectral scanner data, offers some conclusions about this experiment, and suggests some possible applications of this type of radiance measurement. All data show a high correlation between satellite radiance and aircraft reflectance, with reasonable values of path radiance resulting from the calculations.

Background

The investigation of solar and atmospheric effects stems from earlier attempts to use near-ground-level radiometric measurements as aids in analyzing satellite imagery (Heller and others 1974). For similar targets, large differences in LANDSAT-1-measured radiance values were noted between different dates of coverage. LANDSAT-1 radiance values also differed by as much as 30 percent from ground-measured values. These examples, combined with past evidence of haze effects in aerial photography, led us to

search for a method of accounting for variations in solar irradiance and atmospheric interference.

The prospect of using existing complex atmospheric modeling techniques with their detailed computational procedures did not appeal to us. They would require too much software development and costly wavelength-by-wavelength computations to derive meaningful atmospheric coefficients. Accurate modeling probably requires some kind of in situ radiometric measurement anyway. With satellite-matched reflectance measurements we hoped to find a simpler means of finding two coefficients which could linearly transform satellite data.

By collecting reflectance from a low-flying aircraft, we avoided two problems encountered with the tower-mounted instrumentation in the LANDSAT-1 study. The difficulty of maintaining an unattended field site in an often harsh environment was avoided. The problem of the relevance of a few small tower sites to the large satellite study area was also avoided. The tower instruments viewed only one small portion of a few LANDSAT picture elements, whereas the low-flying aircraft could adequately sample dozens of targets easily resolved by LANDSAT.

Study Area

The possibility of acquiring Skylab coverage on more than one date for the Black Hills, South Dakota, and the Atlanta, Georgia, sites gave us hope of demonstrating the use of atmospheric corrections to data in these two areas. One possible application was measuring temporal changes in vegetative spectral signatures. Another application was signature extension from one sub block to another in computer-aided classification work.

The aircraft system for terrain reflectance measurement was flown over the Savoy and Englewood sub blocks in the Black Hills study area on July 27, 1973. A mission was also flown over two study blocks approximately 4,050 hectares (10,000 acres) in size in the original Georgia study area near Carrollton, Georgia, on January 13, 1975. As explained in the Forest Inventory and Forest Stress Detection Sections, these sites were not covered by Skylab during the seasons of our underflight coverage. Therefore, no attempts were made to compute atmospheric effects on Skylab data for these two sites. The Black Hills flight data, however, were analyzed and compared with LANDSAT-1 data.

During the final days of the Skylab program we were able to obtain coverage for a secondary site in northern California. With one day's notice, a test site was selected west of Redding, California (fig. 32). It was a narrow strip along Skylab track 63 extending from a point 8 kilometers (5 miles) northwest of Whiskeytown Reservoir to the airport on the southeast edge of Redding--a distance of 35 kilometers (22 miles).

The western end of the test area is moderately steep terrain with wooded slopes of mixed ponderosa and digger pine (Pinus sabiniana Dougl.), California black oak (Quercus kelloggii), and canyon live oak (Quercus chrysolepis Liebm.). Patches of manzanita (Arctostaphylos sp) and other chaparral species are also present. The central portion and eastern end of the strip are predominantly mixed oak, chaparral, and pastureland, with some rural homesites.

A few fallow fields and fields of winter crops were noted at the time of the Skylab coverage. The waters of Whiskeytown Reservoir and the Sacramento River appeared relatively turbid during the overpass.

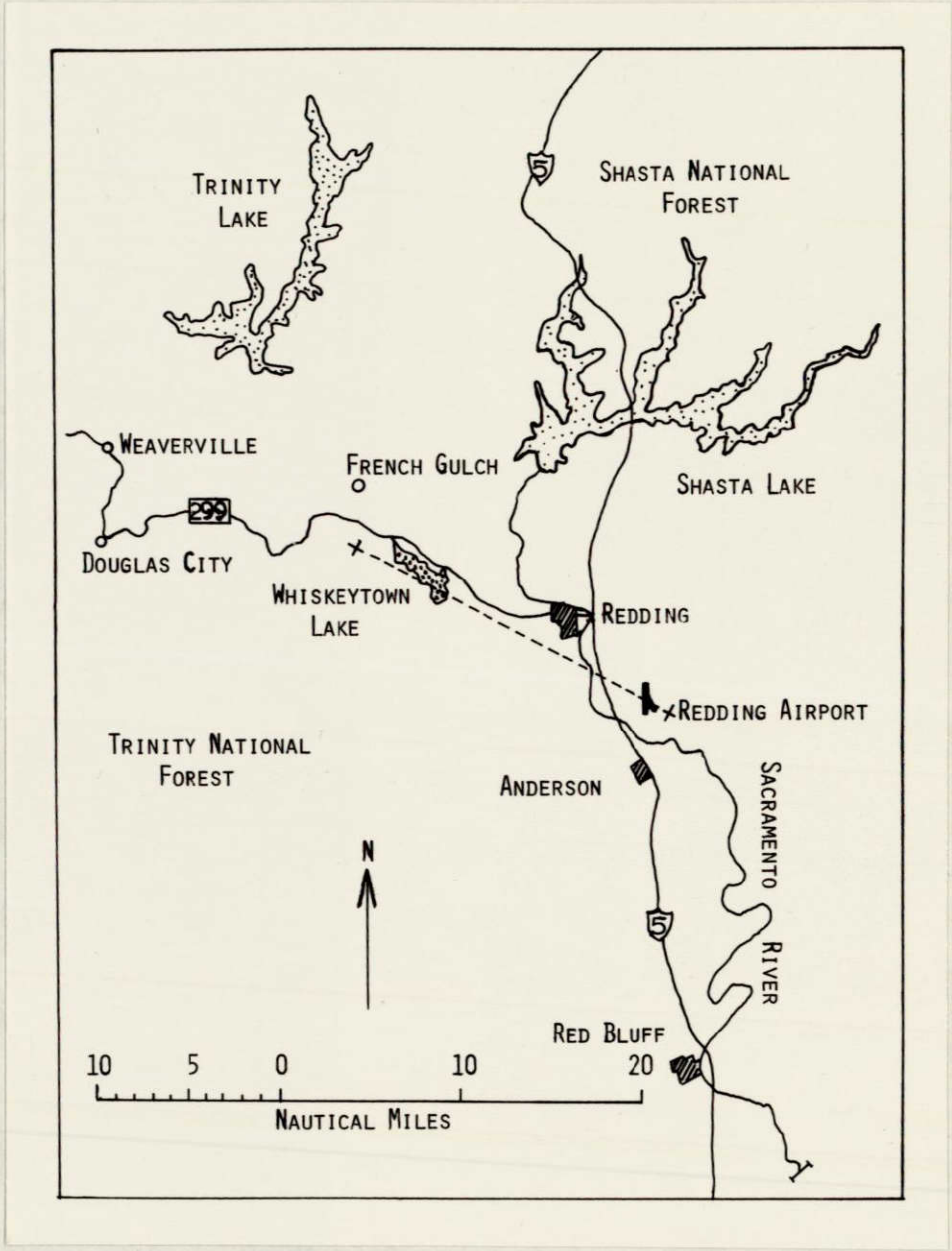

Figure 32.--The test site for measurement of forest terrain reflectance was a 35-kilometer-long (22-mile-long) strip between Redding Airport and Whiskeytown Reservoir.

Instrumentation

The instrumentation for gathering the necessary data was installed in a twin-engine Aero Commander 500B aircraft modified for aerial photography. The equipment consisted primarily of a radiometer, irradiance meter, high-speed recorder, video camera, video tape unit, and wide bandpass filter sets (fig. 33). Power for most components was provided by a stabilized (frequency and voltage) inverter rated at 500W, running off the 28V d.c. aircraft supply.

Reflectance was measured by an upward-pointing irradiance meter and a downward-pointing radiometer. The silicon diode detectors were filtered to match the bandwidths of LANDSAT-1 multispectral scanner and Skylab S190 sensors. The reflectance was derived from the aircraft radiance N_a using Equation 2, in which the altitude is assumed to be low enough to minimize the effects of atmospheric path:

$$\rho = \frac{\pi N_a}{H} \qquad (2)$$

When H or N_a are known at the time of satellite overflight, Equations 1 and 2 can be used to find the beam transmittance:

$$\tau = \frac{\tau(N_s - N_p)}{H\rho} = \frac{N_s - N_p}{N_a} \qquad (3)$$

The Skylab S190A photos to be compared with the reflectance data were scanned by a digital microdensitometer. Programs were written to convert the microdensity values to diffuse density and subsequently to effective film exposure at the film plane.

Figure 33.--Equipment for aircraft target measurements of terrain reflectance. Left to right: video tape recorder, strip chart recorder, radiometer, static inverter, irradiance meter with input probe and filter chamber, TV monitors, vidicon camera and radiometer input probe on aerial camera mount.

Radiometer

The radiometer employed for measurement of terrain radiance is an Optronic Laboratories Model 700F with digital and analog output. It amplifies the signal from a silicon photodiode in a photovoltaic current-to-voltage mode and provides six decades of linear amplitude. The full-scale value of the most sensitive range is about 1×10^{-8} A or about 3×10^{-8} W of light energy on a silicon detector. It is more sensitive than necessary for this experiment because our normal operation was about 1 microamp.

The radiometer was custom-built for low noise and high frequency response. For a square-wave input at the 1 microamp level, the total of the rise and fall times and the transient effect of any underdamping conditions in the output wave is less than 1 millisecond. Therefore, this instrument is responsive enough for measurements at aircraft speeds up to 45 miles per second (100 mph).

The input optical probe was constructed from a machined aluminum block linking a 135-mm camera lens and a planar diffused junction silicon diode, which is masked by a 6-mm diameter aperture. The resultant field of view (FOV) is 44 milliradians or a full angle of 2.6°. At the designed experimental altitude of 300 meters, the ground resolution is 13 meters. Light filtration is accomplished with 50-mm filters mounted on the front of the lens.

Irradiance Meter

Total irradiance at aircraft altitude was measured with an electronics package designed and built in our laboratory. It essentially matches the performance characteristics of the unit used for gathering radiance data.

The silicon target in an RCA Model 4532 tube had a spectral sensitivity curve similar to the curve of the photodiodes used in the radiometer and irradiance meter (fig. 34). The silicon vidicon camera is so sensitive in the absolute sense that normal operation in the plane required a lens f-stop of f/11 and a neutral-density filter of 10 percent transmittance in combination with the bandpass filter.

The vidicon camera was vertically mounted on a mapping camera mount with the boresighted radiometer secured to the camera housing. Two small closed-circuit TV monitors were used--one in the front of the aircraft to aid the pilots in navigating along the flight line, and the other in the rear for the instrument operators.

The video signal was recorded on a commercial-quality half-inch tape recorder (VTR). Although the image resolution with this device is limited to about 300 TV lines per picture height (the camera is capable of 700), this low-cost recorder does allow playback of useful pictures. Analysis can be conducted at normal speed, variable slow speeds, or at a stop-action setting.

The VTR employed in this study had two available audio channels. One channel was used for housekeeping data introduced by a microphone. On the other channel a timing signal was introduced by an audio pulse generator, which synchronously excited an event marker on the chart recorder. This provided time base synchronization of the VTR with the chart recorder.

Filter Sets

In matching the Skylab S190A bands, we were limited by the time and funds available. Three sets of filters were required--one each for the

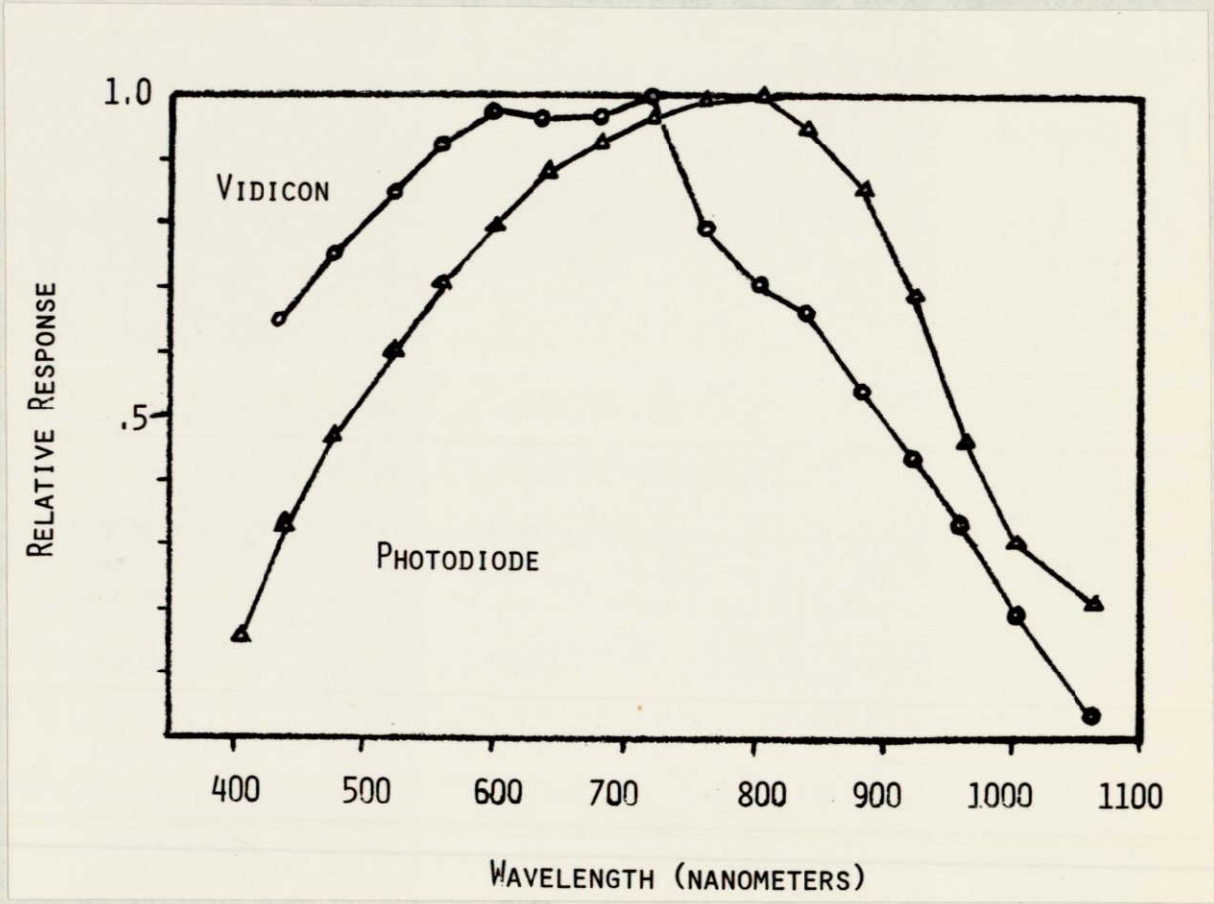

Figure 34.--Spectral response of silicon vidicon and diffused silicon photodiode. Each curve was separately normalized to its highest value.

irradiance meter, radiometer, and vidicon imager. We selected off-the-shelf absorption glass filters in stock thicknesses to meet the time/cost constraints. For each spectral band a cut-on filter was combined with a long wavelength-absorbing glass. The filter sets and their thicknesses, in millimeters, were:

A - Hoya Y-50 (2.5) + Schott BG-18 (1.0)

B - Hoya R-60 (2.5) + Hoya HA-30 (3.0) + Schott BG-20 (2.0)

C - Hoya R-70 (2.5) + Hoya HA-30 (3.0)

D - Hoya IR-80 (2.5) + Hoya B-370 (2.5)

The spectral responses of the vidicon and photodiodes were combined with filter transmittance data to arrive at curves of system spectral response. The spectral response of the S190A camera stations employing black-and-white film was also computed (Appendix 4). The film spectral sensitometry data were taken into account as well as spectral transmittances of all optical components in the system. The bandwidths are summarized in terms of the locations of the half-power points where the response reaches 50 percent of the peak value (table 43).

Although mismatches between the Skylab cameras and the radiometric instruments are apparent, they may not be serious in terms of proper wide-band measurements of terrain reflectance. The most serious difference occurs between set B and station 5, where the radiometer and vidicon pick up excess energy from the strong infrared reflection band of live vegetation, beginning at about 700 nm. This condition would result in a higher reflectance value from some aircraft measurements than that to which the satellite camera responds.

Table 43. Measured bandwidths of Skylab S190A stations 1, 2, 5, 6 and U.S. Forest Service instruments using filters C, D, B, A with either silicon vidicon or Pin 10-DP diffused silicon photodiode[1]

Skylab Camera Station	Design Bandwidth	Actual Bandwidth	USFS Filter Set	Bandwidth (Photodiode)	Bandwidth (Vidicon)
1	700 to 800	713 to 814	C	689 to 779	690 to 780
2	800 to 900	805 to 882	D	810 to 956	805 to 965
5	600 to 700	601 to 695	B	605 to 723	605 to 720
6	500 to 600	517 to 594	A	497 to 622	495 to 615

[1]Units are half power-points in nanometers.

Skylab Data

For the northern California site we requested and received SL-4 photographic data from pass 93 along ground track 6. The pass was made on January 27, 1974. The data included duplicate films for S190A, magazines 73 through 78, and S190B, magazine 94. The western 40 percent of the aircraft flight path over which we obtained reflectance data was cloud-free on the S190A photos. The S190B camera was turned on too late to include any of the test site.

All camera stations of the S190A package were operable except station 5. The critical frame (number 214) was blank for this red band. The green band (station 6) and the normal-color band (station 4) were well exposed, but the three infrared-sensitive bands (stations 1, 2, and 3) were slightly underexposed.

High-resolution images from stations 6 and 4 supported meaningful microdensitometer scanning increments as small as 8 μm (fig. 35). The black-and-white infrared images of stations 1 and 2 were very granular and did not merit scanning increments smaller than 32 μm (fig. 36). Features smaller than 100 meters (327 feet) across were rarely detected by eye on the infrared images.

Procedures for Data Analyses

Radiometric measurements were made over three test sites--near Atlanta, Georgia; in the Black Hills of South Dakota; and near Redding, California. Applicable Skylab coverage was not obtained, however, until the last week of the program on January 27, 1974. On that date a site 15 kilometers (24 miles) west of Redding, in northern California, at Whiskeytown Reservoir was photographed.

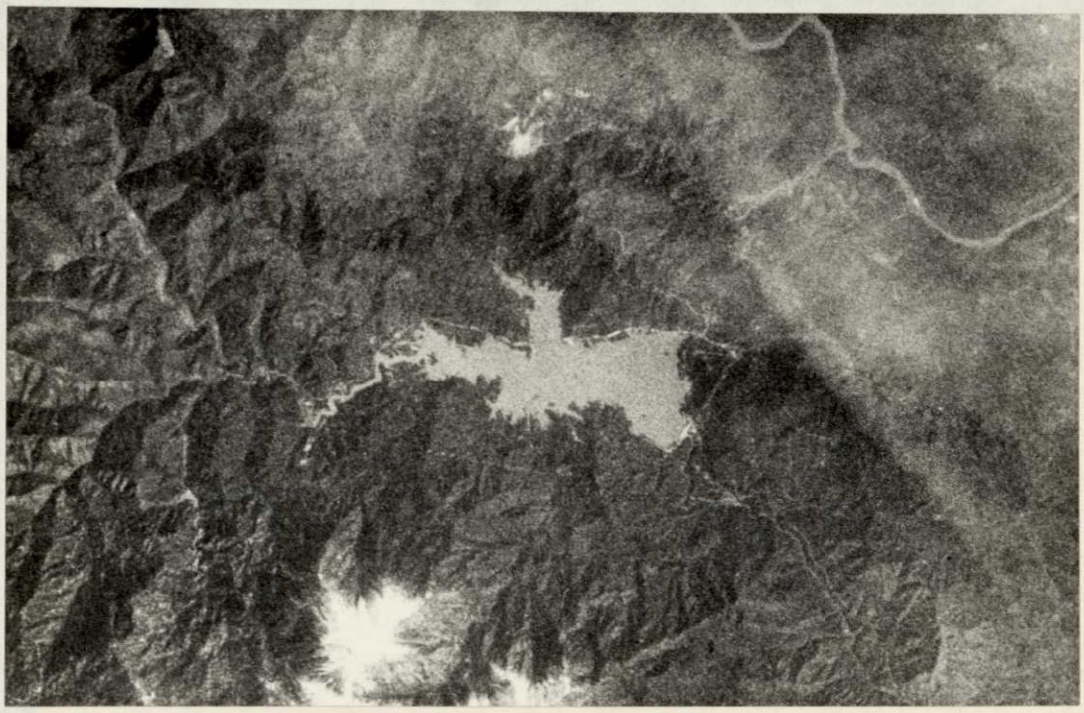

Figure 35.--Northern California site imaged by S190A camera station 6.

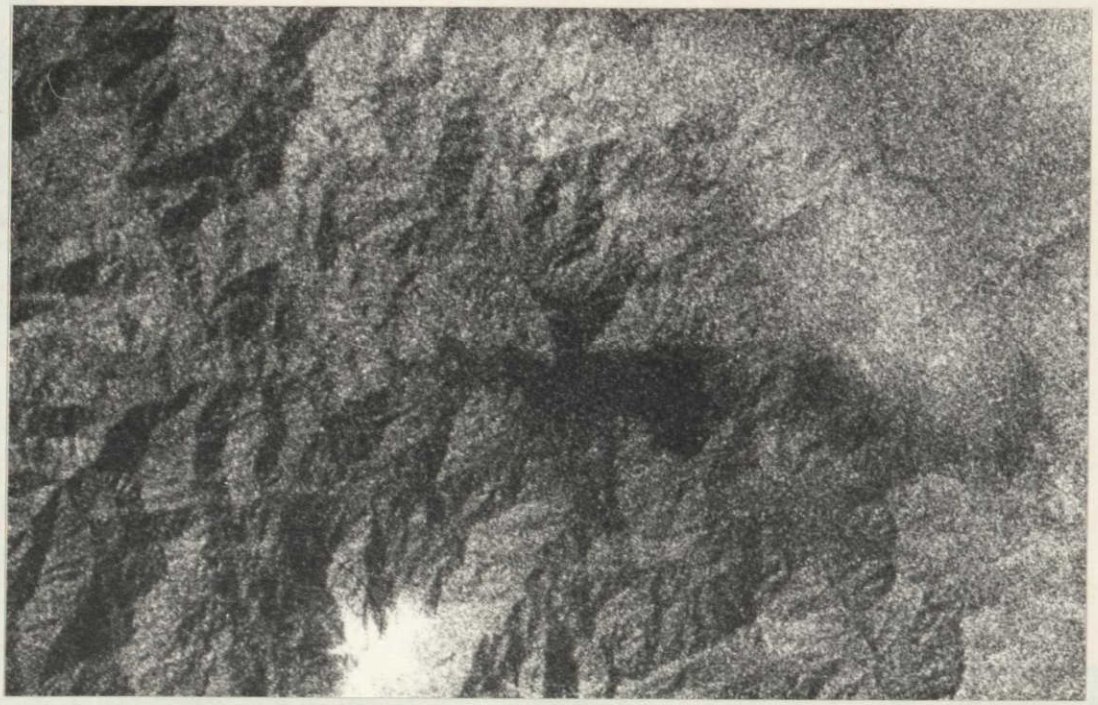

Figure 36.--Northern California site imaged by S190A camera station 1.

This experiment produced three kinds of data to be reduced and analyzed. The first consisted of aircraft radiance and irradiance data recorded on strip chart that had to be reduced to average target reflectance values for specific areas on the ground. Conventional manual and computer-aided techniques were used. The second kind of data was satellite imagery, which required the conversion of photographic density to apparent radiance values. A new computer technique was developed utilizing sensitometric data provided by the Photographic Technology Division of NASA/JSC. The third kind of data was LANDSAT-1 satellite data, which is discussed briefly in Results and Discussion.

Aircraft Radiance and Irradiance Data

Before analyzing the radiance data, we reviewed the video tapes of the flights and plotted the flight paths on available maps and aerial photo coverage. To find the large-scale video paths on 1:2,900,000-scale space photos, it was often necessary to transfer the paths to a medium scale, such as 1:15,000 resource photography. Thus, it was possible to determine which parts of the radiance data stream represent relatively homogeneous areas which are resolvable on the satellite imagery.

The strip chart data were sampled with a digitizer at intervals equaling approximately 20 meters on the ground. The ratios of radiance to irradiance were calculated by computer to generate a data stream of reflectance values. Calibration coefficients for the radiometer, irradiance meter, and chart recorder were derived in our laboratory near the time of the aircraft flights by using a light source with calibration traceable to a National Bureau of Standards source. Portions of the data

stream were selected which transected 6 to 13 homogeneous areas of interest on the photos and mean values of reflectance were computed.

Skylab Photographic Data

The satellite radiance data used were derived from digital microdensitometer (MDM) scans of the test site on duplicate photos by using a Photometric Data Systems Model 1010 unit. The NASA sensitometric data is given in terms of macroscale diffuse density. Cross-calibration scales between microdensity and diffuse density differ considerably for variations in film properties, MDM numerical aperture, and general internal optical design (Weiss 1973; Schmitt 1970). Therefore, it was necessary to calibrate microdensity against the diffuse density scale by using calibrated samples of copy films provided by JSC. Working in diffuse density units, we chose not to use the intermediate steps dealing with the original film sensitometry, but to compare measured duplicate densities to those produced by the exposure values applied to the original film. The system response curve was obtained by polynomial modeling techniques described by Dana (1973).

The analysis and data flow proceeded generally in three parallel paths (fig. 37). From the microdensitometer scan of the test site, a histogram was generated in the first path to establish the range of density values which must be calibrated. This data tape was then ready for the final processing step. In the second path a separate tape containing the JSC step-tablet scans was analyzed by a program called RNSTAB. A least-squares fit of the microdensity M (in digital counts) to diffuse density D produced a second-order equation with a standard error always less than 0.01 diffuse density units for the three copy films used. (A linear form

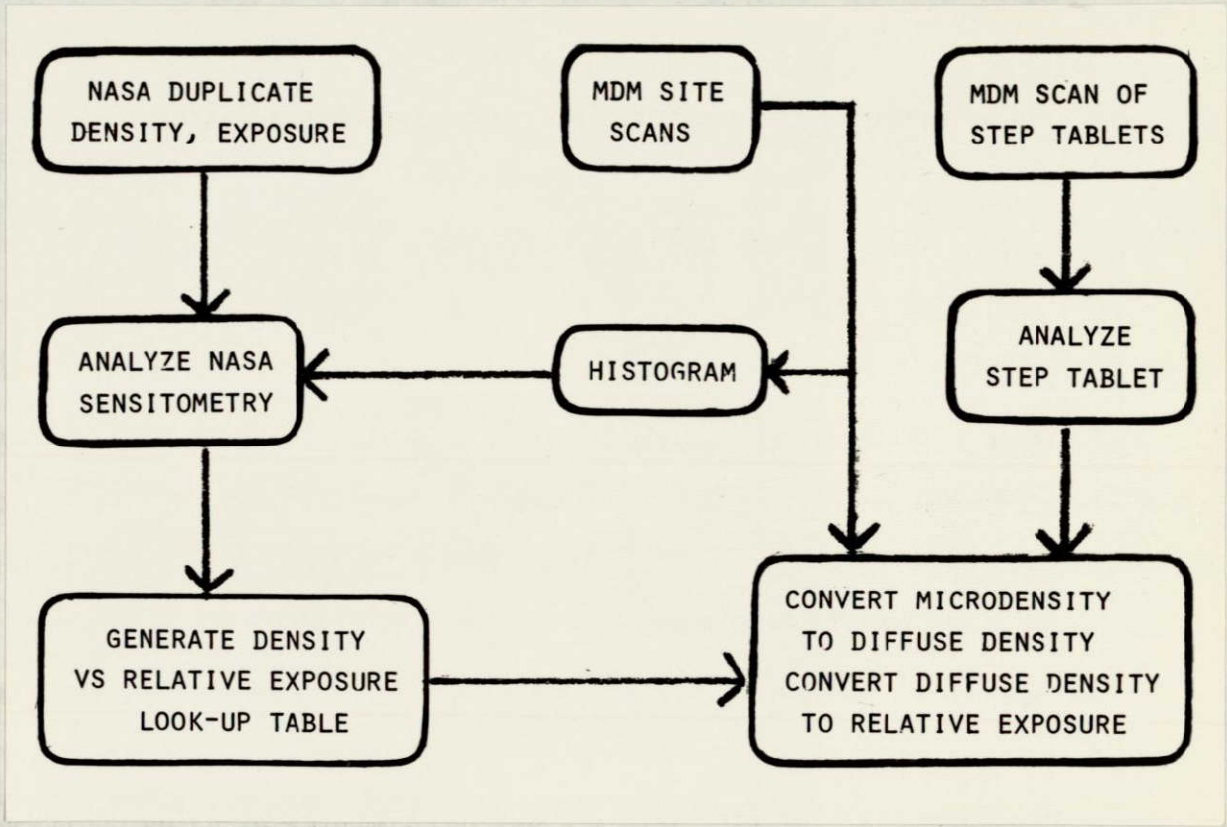

Figure 37.--Flowchart of density calibration program.

was tried, but it produced standard errors of about 0.04.) Conversion to diffuse density could then be made with an equation of the form:

$$D = C_2M^2 + C_1M + C_0 , \qquad (4)$$

where C_2, C_1, and C_0 are modeling coefficients.

In a third path, modeling of the photographic system response generally resulted in an equation for duplicate density that was third order in $\log_{10}$ of relative exposure. Some of the narrower ranges of density could be fit to a second-order curve. From these equations look-up tables were generated to do the actual conversion.

The look-up table, the coefficients of the density conversion equations from RNSTAB, and the site-scan tape were put into a program named XCAL, which derives and prints out a relative exposure value for each microdensity value. Another program, DENCAL, combines the functions of RNSTAB and XCAL, utilizing the look-up table and both MDM input tapes in one computer run. DENCAL writes an exposure tape, as well as a printout, but does not have the flexibility of selecting different combinations of scanning runs from the MDM tapes as do RNSTAB and XCAL.

Once the relative exposure printout was obtained, the data corresponding to particular image blocks were identified and mean values computed for each. The absolute exposure E at the film plane was computed by using additional data provided by NASA. A conversion to equivalent radiance N in engineering units (Jenson 1968) was made by the equation:

$$N = \frac{4F^2}{\pi t T} E, \qquad (5)$$

where F = camera lens f-number, t = integrated exposure time, and T = total transmittance of camera lens, filter, and window.

Results and Discussion

The first set of results to be discussed is from the analysis of the Whiskeytown Reservoir site covered by Skylab photos. The distributions of reflectance (measured on the same day) were recorded and satellite radiance values were computed (figs. 38, 39). The green band results indicate the possibility of two distinct populations of reflectance--one around 0.04 and another around 0.14 (fig. 38). Possibly a high linear correlation is forced on the data, but exclusion of the two high points yields a difference in path radiance of only 3 percent from linear regression. The slope of the new regression line would be 11 percent less. How the reflectance data should be used for classification depends on the distribution of radiance and reflectance values in the training and test areas. Multimodal data might present problems.

Camera station 5 (red band) malfunctioned momentarily over the Whiskeytown area and the photo in that band was not taken. But it was possible to compute the relative exposure values from red-filtered densitometer scans of the normal-color film (SO-356) from camera station 4. Since the red sensitive layer in color film is not exclusively sensitive to the red wavelengths, we did not try to convert exposure to absolute radiance. Nevertheless, reflectance and exposure were closely correlated in the red region (fig. 40) as was noted in the other wavelength regions.

Further evidence of the linear relationship between reflectance and satellite radiance came from a test flight in the Black Hills on August 27, 1973 (fig. 41, 42). Due to anomalies in calibration data, reflectance is shown here in normalized form. The satellite radiance values were from LANDSAT-1 image number 1028-17121 of the same area taken on August 20,

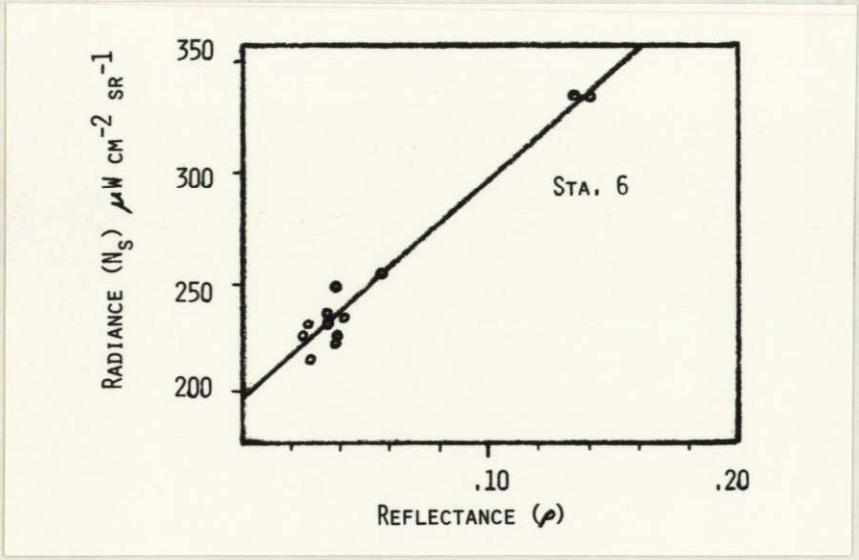

Figure 38.--Skylab radiance and reflectance for the S190A green band (camera station 6).

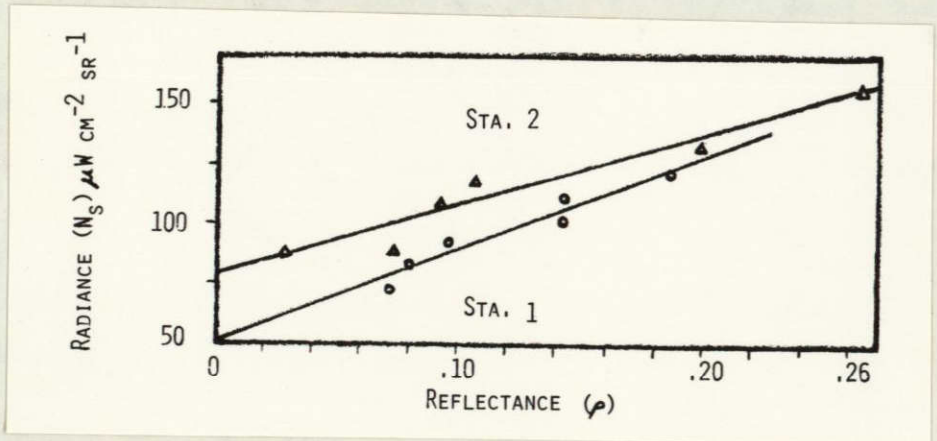

Figure 39.--Skylab radiance and reflectance for the S190A near-infrared bands (camera stations 1 and 2).

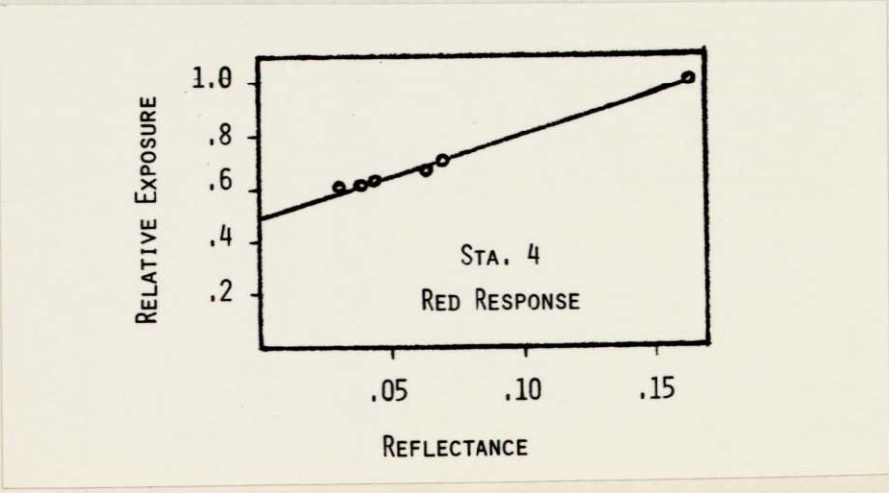

Figure 40.--Relative exposure and reflectance for the red response of the normal-color film of Skylab S190A camera station 4.

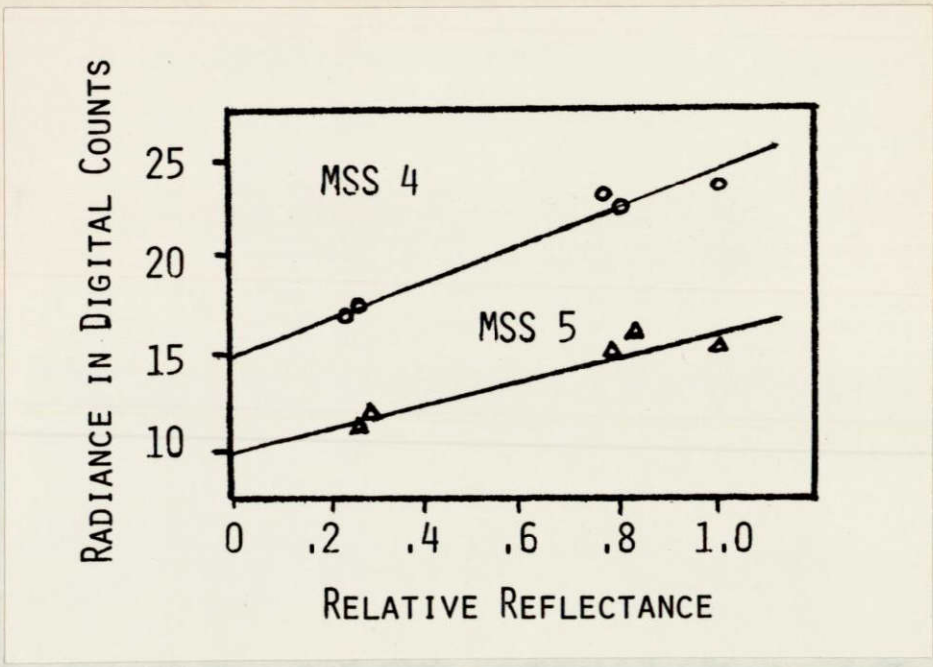

Figure 41.--LANDSAT-1 (ERTS-1) radiance and relative reflectance for the multispectral scanner (MSS) visible bands 4 and 5. Reflectance in each band was separately normalized to its highest value.

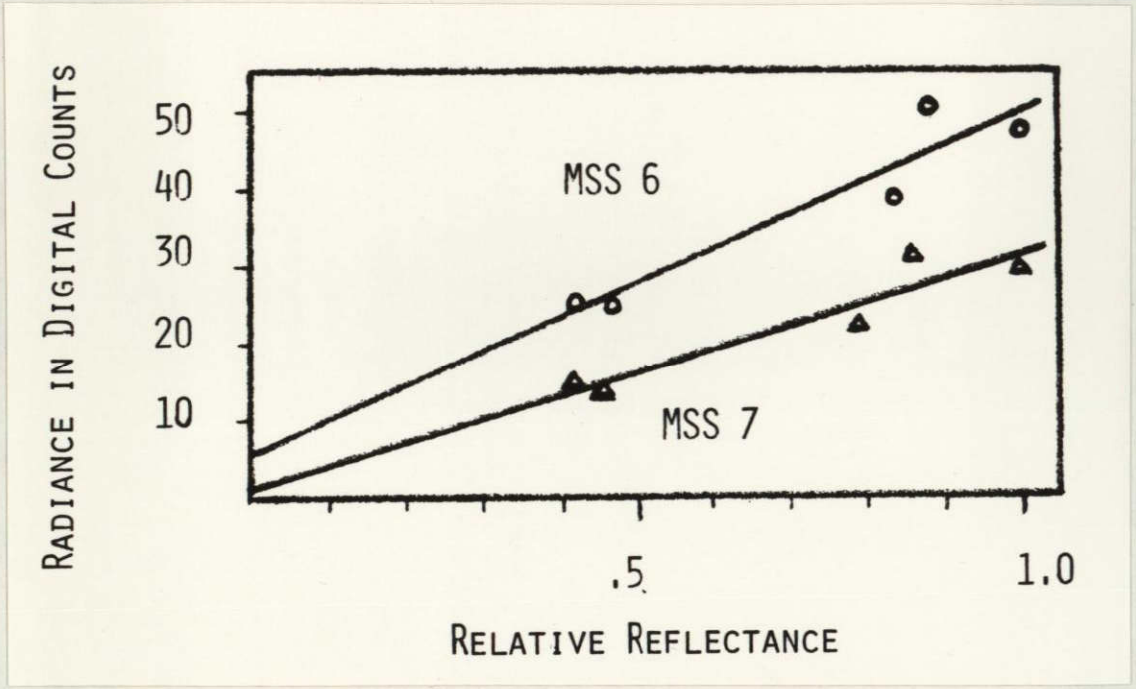

Figure 42.--LANDSAT-1 (ERTS-1) radiance and relative reflectance for the multispectral scanner (MSS) infrared bands 6 and 7. Reflectance in each band was separately normalized to its highest value.

1972. No LANDSAT data from August to September 1973 were useable because of cloud cover. Average radiance values were computed from the system-corrected computer tapes and converted from digital counts to engineering units using conversion data from appropriate NASA publications (NASA 1972; Thomas 1973).

All correlation coefficients exceeded 0,94 and suggest that the radiance Equation 1 is valid (table 44). The path radiance values are all within the range of those reported by Rogers and others (1973) for four different LANDSAT images. We do not understand why camera station 2 recorded more path radiance than camera station 1 since the former represents longer wavelengths and has a narrower bandwidth. One possible source of error is the large factor (roughly 1.5 to 2.3) used in the NASA sensitometry procedure to correct for a wider band Kodak Wratten 89 filter used in the sensitometer rather than the actual flight filters. We also found other unexplained discrepancies in comparing ground-measured radiance data with values from S190A film density, amounting to as much as 40 percent (NASA 1974). The matter deserves further study.

The space photos indicated semitransparent cirrus or cirrostratus clouds in the vicinity of the test site. Also, a very light and variable cirroform veil was noted about 1 hour after the Skylab overflight when the aircraft flight was performed. Therefore, undetected ice crystals or other aerosols might have contributed to the anomaly in near-infrared path radiance.

Despite the increasing cirrus veil, the appearance of strong shadows in the forest at the time of the aircraft flight suggested that the reflectance data would be valid for a clear sky. However, only the radiance and

Table 44. Path radiance and correlation coefficients from linear regression of satellite radiance (or relative exposure) on reflectance

Space Platform, Sensor	Camera Station or Band	Bandwidth nm	Path Radiance $\mu W\ cm^{-2}\ sr^{-1}$	Correlation Coefficient
Skylab S190A	6	517 to 594	196	0.98
	[1]4			0.99
	1	713 to 814	51	0.96
	2	805 to 882	78	0.97
LANDSAT-1, MSS[2]	4	494 to 598	289	0.98
	5	604 to 700	153	0.96
	6	693 to 799	77	0.95
	7	808 to 987	76	0.94

[1]Relative exposure of red response.

[2]Multispectral scanner.

irradiance data acquired early in the flight for the green band could be considered valid for beam transmittance calculations using Equation 3 The result was 0.86 ±0.05.

Applications

This reflectance measurement technique shows much promise as a means of obtaining valid values of the path radiance components of satellite imagery and probably of high-altitude aircraft imagery. Although this method may not be the least expensive one, it may be a valuable adjunct to computational methods or to methods using ground-based instrumentation requiring measurements coincident to the satellite overpass. Plans are under way to compare the aircraft reflectance method with the ground-based method developed by Rogers and Peacock (Rogers and others 1973). This comparison should at least help determine the relationship of the slope of the regression line to total irradiance and beam transmittance.

Several variables affecting the aircraft measurement technique need to be investigated. Most of them concern the question of how closely must the flight conditions match those at the time of satellite overflight. These variables include solar zenith angle, viewing angle, time of day, aircraft altitude, and spectral effects.

Equation 1, which is concerned with spectral effects, is strictly valid only at individual wavelengths or for narrow bandwidths. The factors τ, H, ρ, and N_p are all spectrally dependent. Since the broad-band measurements are actually integrals over wavelength, the results should be checked against measurements made with spectroradiometers (Potter 1974).

Possible applications of linear atmospheric transformation in computer classification have been discussed in the literature (Rogers and others 1973; Hulstrom 1974; Kan 1972). The objective is to extend spectral signatures from a classified scene or data set to a similar unclassified set when the main differences are due to solar and atmospheric effects. Rewriting Equation 1 we have:

$$N_i = a_i \rho_i + b_i, \qquad (6)$$

where the subscript i refers to the wavelength band. Knowing the correct coefficients a_i and b_i, one could convert the radiance sets N_i to reflectanc sets ρ_i before classification. Also, new sets of radiance data N_i' (with coefficients a_i' and b_i') could be converted to the scale of previous sets by the equation:

$$N_i = \frac{a_i}{a_i'} N_i' + \frac{a_i}{a_i'} b_i' + b_i \qquad (7)$$

In a supervised classification scheme requiring training sets, one could transform the discriminant function used in the analysis of the old data set to the scale of the new data set. This method should require the least amount of computation. For example, using a Gaussian linear classifier implies the transformation of the mean vector and the covariance matrix to new functions that are applicable to the new data set.

LITERATURE CITATIONS

1. Aldrich, R. C. 1971. Space photos for land use and forestry. Photogramm. Eng. 37(4):389-401, illus.

2. Ashby, R. W. 1964. Constraint analysis of many-dimensional relations. In Yearb. for the Soc. of Gen. Syst. Res. Vol. 9, p. 99-105.

3. Brooner, W. G., R. M. Haralick, and I. Dinstein. 1971. Spectral parameters affecting automated image interpretation using Bayesian probability techniques. In Proc. Seventh Int. Symp. on Remote Sensing of Environ. Univ. of Mich., Ann Arbor. Vol. 3, 1971:1929-1949.

4. Canfield, R. H. 1942. Sampling ranges by the line-interception method. USDA, Forest Serv., Southwest Forest and Range Exp. Stn. Res. Rep. 4. 28 p.

5. Dana, R. W. 1973. Digital sensitometry of color infrared film as an aid to pattern recognition studies. In Remote Sensing of Earth Resour., Vol. II. p. 435-452. Univ. of Tennessee, Tulahoma, Tenn., Space Inst.

6. Daubenmire, R. F. 1952. Forest vegetation of northern Idaho and adjacent Washington and its bearing on concepts of vegetation classification. Ecol. Monogr. 22:301-330.

7. Draeger, W. C., L. R. Pettinger, and A. S. Benson. 1971. The use of small scale aerial photography in a regional agricultural survey. In Proc. Seventh Int. Symp. on Remote Sensing of Environ. Univ. of Mich., Ann Arbor. Vol. 2, 1971:1205-1217.

8. Driscoll, R. S. 1969. Aerial color and color infrared photography--some applications and problems for grazing resource inventories. In Proc. Aerial Color Photogr. in Plant Sci. Aerial Color Photogr. Workshop, Univ. of Florida, Gainesville. 1969:140-149.

9. Driscoll, R. S., and R. E. Francis. 1972. Multistage, multiband, and sequential imagery to identify and quantify non-forest vegetation resources. Final Prog. Rep., Earth Resour. Surv. Program, OSSA/NASA. Rocky Mountain Forest and Range Exp. Stn. 49 p.

10. Ecosystem Task Force. 1973. ECOCLASS--a method for classifying ecosystems. USDA, Forest Serv., mimeo rep. 52 p.

11. Eppler, W. G. 1974. An improved version of the table look-up algorithm for pattern recognition. In Proc. Ninth Int. Symp. on Remote Sensing of Environ. Univ. of Mich., Environ. Res. Inst. of Mich., Ann Arbor. Vol. 2, 1974:793-812.

12. Eppler, W. G., C. A. Hemke, and R. H. Evans. 1971. Table look-up approach to pattern recognition. In Proc. Seventh Int. Symp. on Remote Sensing of Environ. Univ. of Mich., Ann Arbor. Vol. 2, 1971: 1415-1425.

13. Forest-Range Task Force. 1972. The Nation's range resources--a forest-range environmental study. USDA, Forest Serv. For. Resour. Rep. No. 19. 147 p., illus.

14. Fukunaga, K. 1972. Introduction to statistical pattern recognition. Academic Press, New York and London. 369 p.

15. Gates, D. M. 1966. Spectral distribution of solar radiation at the Earth's surface. Science. 151(3710):523-529.

16. Heller, R. C., J. L. Bean, and F. B. Knight. 1959. Aerial surveys of Black Hills beetle infestations. Stn. Pap. 46, Rocky Mountain Forest and Range Exp. Stn., Fort Collins, Colo. 8 p.

17. Heller, R. C., R. C. Aldrich, R. S. Driscoll, R. E. Francis, and F. P. Weber. 1974. Evaluation of ERTS-1 data for inventory of forest and rangeland and detection of forest stress. Final Report for NASA, Contract No. S-70251-AG. Pacific Southwest Forest and Range Exp. Stn., Berkeley, Calif., and Rocky Mountain Forest and Range Exp. Stn., Fort Collins, Colo. 255 p., illus.

18. Hildebrandt, G. 1973. Use of earth satellites for supranational inventories of forest and agricultural areas. Raumfahrtforschung, Vol. 17. p. 164-168.

19. Hulstrom, R. L. 1974. Spectral measurements and analyses of atmospheric effects on remote sensor data: proc. of the Soc. of Photo-optical Instrum. Eng. Semin. on Scanners & Imagery Syst. for Earth Obs. [San Diego, Calif., August 19-20, 1974], Vol. 51, p. 90-100.

20. Jensen, N. 1968. Optical photographic reconnaissance systems. p. 73-76. John Wiley and Sons: New York, London, Sydney.

21. Kan, E. P. F. 1972. Effects of atmospheric correction on classification. Lockheed Electron. Co., Inc., Houston Aerospace Syst. Div., Houston. Publ. LEC Number TM642-620. 9 p.

22. Kuusela, K., and S. Poso. 1972. Multi-stage acquisition of forest information from space and aircraft imagery and ground sampling. In Space Research III. Proc. of the Fifteenth Plenary Meet. Vol. 1, p. 113-117.

23. Langley, P. G., R. C. Aldrich, and R. C. Heller. 1969. Multistage sampling of forest resources by using space photography. In Second Annu. Earth Resour. Aircr. Program Status Rev. Vol. 2, Agric./For. and Sens. Studies. NASA Manned Spacecr. Cent., Houston. p. 19-2 to 19-21.

24. National Aeronautics and Space Administration, Goddard Space Flight Center. 1972. Data users handb.: NASA Earth Resour. Technol. Satellite. Doc. No. 71SD4249. NASA Goddard Space Flight Center, Greenbelt, Md. p. G-14.

25. National Aeronautics and Space Administration, Johnson Space Center, 1974. Earth Resources Experiment Package: Sensor Performance Report, Vol. I., S190A. (Eng. Baseline, SL2, SL3, & SL4 Evaluation). Publ. MSC-05528. NASA Johnson Space Center, Houston. p. 5-8p to 5-8q.

26. Nichols, J. D., M. Gialdini, and S. Jaakkola. 1973. A timber inventory based upon manual and automated analysis of ERTS-1 and supporting aircraft data using multistage probability sampling. Vol. 1: Tech. Presentations, Sec. A. Third Earth Resour. Tech. Satellite-1 Symp. NASA Goddard Space Flight Center, Greenbelt, Md. p. 145-157.

27. Peterken, G. R. 1970. Guide to check sheet for IBP [Int. Biol. Program] areas; including a classification of vegetation for general purposes by F. R. Fosberg. IBP Handb. 4. Blackwell Sci. Publ., Oxford. 133 p.

28. Potter, J. F. 1974. Haze and sun angle effects on automatic classification of satellite data-simulation and correction: proc. of the Soc. of Photo-optical Instrum. Eng. Semin. on Scanners & Imagery Systems for Earth Obs. [San Diego, Calif., August 19-20, 1974], Vol. 51, p. 73-83.

29. Rogers, R. H., K. Peacock, and N. J. Shah. 1973. A technique for correcting ERTS data for solar and atmospheric effects: proc. of Third ERTS Symp., Washington, D.C. Vol. 1, Sec. B, p. 1787-1804.

30. Schmitt, H. C., Jr., and J. H. Altman. 1970. Method of measuring diffuse RMS granularity. Appl. Optics. 9(4):871-874.

31. Thomas, V. L. 1973. Generation and physical characteristics of the ERTS MSS system corrected computer compatible tapes. Publ. No. X-563-73-206. NASA Goddard Space Flight Center, Greenbelt, Md. p. E-1 to E-4.

32. Weber, F. P. 1969. Remote sensing implications of water deficit and energy relationships for ponderosa pine attacked by bark beetle and associated disease organisms. Doctoral dissertation. Univ. of Mich., Ann Arbor. 143 p.

33. Weber, F. P., and F. C. Polcyn. 1972. Remote sensing to detect stress in forests. Photogramm. Eng. 38(2):163-175.

34. Weber, F. P., R. C. Aldrich, F. G. Sadowski, and F. J. Thomson. 1973. Land use classification in the southeastern forest region by multispectral scanning and computerized mapping. In Proc. Eighth Int. Symp. on Remote Sensing of Environ., Univ. of Mich., Environ. Res. Inst. of Mich., Ann Arbor. Vol. 1, 1973:351-373.

35. Weber, F. P. 1975. Computer-assisted processing of Skylab and ERTS-1 imagery for forest land classification and disturbance detection. Proc. Forty-first Amer. Soc. of Photogramm. Meet., Washington, D.C. March 10-14, 1975.

36. Weimer, R. J., and J. D. Haun, eds. 1960. Guide to the geology of Colorado. 310 p., illus. Geol. Soc. Amer., New York.

37. Weiss, J. P. 1973. Densitometry. In SPSE Handb. of Photogr. Sci. and Eng. p. 829-877. John Wiley & Sons: New York, London, Sydney, Toronto.

APPENDIX

1. Processing of Skylab S190B Diffuse Film Densities Recorded on Computer-Compatible Tapes

Nancy X. Norick

An automatic land-use recognition system, designed and implemented by the PSW Remote Sensing Work Unit was modified for the processing of Skylab diffuse film densities recorded on computer-compatible tapes. Considerable flexibility is built into the system so that the individual program components can be used in various combinations. The system programs run on a CDC 7600 at the University of California Lawrence Berkeley Laboratory, with input and output from a remote batch terminal at the PSW Forest and Range Experiment Station. The terminal consists of a Westinghouse 2500 with a line printer and other components. An Electronic Associates Inc. (EAI) model 430 off-line plotter is used with combinations of color pens to plot forest and land-use classification maps in the final classification process.

Skylab film densities recorded on CCT's are used as the first-step data input. Histograms and gray-scale maps are printed for each channel on a line printer so that study areas can be accurately located. If a study area falls on the boundary between two tapes, the needed portion of the data on the second tape is rewritten onto one tape. An area surrounding and including the study area is plotted for one channel using a color-coded gray scale. The corners of the rectangular study area are then located precisely on this plot.

The basic "ground truth" units we have been working with for Skylab are rectangular land-use maps at a scale of 1:24,000 which have been

constructed from small-scale aerial photos and ground checks. The size of the areas covered is 10,000 meters (6.2 miles) on a side or 40.6 centimeters (16 inches) on a map of this scale. After finding the corners of a rectangular study area on a gray-scale plot, a "rubber sheet-stretching" routine scales the corresponding nonrectangular Skylab area to the rectangular ground truth maps. This routine does a linear transformation of data array coordinates conforming to ground truth map coordinates. Nearest pixel data values are assigned to the new array elements. This is done in such a way that no data element is lost. Here and there an original data element will be used twice.

Upon completion of these corrections and calibrations a new tape is written, which becomes the data input to all subsequent programs.

The next step in the processing is to produce an EDMAP--empirical distribution map. The EDMAP is used to locate ground truth training samples and to visually screen the channels as potential contributors to the discrimination between land-use classes. Using information from the previously mentioned histograms, the range of radiance values for each channel is divided into any number of equal frequency intervals. Cartesian products of these intervals are formed for two or more selected channels. Data points falling into any product interval are assigned a mapping color and the EAI plotter is programmed to map. From the resulting sets of color-coded maps, with varying combinations of channels included or excluded, a subjective evaluation of the potential contribution of each channel for discerning each land-use class can be made. We decided to use all four filter scans in our classification analyses.

The system has an option of three classification procedures. The first uses a boundary-finding algorithm to locate clusters of spectrally similar and adjacent pixels. A pixel is put into the same cluster as its neighbor if the distance between the two in the spectral space is less than some threshold value. Locations of all cluster elements are kept track of by a sequence of pointers. This storage technique allows the combining of clusters to be very efficient. The sums of radiance values and the sums of their cross-products are accumulated for each cluster during the process of cluster assignment. After all cluster assignments are made, the cluster mean vectors and covariance matrices are used for comparison with mean vectors and covariance matrices of samples of pixels of known land use, by means of the Bhattacharyya distance function (Fukunaga 1972). A cluster is assigned to the land use for which this distance is a minimum.

A weighting factor can be applied conforming to the expected frequencies in each land-use class or conforming to any loss function.

The second classification procedure compares the radiance vector for each pixel with the mean radiance vector for a sample of pixels from each land use. The land-use classification corresponding to the minimum Euclidean distance is assigned to the pixel. This classification can also use any set of weighting factors.

The third and last classification procedure available in our system is a linear discriminant analysis with maximum likelihood and Gaussian assumptions.

The final computer output consists of the listing of acreages of land assigned to each land-use class, confusion matrices for the training

and test areas, and color-coded land-use maps. The maps are plotted in any desired scale and color code set on the EAI plotter. There is virtually no limitation upon the number of colors that can be used; however, the plotter can accommodate only eight pens at one time.

All programs are available and documented at PSW.

2. Processing of Skylab S192 Multispectral Scanner Data

Robert Haralick and Gary Minden[11]

Scan Line Straightening Mapping Functions

The path on the Earth's surface traced by the S192 scanner is a portion of a circle. The following diagram is an example of one scan line plotted on the surface.

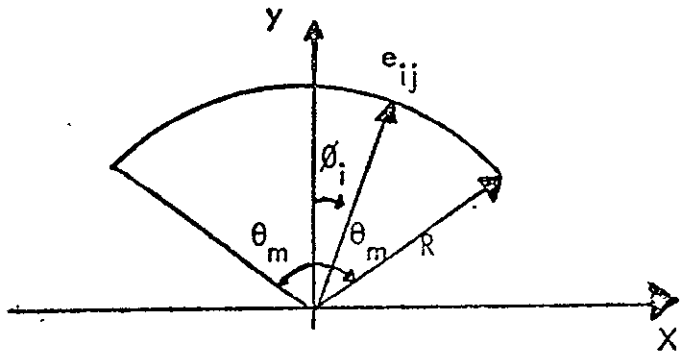

We assume the spacecraft's ground track is along the Y-axis and the arc is symmetrical about the Y-axis. We wish to take the point e_{ij} and compute its coordinates X_{ij} and Y_{ij}. The following equations specify this transform.

$$X_{ij} = (R/P) * \text{Sin}\ (\emptyset_i) \tag{8}$$

$$Y_{ij} = (R/Q) * \text{Cos}\ (\emptyset_i) + \frac{i-1}{n-1} * \frac{\theta m}{180^\circ} + j - 1 \tag{9}$$

$$\emptyset_j = \frac{2i-1-n}{n-1}\ \theta m \tag{10}$$

---

[11]University of Kansas Space Technology Center, Lawrence, Kansas.

Where:

R = H Tan (5.53°) = ground scan arc radius

H = altitude

Q = V_g/S = spacing between scan lines at the Earth's surface

V_g = ground velocity

S = scan rate = 94.792 scans/second

θm = scan angle

P = (Rθm)/(90(n-1)) = spacing between picture elements

n = number of picture elements per scan line (either 1240 or 2480)

To straighten or congruence the image, we select every point (x, y) of interest in the straightened image and find the nearest point e_{ij} in the conical image. This step requires two functions to specify I_{xy} and J_{xy}, the picture element and scan line in the conical image. We find these functions by taking the inverse of equations 8 and 9.

$$\phi_i = \text{Arcsin}\ (x\ (P/R)\ ) \tag{11}$$

$$\frac{I_{xy} = \left(\frac{\phi_i}{\theta_m} - 1\right)\ \frac{n-1}{2}}{I_{xy}} \tag{12}$$

$$J_{xy} = y - (R/Q)\ \text{Cos}\ (\phi_i) - \frac{I_{xy} - 1}{n-1}\ \frac{\theta m}{180^\circ} + 1 \tag{13}$$

Thus, given the point (x, y) we can compute ϕ_i from x and then I_{xy} from θ_i. Using ϕ_i and I_{xy} we can compute J_{xy}. The value e_{ij} is then transferred to e_{xy}.

We further reduce equations 11, 12, and 13 to get:

$$I_{xy} = \left(\frac{\text{Arcsin}\left(x(P/R)\right)}{\theta m}\right)\frac{n-1}{} + \frac{-n-1}{2} \qquad (14)$$

$$J_{xy} = y - (R/Q)\,\text{Cos}\left(\text{Arcsin}\left(x(P/R)\right)\right) - \frac{i-1}{n-1}\frac{\theta m}{180^{o}} \qquad (15)$$

Parameters for Mapping Functions

The parameters used to straighten the S192 MSS image were obtained from header and ancillary records on the computer-compatible tape and NASA publications.[12] The parameters thus obtained were:

H = 468.8 km = altitude

R = 45.14 km = ground scan arc radius

V_g = 7.157 km/sec = ground velocity

S = 94.792 scans/sec = scan rate

Q = 0.0755 km/scan = scan line spacing

θm = 1.015 rad = scan angle

P = 0.075 km/picture element = picture element spacing

n = 1240 picture elements per scan line

The equations used are then:

i = 10.69 Arcsin (X/601.68) + 620.5

j = y-597.88 Cos (0.094 i-58.21) + 1

---

[12] Earth Resources Production Processing Requirements for EREP Electronic Sensors, NASA, Rev. A, Change 1, Jan. 3, 1974, pp. 5-20 to 5-24.

KANDIDATS Operational Overview

KANDIDATS (KANsas Digital Image DATa System) refers to the entire interactive image processing facility at the Remote Sensing Laboratory, University of Kansas.

KANDIDATS is an interactive/batch-mode digital multi-image pattern-recognition system designed to facilitate the man-machine interface between the user and the PDP-15/IDECS/IBM 7094 II complex. It is intended to allow users with an interest in image processing and varied degrees of sophistication with computer hardware and software an easy access to the image processing facilities available. KANDIDATS provides a great deal of flexibility and degree of freedom to the operator. It is designed primarily as a tool to be used in a research environment. The type of image processing it provides is the flexible, relatively small quantity image processing tasks necessary in formulating and evaluating algorithms which will later be applied to large amounts of image data. KANDIDATS runs on the PDP-15/IBM computer system and uses the IDECS as an image acquisition and display device. Digital image data may be introduced through magnetic tape units on the IBM machine.

The entire system is guided by an operator at a console directing the system either by initiating commands or by directing input to be taken from a command file. KANDIDATS then manipulates the particular image data accordingly.

Once image data is entered into the system, KANDIDATS automatically maintains and processes multiple digital images in a standard format which provides a complete processing history for the image from the time it enters the system until the time it is no longer needed.

Image processing capabilities currently implemented in the KANDIDATS system include:

1. Equal-interval and equal-probability quantizing
2. Subimage cutting and pasting
3. Gradient operations
4. Spatial clustering
5. Computing textural feature images
6. Histogram and Scattergram determination
7. Decision rule determination and image classification according to these decision rules
8. Image display
9. Image transformation
10. Image convolution
11. Expansion and Compression of image scales
12. Reformatting of images
13. Creation of images
14. Addition of ground truth information or maps to images

There exists a set of specific image operations for each one of the above-mentioned image processing tasks. The operator selects the appropriate operation by inputting commands to KANDIDATS via the teletype or the CRT terminal. The KANDIDATS package provides extensive error checking and frees the user from the bookwork and housekeeping necessary to set up these operations on the computer. The commands all have the same simple form and are decoded by the KANDIDATS command string interpreter. Each command string contains certain basic information:

1. The abbreviated name of the operation
2. The name of the destination device on which to place the output image
3. The name of the created image
4. The name of the origination device on which to find the input image
5. The name of the input image

The rationale for the command string being set up this way can be illustrated by an analogy with a busy office. In the office there are many workers, each equipped with particular talents. The office has many kinds of file cabinets for storing information. The investigator gets work done by making a request of or by giving a command to one of the workers. He identifies for the worker which file cabinet and the name of the folder in the cabinet where he can find the material which needs to be worked on. Then, he identifies for the worker which file cabinet and the name of the folder into which he must place the material he creates by working.

In KANDIDATS, every image has a name and is stored in a folder with that name. The cabinet into which the folder containing the image is placed is really the physical device on which the image resides. KANDIDATS has the following peripheral devices on which an image as well as other information can reside:

1. IBM compatible magnetic tape drives
2. Disk pack (movable head)
3. Cardreader
4. IDECS disk

The operator guides the various image data sets between the various devices applying various processing algorithms to them.

In addition, KANDIDATS allows the batch processing of image data through the creation of image processing task files. These task files known as KANDIDATS run files may be entered in the same format as that used when the operator enters command strings and responses at the teletype. This run file is stored on the disk and can be summoned at any point and used to instruct KANDIDATS in lieu of operator interaction.

KANDIDATS has a monitor which resides in memory throughout a KANDIDATS program run. This monitor takes user input in the form of a KANDIDATS command string, decodes it, and calls in the appropriate subsystem to perform the designated function. The subsystem requests any additional information needed to perform the process and initiates the process. After the processing has begun, it is carried to completion unless the operator interrupts it or an error occurs. In all cases, return is made to the KANDIDATS monitor and appropriate action is taken. On normal return, KANDIDATS requests another command from the operator or run file. If the operator terminates the operation prematurely, return is made to the monitor and the termination noted. If termination occurs during processing from a KANDIDATS run file, the monitor asks for permission to continue or exit from the run file. When the system encounters a recoverable error, an error flag is set and the KANDIDATS monitor prints out a list of subroutine names whose calls led to the error along with the event number returned. The number can then be matched to an error list to determine the cause of the error. If the error occurs during run file operation, the operator is asked whether to continue with the operation or abort it.

KANDIDATS Table Look-up Approach

Brooner, Haralick, and Dinstein (1971) used a table look-up approach on high-altitude multiband photography flown over Imperial Valley, California, to determine crop types. Their approach to the storage problem was to perform an equal-probability quantizing from the original 64 digitized grey levels to ten quantized levels for each of the three bands: green, red, and near infrared. Then after the conditional probabilities were empirically estimated, they used a Bayes rule to assign a category to each of the 10^3 possible quantized vectors in the 3-dimensional measurement space. Those vectors which occurred too few times in the training set for any category were deferred assignment.

The rather direct approach employed by Brooner and others (1971) has the disadvantage of requiring a rather small number of quantized levels. Furthermore, it cannot be used with measurement vectors of dimension greater than four: for if the number of quantized levels is about 10, then the curse of dimensionality forces the number of possible quantized vectors to an unreasonably large size. Recognizing the grey-level precision restriction forced by the quantizing coarsening effect, Eppler, Hemke, and Evans (1971) suggest a way to maintain greater quantizing precision by defining a quantization rule for each category-measurement dimension as follows:

1. Fix a category and a measurement dimension component
2. Determine the set of all measurement patterns which would be assigned by the decision rule to the fixed category
3. Examine all the measurement patterns in this set and determine the minimum and maximum grey levels for the fixed measurement component

4. Construct the quantizing rule for the fixed category and measurement dimension pair by dividing the range between the minimum and maximum grey levels into equal-spaced quantizing intervals.

This multiple quantizing rule in effect determines for each category a rectangular parallelepiped in measurement space which contains all the measurement patterns assigned to it. Then as shown in Figure 43, the equal-interval quantizing lays a grid over the rectangular parallelepiped. Notice how for a fixed number of quantizing levels, the use of multiple quantizing rules in each band allows greater grey-level quantizing precision compared to the single quantization rule for each band.

A binary table for each category can be constructed by associating each entry of the table with one corresponding cell in the gridded rectangular parallelepiped. Then define the entry to be a binary 1 if the decision rule has assigned a majority of the measurement patterns in the corresponding cell to the specified category; otherwise, assign the entry to be a binary 0.

The binary tables are used in the implementation of the multiple quantization rule table look-up in the following way. Order the categories in some meaningful manner such as by prior probability. Quantize the multispectral measurement pattern using the quantization rule for category c_1. Use the quantized pattern as an address to look up the entry in the binary table for category c_1 to determine whether or not the pre-stored decision rule would assign the pattern to category c_1. If the decision rule makes the assignment to category c_1, the entry would be a binary 1 and all is finished. If the decision rule does not make the assignment to category c_1, the entry would be a binary 0 and the process would repeat in a similar manner with the quantization rule and table for the next category.

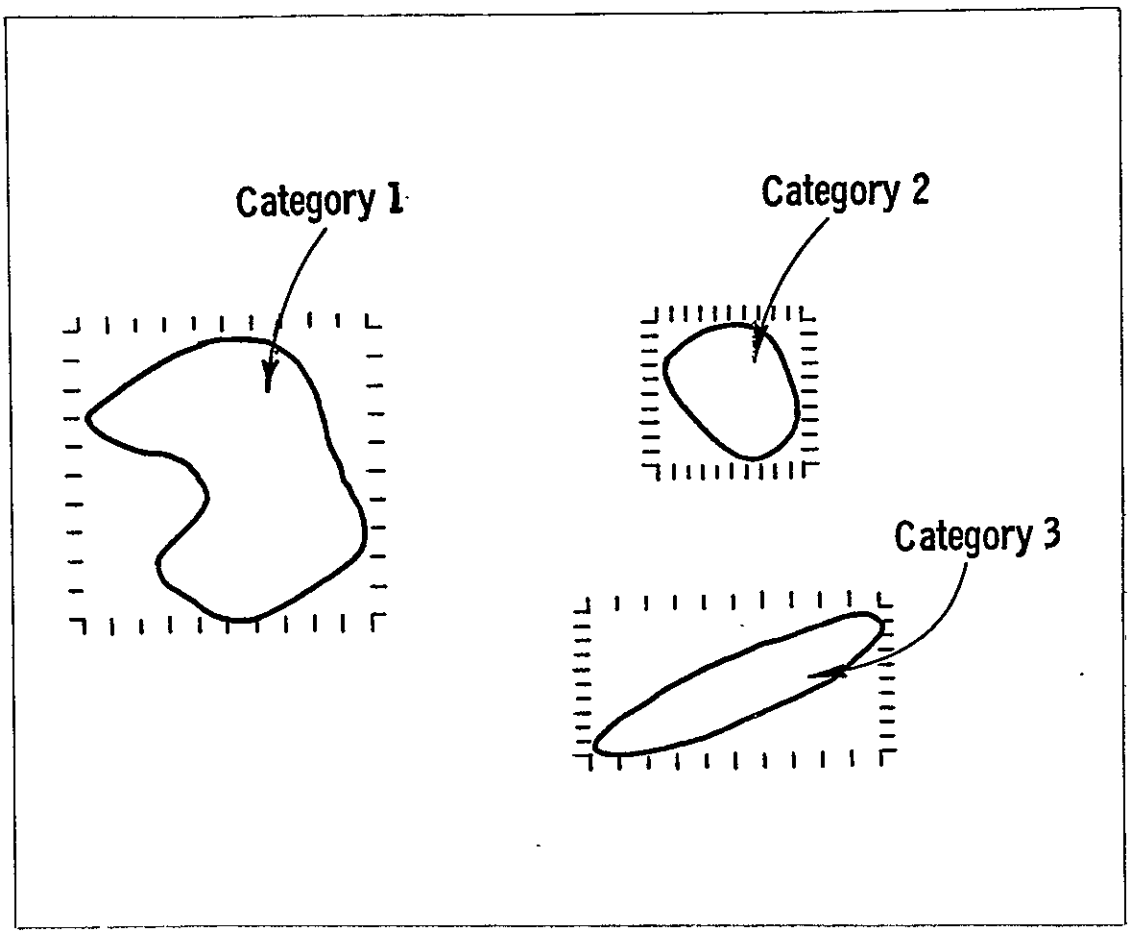

Figure 43. The three drawings illustrate how quantizing can be done differently for each category thereby enabling more accurate classification by the following table look-up rule: (1) quantize the measurement by the quantizing rule for category one, (2) use the quantized measurement as an address in a table and test if the entry is a binary one or binary zero, (3) if it is a binary one assign the measurement to categor one; if it is a binary zero, repeat the procedure for category two.

One advantage to this form of the table look-up decision rule is the flexibility to use different subsets of bands for each category look-up table and thereby take full advantage of the feature-selecting capability to define an optimal subset of bands to discriminate one category from all the others. A disadvantage to this form of the table look-up decision rule is the large amount of computational work required to determine the rectangular parallelepipeds for each category and the still large amount of memory storage required (about 5,000 8-bit bytes per category).

Eppler (1974) discusses a modification of the table look-up rule which enables memory storage to be reduced by five times and decision rule assignment time to be decreased by two times. Instead of pre-storing in tables a quantized measurement space image of the decision rule, he suggests a systematic way of storing in tables the boundaries or endpoints for each region in measurement space satisfying a regularity condition and having all its measurement patterns assigned to the same category.

Let $D = D_1 \times D_2 \times \ldots \times D_N$ be measurement space. A subset $R \subseteq D_1 \times D_2 \times \ldots \times D_N$ is a regular region if and only if there exists constants L_1 and H_1 and functions $L_2, L_3, \ldots, L_N, H_2, H_3, \ldots, H_N$

$$\left(L_n: D_1 \times D_2 \times \ldots \times D_{n-1} \rightarrow (-\infty, \infty);\ H_n: D_1 \times D_2 \times \ldots \times D_{n-1} \rightarrow (-\infty, \infty)\right)$$

such that

$$R = \left\{(x_1, \ldots, x_N) \in D \mid \begin{array}{l} L_1 \leq x_1 \leq H_1 \\ L_2(x_1) \leq x_2 \leq H_2(x_1) \\ \quad \vdots \\ L_N(x_1, x_2, \ldots x_{N-1}) \leq x_N \leq H_N(x_1, x_2, \ldots, x_{N-1}) \end{array}\right\}$$

From the definition of a regular region, it is easy to see how the table look-up by boundaries decision rule can be implemented. Let $d = (d_1, \ldots, d_N)$ be the measurement pattern to be assigned a category. To determine if d lies within a regular region R associated with category c we look up the numbers L_1 and H_1 and test to see if d_1 lies between L_1 and H_1. If so, we look up the numbers $L_2(d_1)$ and $H_2(d_1)$ and so on. If all the tests are satisfied, the decision rule can assign measurement pattern d to category c. If one of the tests fails, tests for the regular region corresponding to the next category can be made.

The memory reduction in this kind of table look-up rule is achieved by only storing boundary or endpoints of decision regions and the speedup is achieved by having one-dimensional tables whose addresses are easier to compute than the three- or four-dimensional tables required by the initial table look-up decision rule. However, the price paid for these advantages is the regularity condition imposed on the decision regions for each category. This regularity condition is stronger than set connectedness but weaker than set convexity.

Another approach to the table look-up rule can be based on Ashby's (1964) technique of constraint analysis. Ashby suggests representing in an approximate way subsets of Cartesian product sets by their projections on various smaller dimensional spaces. Using this idea for two-dimensional spaces we can formulate the following kind of table look-up rule.

Let $D = D_1 \times D_2 \times \ldots \times D_N$ be measurement space, C be the set of categories, and $J \subseteq \{1, 2, \ldots, N\} \times \{1, 2, \ldots, N\}$ be an index set for the selected two-dimensional spaces. Let the probability threshold α be given. Let $(i, j) \in J$; for each $(x_1, x_2) \in D_i \times D_j$ define the set $S_{ij}(x_1, x_2)$ of categories having the highest conditional probabilities given (x_1, x_2) by

$$S_{ij}(x_1, x_2) = \{c \in C \mid P_{x_1, x_2}(c) \geq \alpha_{ij}\}$$, where α_{ij} is the largest number which satisfies

$$\sum_{c \in S_{ij}(x_1, x_2)} P_{x_1, x_2}(c) \geq \alpha$$

$S_{ij}(x_1, x_2)$ is the set of likely categories given that components i and j of the measurement pattern take the values (x_1, x_2).

The sets S_{ij}, $(i, j) \in J$, can be represented in the computer by tables. In the $(i, j)^{th}$ table S_{ij} the $(x_1, x_2)^{th}$ entry contains the set of all categories of sufficiently high conditional probabilities given the marginal measurements (x_1, x_2) from measurement components i and j, respectively. This set of categories is easily represented by a one-word table entry: a set containing categories c_1, c_7, c_9, & c_{12}, for example, would be represented by a word having bits 1, 7, 9, and 12 on and all other bits off.

The decision region R(c) containing the set of all measurement patterns to be assigned to category c can be defined from the S_{ij} sets by

$$R(c) = \left\{(d_1, d_2, \ldots, d_N) \in D_1 \times D_2 \times \ldots \times D_N \mid \{c\} = \bigcap_{(i,j) \in J} S_{ij}(d_i, d_j)\right\}$$

This kind of a table look-up rule can be implemented by using successive pairs of components (defined by the index set J) of the (quantized) measurement patterns as addresses in the just-mentioned two-dimensional tables. The set intersection required by the definition of the decision region R (c) is implemented by taking the Boolean AND of the words obtained from the table look-ups for the measurement to be assigned a category. Note that this Boolean operation makes full use of the natural parallel compute capability the computer has on bits of a word. If the k^{th} bit is the only bit which remains on in the resulting word, then the measurement pattern

is assigned to category c_k. If there is more than one bit on or no bits are on, then the measurement pattern is deferred its assignment (reserved decision).

Thus we see that this form of a table look-up rule utilizes a set of "loose" Bayes rules in the lower dimensional projection spaces and intersects the resulting multiple category assignment sets to obtain a category assignment for the measurement pattern in the full measurement space.

Because of the natural effect which the category prior probabilities have on the category assignments produced by a Bayes rule, it is possible for a measurement pattern to be the most probable pattern for one category yet be assigned by the Bayes rule to another category having much higher prior probability. This effect will be pronounced in the table look-up rule just described because the elimination of such a category assignment from the set of possible categories by one table look-up will completely eliminate it from consideration because of the Boolean AND or set intersection operation. However, by using an appropriate combination of maximum likelihood and Bayes rules, something can be done about this.

For any pair (i, j) of measurement components, fixed category c, and probability threshold β, we can construct the set of $T_{ij}(c)$ having the most probable pairs of measurement values from components i and j arising from category c. The set $T_{ij}(c)$ is defined by

$$T_{ij}(c) = \left\{(x_1, x_2) \in D_i \times D_j \mid P_c(x_1, x_2) \geq \beta_{ij}(c)\right\},$$

where $\beta_{ij}(c)$ satisfies

$$\sum_{(x_1, x_2) \in T_{ij}(c)} P_c(x_1, x_2) = \beta$$

Tables which can be addressed by (quantized) measurement components can be constructed by combining the S_{ij} and T_{ij} sets. Define $Q_{ij}(x_1, x_2)$ by

$$Q_{ij}(x_1, x_2) \quad \{c \in C \mid (x_1, x_2) \in T_{ij}(c)\} \quad \cup S_{ij}(x_1, x_2)$$

The set $Q_{ij}(x_1, x_2)$ contains all the categories whose respective conditional probabilities given measurement values (x_1, x_2) of components i and j are sufficiently high (a Bayes rule criteria) as well as all those categories whose more probable measurement values for components i and j, respectively, are (x_1, x_2) (a maximum likelihood criteria). A decision region R(c) containing all the (quantized) measurement patterns can then be defined as before using the Q_{ij} sets:

$$R(c) = \left\{(d_1, d_2, \ldots, d_N) \in D_1 \times D_2 \ldots \times D_N \mid c \right\} = \bigcap_{(i,j) \in J} Q_{ij}(d_i, d_j)$$

A majority vote version of this kind of table look-up rule can be defined by assigning a measurement to the category most frequently selected in the lower-dimensional spaces.

$$R(c) = \{(d_1, d_2, \ldots, d_N) \quad D_1 \times D_2 \times \ldots \times D_N \mid$$

$$\# \{(i,j) \in J \mid c \in Q_{ij}(d_i, d_j)\} \geq \# \{(i,j) \in J \mid c \in Q_{ij}(d_i d_j)$$

$$\text{for every } c \quad C - \{c\}\}$$

All single band pair classification results used probability threshold parameters $(\alpha, \beta) = (0.1, 0.)$ thereby making the decision rule a true Bayes rule. The multiband pair classification results were run with $\beta = 0.07\alpha$ and α chosen to minimize the number of reserved decisions.

Intentionally left blank

3. Angular Corrections for the Input Probe of an Irradiance Meter

Robert W. Dana

The power per unit area incident on a horizontal surface from a point source such as the sun is proportional to the cosine of the zenith angle (θ). The zenith angle is the angle between the normal to the surface and line from the surface to the sun. The flat, uniformly thick (3 mm) acrylic diffuser used as the first element in the irradiance probe transmits the increasing off-angle (large θ) radiation from a point source with decreasing efficiency. Therefore, as with most so-called "cosine receptors," some angular correction is necessary, especially for θ greater than 45°.

To measure the angular dependence to point source or direct radiation, we mounted the probe on a turntable with vernier angular readout. The turntable was mounted on an optical bench a fixed distance from a stable tungsten lamp.

Rotation of the probe about an axis perpendicular to a line between the probe and the lamp produced a response curve $f(\theta)$ somewhat lower than the cosine function (fig. 44). For example, the correction factor $\cos\theta/f(\theta)$ of the direct component of irradiance at a zenith angle of 60° is a multiplier of 1.114. No significant spectral differences were noted in the correction factor when all four broadband filters were used with the probe.

The next step is to compute the correction on the broadband irradiance H_m measured by the imperfect receptor. The true total irradiance on a horizontal surface is the sum of the direct component H_r and a diffuse

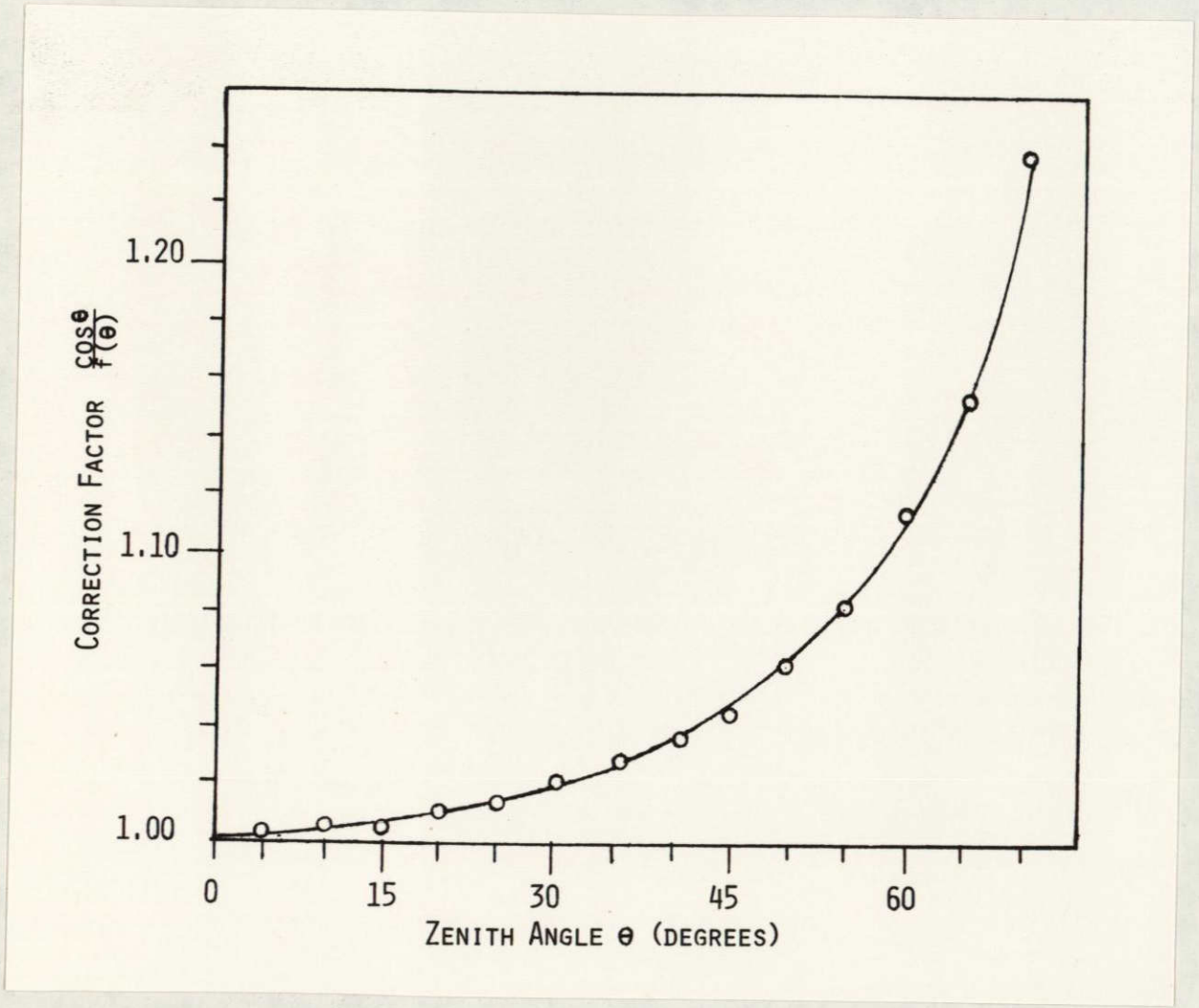

Figure 44.--Correction factors for direct irradiance.

Table 45. Ratio (g) of sky irradiance to total irradiance with angular correction factor ($g' = \frac{F}{1 + g(F - 1)}$) shown in parentheses.

Zenith Angle θ	Direct Component Correction (F)	Spectral Band[1] A	B	C	D
0	1.0000	0.0530(1.0000)	0.0394(1.0000)	0.0467(1.0000)	0.0133(1.0000)
48°11'	1.0562	0.1095(1.0497)	0.0739(1.0518)	0.0589(1.0527)	0.0251(1.0547)
60°	1.1152	0.1665(1.0942)	0.1186(1.1002)	0.0944(1.1032)	0.0397(1.1107)

[1]Defined in Table 43.

wavelength band. The visible bands at zenith angles greater than 45° show the greatest discrepancy between (g) and ($\bar{g}$).

The data used for this computation of sky-to-total irradiance ratio pertains to a moderately clear sky. For a heavy haze condition the factor (g) would be considerably higher producing larger values at a given zenith angle. Therefore, in cases of heavy haze the sky irradiance, as well as total irradiance, should be monitored to arrive at the proper irradiance meter angular correction.

Intentionally left blank

4. Computation of the Effective Shapes and Bandwidths of Skylab S190A Bandpasses.

Robert W. Dana

To provide a measure of the accuracy of match of the detectors and filters used in our airborne measurements, the effective shapes and bandwidths of the S190A bandpasses were computed from the SL-2 Sensitometric Data Package, JL12-502.

First we computed the product function of the various transmittances of the optical elements in front of the S190 films. They are the lens (T_L), window (T_W), and filter (T_f) transmittance values. The products $T_L T_W T_f = T_t$ were computed at 10 nanometer intervals.

Next, a representative set of film spectral sensitivity values for each original film (SO-022, 2424) was derived. We first plotted several columns of log spectral sensitivity values (X) against wavelength for different density levels. As expected with each film, the curves tracked quite well, so that the data at density D = 1.0 could be taken as typical. Also, little spectral difference was seen between the premission and postmission sensitometry. To remove overall sensitivity differences, we normalized the eight data sets for SO-022 film and the seven sets for 2424 film. To do this we subtracted from X values in the D = 1.0 column the peak value which occurred at 450 nm for SO-002 film and 800 nm for 2424 film. We then computed the mean value X of the seven or eight sets of normalized X values, wavelength by wavelength (10 nm intervals). Standard deviations ranged from 0.01 to 0.03 cm^2/erg at most wavelengths but reached 0.15 at the long wavelength ends. Finally, we computed the products:

$$T_t(\lambda)10^{\bar{x}(\lambda)} = \bar{S}(\lambda).$$

Stations 1, 5, and 6 are characterized by relatively gradual gradients on the low wavelength side and peak values very near to the long-wave limits (fig. 43). This shape is due entirely to the film curve because the filter functions are all quite square. The characteristic dip at 630 to 650 nanometers for aerial black-and-white films is seen in the station 5 bandpass. The curve for station 2 is very symmetrical about its peak value. The curve is not certain beyond 900 nanometers due to incomplete X data in the JL12-502 package. An integrated bandwidth measurement was calculated by finding the integral $\int \bar{S}(\lambda)\, d\lambda$ and dividing by the peak value of $\bar{S}(\lambda)$. This proved to be different in some cases from the distance between half-power points due to the irregular shapes. Bandwidth information is summarized in Table 46.

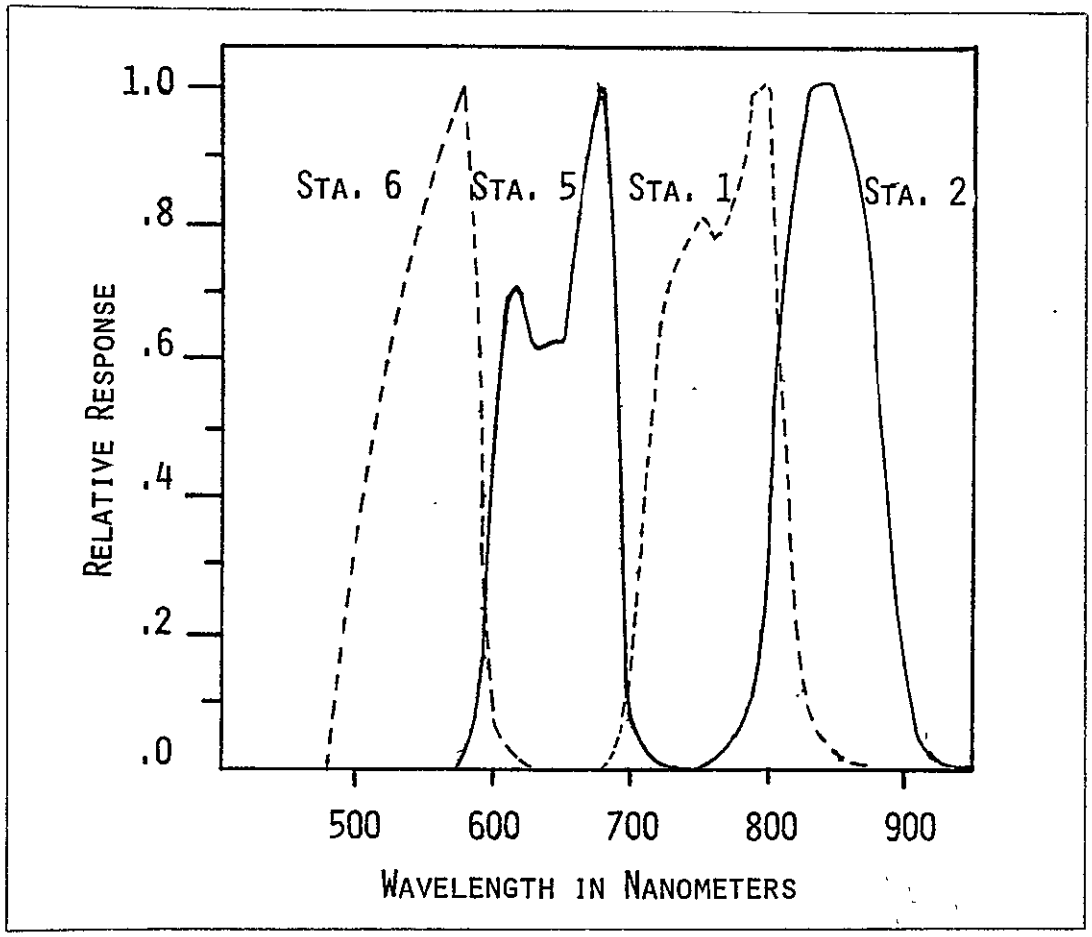

Figure 45.--System spectral response curves for Skylab S190A camera stations 6, 5, 1, and 2. Curves are separately normalized.

Table 46. Measured bandwidths of S190A stations 1, 2, 5, and 6 for SL-2.

Station	Design Bandwidth[1]	Actual Half-power Points	Wavelength at Peak Response	Half-Bandwidth	Integrated Bandwidth
			nanometers		
1	700 to 800	713, 814	800	101	91
2	800 to 900	805, 882	850	77	81
5	600 to 700	601, 695	680	94	75
6	500 to 600	517, 594	580	77	75

[1]EREP Investigators Information Book MSC - 07874

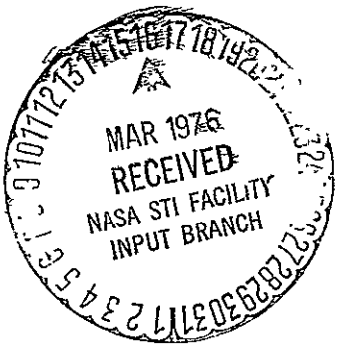
MAR 1976
RECEIVED
NASA STI FACILITY
INPUT BRANCH